Untersuchung der Degradation von Fluorpolymermaterialien im Niedertemperatur-Sauerstoffplasma mittels physikalisch-chemischer Oberflächenanalytik

Investigation of the Degradation of Fluoropolymer Materials in a Low Temperature Oxygen Plasma using Physical-Chemical Surface Analysis

Dem Fachbereich 08 - Biologie und Chemie - der Justus-Liebig-Universität Gießen vorgelegte Dissertation zur Erlangung des akademischen Grades

Doktor der Naturwissenschaften

- Dr. rer. nat. -

Tobias Wagner

Dekan / Dean	Prof. Dr. Holger Zorn
Erstgutachter / 1st Reviewer	Prof. Dr. Dr. h.c. Jürgen Janek (Justus-Liebig-Universität Gießen)
Zweitgutachter / 2nd Reviewer	Prof. Dr. Peter Klar (Justus-Liebig-Universität Gießen)
Eingereicht / Submitted	29.04.2026

Selbstständigkeitserklärung

Ich erkläre: Ich habe die vorgelegte Dissertation selbstständig und ohne unerlaubte fremde Hilfe und nur mit den Hilfen angefertigt, die ich in der Dissertation angegeben habe. Alle Textstellen, die wörtlich oder sinngemäß aus veröffentlichten Schriften entnommen sind, und alle Angaben, die auf mündlichen Auskünften beruhen, sind als solche kenntlich gemacht. Ich stimme einer evtl. Überprüfung meiner Dissertation durch eine Antiplagiat-Software zu. Bei den von mir durchgeführten und in der Dissertation erwähnten Untersuchungen habe ich die Grundsätze guter wissenschaftlicher Praxis, wie sie in der „Satzung der Justus-Liebig-Universität Gießen zur Sicherung guter wissenschaftlicher Praxis“ niedergelegt sind, eingehalten.

Angaben zu auf künstlicher Intelligenz (KI) basierender Hilfen wie ChatGPT oder SchulKI von OpenAI oder Gemini von Google zur Erstellung meiner Dissertation (Zutreffendes angekreuzt):

☒ Ich habe bei der Erstellung dieses Textes kein KI-Tool verwendet.

☐ Ich habe ein KI-Tool in den folgenden Bereichen eingesetzt (Mehrfachnennungen möglich):

☐ Ideen finden, meine Kreativität anregen

☐ Verstehen von Konzepten, Recherche von Fakten und Definitionen

☐ Optimierung eines von mir verfassten Textes

☐ Erstellen ganzer Textpassagen nach meinen Vorgaben

Folgende KI-Tools habe ich verwendet, damit aufgeführte Teile meines Textes von dem Tool wie folgt profitiert haben

Gießen, den

Tobias Wagner

Acknowledgement

First of all, I want to thank the supervisor of this work, Prof. Dr. Dr. h.c. Jürgen Janek, for giving me the opportunity to work, research and study in his group, as well as providing direction for my doctoral thesis. I am grateful for the many hours he has dedicated despite his extremely busy schedule to discuss my work.

Furthermore, I want to thank Prof. Dr. Peter Klar for being the second reviewer of this thesis.

Special thanks are dedicated to apl. Prof. Dr. Marcus Rohnke for further supervising and supporting me. Being able to work, learn and being mentored in his subgroup was a great opportunity that has allowed me to grow personally. Without his continuous support and technical expertise, this work would simply not have been possible.

Additional thanks go to the workshop and electricians of the institute, as well as the facility management team of the old chemistry building.

I would then like to thank the many people, I had the pleasure of working and discussing with. Particularly, I thank my current and former colleagues and friends in the Janek group and beyond, especially Dr. Svenja Otto, Dr. Yannik Moryson, David Schäfer, Pascal Dippell, Tobias Zeller, Mario Lorenz, Dennis Pietruschka, Linus Pohl, Dr. Jannis Jung, Dr. Sebastian Schwan, Alix Kaczmarek and Frances Pauelsen, as well as Lea Aydin, Ayşe Gül Karaaslan, and Dr. Felix Bödeker.

I also thank my parents Anke and Dietmar, whose emotional and financial support, encouragement and unconditional love have enabled me to study full time and who have thus have laid the groundwork for this thesis; my sister Tamara, who has always been able to make me laugh and have a positive outlook; and my parents- and sister in-law Aysun, Halis and Sila Bayram, for always giving me a different perspective and the many, many, many delicious meals they have provided me with during stressful and relaxed periods alike. Last but most definitely not least, I thank my wife, Kardelen, who has supported me throughout the entire journey of my studies, has always encouraged me to push and grow further and cushioned a lot of stress, especially so during the last weeks of writing.

Zusammenfassung

Der so genannte low Earth orbit (LEO, dt.: Erdnaher Orbit) spielt eine wichtige Rolle in der Erforschung des Weltraums, moderner Telekommunikation und der Beobachtung der Erde. Durch seine Nähe zur Erde ist der LEO besonders attraktiv für diese Nutzungsformen, jedoch sind die Umweltbedingungen in diesem Orbit besonders harsch und können zu einer raschen Degradation von Materialien führen. Viele Satelliten verbleiben für Jahrzehnte im LEO, wodurch die Wahrscheinlichkeit auf katastrophales Materialversagen während des Lebenszyklus steigt. Besondere Gefahr für Materialien im LEO geht von atomarem Sauerstoff (AO) aus, welcher besonders in den erdnähesten Bereichen die am häufigsten vorkommende Gasspezies darstellt und hochreaktiv ist. Ein Verständnis für die chemische Degradation, welche auftritt, sobald ein Stoff AO ausgesetzt ist, ist unerlässlich, um bessere Materialien für die Nutzung im LEO zu entwickeln. Niedertemperatur-Sauerstoffplasmen werden häufig genutzt, um AO zu erzeugen und Bedingungen ähnlich denen im LEO zu schaffen. Fluorpolymere besitzen typischerweise geringe Dichten, thermisch und elektrisch isolierende Eigenschaften, sowie für Polymere geringe Reaktivitäten gegenüber AO. Diese Merkmale machen Fluorpolymere zu geeigneten Materialien für die Nutzung im LEO. Die meisten Studien auf dem Feld der Materialdegradation im LEO beschäftigen sich in erster Linie mit den Veränderungen mechanischer Eigenschaften und nutzen nur selten Methoden der physiko-chemischen Materialcharakterisierung. Dem folgt eine Wissenslücke im Bereich der chemischen Prozesse, die auf der Materialoberfläche unter LEO-Bedingungen stattfinden.

Im Rahmen dieser Doktorarbeit wurde die chemische Degradation zweier Fluorpolymere, Polyvinylfluorid (PVF) und Polytetrafluorethylen (PTFE), im Niedertemperatur-Sauerstoffplasma untersucht. Letzteres wird häufig als Kabelisolation auf der Außenseite von Raumfahrzeugen im LEO genutzt, wo es durch Kontakt mit AO korrodiert. Ersteres findet hingegen seltener Anwendung, bei der es AO ausgesetzte wäre, und wurde als weniger stark fluoriertes Vergleichsmaterial ausgewählt. Der Degradationsmechanismus wurde mit oberflächensensitiven Methoden der chemischen Materialcharakterisierung, namentlich Flugzeit-Sekundärionen-Massenspektrometrie (ToF–SIMS) und Röntgenphotoelektronenspektroskopie (XPS) untersucht. Gleichzeitig wurde die Zusammensetzung des Plasmas mittels Quadrupol-Massenspektrometrie (QMS) überwacht. Multivariate Statistische (MVS) Methoden wurden genutzt, um die aufgenommenen Daten tiefgreifender zu verstehen. Durch ToF–SIMS- und XPS-Messungen konnten in dieser Arbeit Degradationsprodukte auf der Probenoberfläche identifiziert werden, während in QMS-Messungen Kohlenstoffspezies ohne chemische Bindung zu Sauerstoff im Plasma detektiert wurden, was auf eine unvollständige Oxidation hinweist.

Die Ergebnisse dieser Dissertation erweitern das Wissen um die chemischen Prozesse, welche während der Degradation von Fluorpolymeren in weltraumähnlichen Bedingungen ablaufen. Die hier genutzten Methoden der chemischen Oberflächenanalytik bieten einen enormen Mehrwert zur Untersuchung der Materialdegradation unter Weltraumbedingungen, der bisher nicht ausgeschöpft wird. Weiterhin zeigt der durch MVS-Anwendung gewonnene Einblick in die generierten Daten den Nutzen dieser Methoden zur Beantwortung verschiedenster wissenschaftlicher Fragestellungen.

Abstract

The low Earth orbit (LEO) plays an important role for space exploration, modern telecommunication and Earth observation. While the proximity to Earth makes the LEO particularly attractive for these applications, the environmental conditions inside the LEO are harsh and can lead to rapid material degradation. Many satellites remain in the LEO for years and even decades, increasing the chance for catastrophic material failure during its lifecycle. One significant threat to materials in the LEO is atomic oxygen (AO), which is the most abundant species of gas in parts of the LEO and extremely reactive. Understanding the chemical degradation that occurs when a surface is in contact with AO is crucial for improving material design for applications in the LEO. To generate AO and partially simulate LEO conditions, low temperature oxygen plasmas are commonly employed.

Fluoropolymers have favorable features for use in the LEO. Among these are low density, thermal and electrical insulating properties and a relatively high resistance towards AO, compared to other polymers. Most studies investigating the degradation of fluoropolymers and other materials in space focus on changing mechanical properties. Physical-chemical characterization methods are utilized much more sparingly, leading to a gap in the knowledge about the chemical processes at the surface of materials exposed to LEO conditions.

In the framework of this doctoral thesis the chemical degradation of two fluoropolymers, polyvinyl fluoride (PVF) and polytetrafluoroethylene (PTFE), in a low temperature oxygen plasma was investigated. The latter is often employed in the LEO as a wiring insulator on the exterior of spacecraft, coming in contact with AO. The former is used less frequently in space applications and was chosen as a less fluorinated reference material. The degradation mechanism was studied by employing surface sensitive chemical analysis techniques such as time-of-flight secondary-ion mass spectrometry (ToF–SIMS) and X-ray photoelectron spectroscopy (XPS) on the sample, as well as by monitoring the plasma composition via quadrupole mass spectrometry (QMS). Multivariate statistical (MVS) tools were used to obtain a deeper understanding of the measurement data. By ToF–SIMS and XPS measurements, degradation products on the sample surface were identified, while QMS measurements revealed unoxygenated carbon species in the atmosphere, indicating incomplete oxidation.

Overall, the results of this doctoral thesis expand the knowledge about the chemical processes involved in the degradation of fluoropolymers under space-like conditions. The use of methods for chemical surface analysis techniques in this work yields a significant benefit for the investigation of material degradation under space-like conditions that is currently not fully realized. Additionally, the insight gained into the measurement data by the use of MVS tools for data evaluation demonstrates their usefulness to assist in answering a variety of scientific questions.

List of Abbreviations

AES	Auger electron spectroscopy
AFM	Atomic force microscopy
BE	Binding energy
CCP	Capacitively coupled plasma
ICP	Inductively coupled plasma
LEO	Low Earth orbit
MCR	Multivariate curve resolution
MVS	Multivariate statistics
PC	Principal component
PCA	Principal component analysis
PI	Primary ion
PTFE	Polytetrafluoroethylene $(CF_2CF_2)_n$
PVF	Polyvinyl fluoride $(CH_2CHF)_n$
QMS	Quadrupole mass spectrometry
RF	Radio frequency
SEM	Scanning electron microscopy
SI	Secondary ion
SIMS	Secondary ion mass spectrometry
ToF	Time-of-flight
ToF–SIMS	Time-of-flight secondary ion mass spectrometry
UHV	Ultra-high vacuum
UV	Ultraviolet
VLEO	Very low Earth orbit
XPS	X-ray photoelectron spectroscopy

Table of Contents

1. Introduction

"*Scientiae enim naturalis non est simpliciter narrata accipere, sed in rebus naturalibus inquirere causas.*"
"*For natural science must not simply accept what is said, but must seek the causes in nature itself.*"
- Albertus Magnus[1]

Space, and the low Earth orbit (LEO) in particular are of significant interest for societies around the planet. The worldwide number of launches into space is increasing year by year, with the most common destination being the LEO, the orbit between 200 and 2000 km above Earth's surface (Figure 1).[2][3] Commercial telecommunication satellites dominate the number of spacecrafts in the LEO, with scientifically and militarily used objects making up the remainder. Prominent examples of LEO spacecraft include the Hubble Space Telescope[4], the FIRMS wildfire detection satellites[5], and the International Space Station.[6] While the close distance to Earth makes the LEO well suited for the aforementioned applications, the environmental conditions inside this orbit are unique and harsh: Up to an altitude of ~650 km, the most abundant species of gas in the LEO is atomic oxygen (AO).[7] This gas is highly reactive, leading to constant chemical material degradation during spaceflight. Understanding and reducing the effects of this degradation is crucial for successful LEO missions.[8]

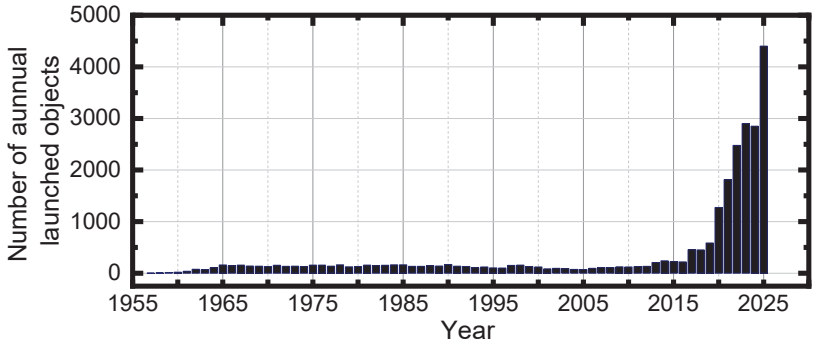

Figure 1: Annual launched objects into space. A rapidly increasing trend is visible from the late 2010s onward. In the years 2022-2025, more objects have been launched than up to 2022. Data obtained from UNOOSA[3].

In order to prevent, or at least delay, catastrophic material failure, the outside of LEO spacecraft is often made up of material resistant to AO.[9] At the same time, other important physical and mechanical properties need to be considered: High density is associated with great monetary cost, especially during the launch.[10] Stability to other LEO conditions, such as UV radiation, extreme temperatures and the impact of micrometeoroids are crucial in this environment.[11][12] Of course, the material still needs the properties to fulfil its intended purpose. Polymers typically have a low density and can be tailored to specific needs. Fluoropolymers in particular are of great interest for application in the LEO, as they typically have lower reactivities towards AO than the respective unfluorinated polymers.[13] They are often employed for their thermal and electrical insulating properties, e.g. as wiring insulation on the outside of spacecraft, where they are exposed to the LEO environment, including AO.

Although space flight experiments are conducted to investigate the effect of LEO conditions on spacecraft materials, these kinds of experiments carry a high cost in time, money and planning. The more common approach for such degradation studies therefore utilizes laboratory facilities on Earth's surface to conduct simulation experiments. Oxygen plasmas are typically employed in this manner to generate AO, to which a sample is then exposed.[14] Although not accounting for synergistic degradation effects from different sources, these types of experiments provide a decent knowledge basis that can be expanded upon with more complex experimental setups, up to the aforementioned space flights.[15]

The most important concern regarding LEO induced degradation is material failure. Therefore, the effect of AO exposure on physical and mechanical properties, such as the Young's modulus or volume shrinkage of spacecraft materials is commonly studied.[16] This symptomatic approach is well suited to determine the best material for a given task, but can fall short on understanding the degradation process, which is, especially in the case of AO, primarily chemical. Surface science can bridge this knowledge gap and elucidate the causes for material failure by monitoring the chemical structure of the material layers in contact with AO, as well as potentially with other environmental factors.

In this doctoral thesis, the degradation mechanisms of fluoropolymers under atomic oxygen are investigated. The overall aim is to better understand the mechanisms of degradation and the impact of fluorine in the polymer on the reactivity towards AO. Furthermore, the combination of time-of-flight secondary ion mass spectrometry (ToF–SIMS) and X-ray Photoelectron Spectroscopy (XPS) is showcased as a powerful tool to study spacecraft material decay.

In the first publication of this thesis, entitled: Publication *1: "Long-term degradation study of Polytetrafluoroethylene in a low* temperature oxygen plasma", the degradation mechanism of polytetrafluoroethylene (PTFE) under AO is investigated. Surface science methodology is applied to samples of this fluoropolymer exposed to an oxygen plasma for varying durations. Further analytical methods are tested with varying degrees of suitability for the sample system at hand. Degradation products and changes in the chemical surface composition and plasma atmosphere during exposure to the plasma are identified. Evidence for scission of the polymer chain during the exposure to AO is presented. The value of Multivariate Statistical (MVS) methods for data processing is showcased, establishing a set of analytical and mathematical procedures for further investigations.

In the second publication of this thesis, entitled: Publication *2: "Investigation of the polyvinyl fluoride degradation mechanism under* atomic oxygen exposure", the degradation of polyvinyl fluoride (PVF) in an oxygen plasma is studied. The established methods from the first publication are adapted to the requirements of this sample system and successfully employed. Again, degradation products are observed and changes in the composition are noted. The lower degree of fluorination in this polymer compared to PTFE is presented as the cause for higher reactivity towards AO. Furthermore, X-ray damage to the sample during XPS measurements is observed and, with the assistance of PCA, partially unraveled. Importantly, the F1s signal is established as the best reference signal for calibration despite it being affected by X-ray damage.

Overall, the results expand the understanding about the reaction between AO and fluoropolymers and can help to develop new and improve old materials for use in space. Analytical and statistical methods not yet commonly used to study the effects of LEO-like conditions on materials are proven to be well suited for this field of research and able to provide new insights into the mechanisms at play. For these methods, possible limitations are described as well, yielding a framework complementary to prior knowledge for application in further studies.

2. Fundamentals

2.1. Degradation of Spacecraft Materials

"Quid autem caelo pulchrius, nempe quod continet pulcra omnia?"

"*But what indeed is more beautiful than the skies, which of course contain all things of beauty?*"

- Nicolaus Copernicus[17]

In the following pages, the conditions in the low Earth orbit (LEO), as well as human use of the LEO are explained. The second part of this chapter contains an overview of the current understanding of degradation materials undergo while inside the LEO.

2.1.1. The Low Earth Orbit

Many aspects of modern life, from commercial to research and defense, are heavily dependent on human use of the LEO, located between 200 – 2000 km above sea level. The number of annually launched objects into space, the majority of which are intended to remain in the LEO, has increased twentyfold from 221 in 2016 to 4400 in 2025, marking a clear trend for the foreseeable future.[3] The attractiveness of the LEO stems in part from the small distance to Earth, which does not only equate to lower launching costs than for orbits further away, but is also necessary to obtain images of the Earth's surface with a high resolution. For telecommunications, the lower latency achieved by the use of satellites closer to Earth, is crucial. The parts of the LEO closest to Earth, below 450 km, are often to referred as the very low Earth orbit (VLEO).[18] There, the aforementioned advantages of the LEO over further distant orbits are even more pronounced. Heliosynchronous orbits, i.e. orbits, in which a satellite passes over a given spot on Earth at the same solar time each cycle, are restricted to narrow heights, many of which can be found in the LEO region.

For most use cases of the LEO, there is no viable alternative. Therefore, satellites traversing it need to be equipped to handle the environmental conditions inside it. These are extremely harsh and unique: Located outside of Earth's protective atmosphere, the LEO is exposed to the entire solar spectrum, including high energy UV radiation. At wavelengths below 242 nm, these photons carry enough energy to photodissociate the 5.12 eV diatomic bond of O_2.[19] The resulting atomic oxygen (AO) atoms are unlikely to recombine, due to the pressure in the 10^{-10} mbar range. Below ~650 km, AO is the dominant species of gas, especially so in the VLEO.[20] Although the low pressure would suggest that collisions between AO and a spacecraft's outer layer are rare, the spacecraft needs to maintain a velocity of >7 km/s to travel on stable orbital path. As a result, the spacecraft is exposed to an AO flux of ~10^{14} - 10^{15} atoms $\cdot$ cm^{-2} $\cdot$ s^{-1}. This value, of course, is dependent on multiple further factors, such as the angle of the material relative to the flight path or the position of the spacecraft relative to sun and Earth. Upon contact with AO, many materials undergo chemical degradation, as AO is highly reactive. The yellowish glow around the silhouette of a spacecraft, first reported on the space shuttle, is emitted from excited products of this reaction.[21][22] While the chemical etching of spacecraft materials by AO is unique to the LEO, it is not the only degradation path occurring in this region of space.

The UV-radiation causing the atomization of O_2 has degrading effects on many other chemical bonds, especially in organic polymers. Solar flares cause temporarily increased radiation fluxes along the electromagnetic spectrum, from X-rays to radio waves. The former carry enough energy to ionize atoms, which leads to the deterioration of materials. Another effect of the exposure to the sun's radiation is thermal cycling. Depending on the position relative to the sun, a satellites outer material can reach temperatures between −100 to 100 °C.[23] As a spacecraft in the LEO needs to maintain a velocity to travel around the Earth in 80-120 minutes, the exposure to the sun and temperature is consequently changing several times a day. In 1997, less than seven years after the launch of the Hubble Space Telescope, thermal cycling caused significant damage to the telescopes thermal blanket

Cosmic rays, i.e. charged subatomic particles with a kinetic energy far beyond the MeV range, are mostly deflected by Earths magnetosphere at a height of ~60.000 km.[24] A notable exception occurs above the southern atlantic, in the appropriately named south atlantic anomaly, where the Earth's magnetic field is weaker and high fluxes of cosmic rays can be observed even the lower parts of the LEO. Lastly, impacts of meteoroids, as well as of manmade debris can damage spacecraft materials. Small particles on the µm scale, which make up the vast majority of naturally occurring space debris, can remain on the surface of the spacecraft, comparable to dust. This can then lead to a loss of function, even if the contaminated material is otherwise undamaged. Collisions with larger objects can leading to macroscopic physical damage. With the unprecedented number of yearly launches into space, the probability of a collision between two satellites is rising. Previous collisions, such as in 2009, have led to large debris clouds that can remain on the orbital path of the satellite for long time periods.[25] In the worst case, a collision with a large object can lead to the Kessler syndrome, i.e. the cascade of further collisions, that makes an orbit completely unusable for mankind for many decades.[26] The real threat posed by the Kessler syndrome is underscored by the strategy of military planners to not kinetically destroy adversary satellites, but rather to disable their communication and systems[27]. To avoid incidents leading to the Kessler syndrome, it is therefore crucial to reduce the risk of a spacecraft becoming unmaneuverable, e.g. by material failure.

While each of these conditions can be extremely destructive to materials by itself, material degradation in the LEO shows synergistic effects between different environmental factors, making an accurate simulation of the LEO extremely challenging. Nonetheless, understanding each degradation by itself is necessary to obtain a more holistic picture.

2.1.2. Materials and their Degradation in the LEO

During a flight in the LEO, many parts of a spacecraft are exposed to the environmental conditions. From the paint on the outside of the spacecraft itself, to the glass lenses of a telescope or the protective heat shield, as well as electrical insulation and lubricants, a vast array of materials need to withstand LEO conditions.[28][29] Each of these materials needs to have properties that make it suitable for its task regardless of the environment. Another important requirement for space applications is a low weight. As the launch from Earth into space is associated with high costs, up to 35000 $/kg, reducing the necessary mass has a high priority in space material design.[30]

Metals are used for a variety of different applications in space. Lightweight metals, such as aluminum, serve to support the structure of a spacecraft, while a high conductivity is employed in the generation and transfer of electrical energy. Silver is used in solar cells on the outside of a spacecraft, where it can be exposed to AO. Instead of the mass loss, that is typically observed for organic materials, metallic samples can experience mass gain upon AO exposure, due to the formation of an oxide layer at the surface. This can be as, if not more detrimental to the applicability of the material than erosion would be, as the surface loses its metallic properties upon oxidation. Organic materials, on the other hand, form volatile oxidated species, which lays bare a new layer of the material, which ideally retains many properties of the original surface.[28][29]

To quantify the erosion of a material M in contact with AO, the erosion yield E_M is typically used. This property is defined by the volume lost per AO impact and lies in the 10^{-24} cm³/atom range for many polymers. At a LEO fluence of 10^{15} atoms/cm²·s, this translates to the ablation of 10^{-9} cm/s, or 0.1 Å/s. Over the course of a year, ~10 µm are removed at this rate. Despite the relatively high erosion of organic materials, polymers are often used in the LEO environment, not least because of their low weight.[31] A prominent example is the polyimide Kapton, which is used as a solar array blanket on the International Space Station.[32] To reduce the impact of AO degradation, polymers are often employed as part of a composite material. In the example above, a coating of aluminum is used. Other coatings, such as silicon are also considered.[33] Instead of applying a coating to the polymer, a more resilient approach utilizes nanoparticles inside the polymer matrix. Once the organic material is degraded and a nanoparticle is uncovered, it protects the underlying material from further AO induced erosion.[34] A great advantage of this technique is the resistance towards other LEO conditions: Debris impact can destroy a coating, rendering the underlying material completely unprotected, whereas the destruction of the *in-situ* composite coating will lead to the formation of a new protective layer from the particles below.[35] As the thermal expansion coefficient of an AO resistant coating and the protected polymer are always slightly different, the extreme temperature changes will inevitably lead to the formation of cracks, which again limit the effectiveness of the coating. As thermal cycling can also lead to cracks in an uncoated polymer, modern composites can prevent catastrophic failure: So-called *self-healing* composites include microcapsules filled with a healing agent, which will empty upon being reached by a crack. Catalyst particles embedded in the matrix will then accelerate the polymerization of the agent and the recovery of the original surface.[36][37][38] By choosing a polymer matrix that is inherently more resistant towards AO, the degradation can be slowed down even further.

Among the more resistant are the aforementioned Kapton, as well as fluorinated polymers.[39] Because the erosion yield E_{Kapton} (= $3.0 \cdot 10^{-24}$ cm³/atom) of Kapton is well studied, its observed mass loss is often used to calculate the AO fluence in a given system.[40] Fluoropolymers exhibit even lower erosion yields ($E_{PTFE} < 0.05 \cdot 10^{-24}$ cm³/atom), but are typically more susceptible to damage by UV radiation. This effect is less pronounced with a lower the degree of fluorination.[11] The two fluoropolymers that were studied in this thesis are polytetrafluoroethylene (PTFE) and polyvinyl fluoride (PVF).

Both consist of a carbon chain with four substituents for every two carbon atoms. In the case of PTFE, all substituents are fluorine, whereas for PVF only one is. The remaining three spots in PVF are hydrogenated. PTFE is typically used as a wiring insulator or as a thermal shield, where it is exposed to the harsh LEO environment.[41] PVF on the other hand is currently not used on the outside of LEO spacecrafts but its suitability has been tested in space flight experiments.[42] This polymer is of particular interest, as it has a higher resistance towards UV than PTFE and serves as a comparable material due to its similar molecular structure. In many publications and reports, PVF is referred to by its brand name *Tedlar*, which can be distinguished further into clear Tedlar (pure PVF) and the far more AO resistant composite white Tedlar (TiO_2/PVF). As the scientific question for this dissertation regards the chemical degradation of fluoropolymers under AO, no composite materials were investigated.

Most studies in literature concerned with the degradation of fluoropolymers in the LEO are undertaken not from the perspective of a chemist, but rather that of a material engineer. The decay of material properties is therefore much more prevalent than the change in surface chemistry.[43][44] Nonetheless, some publications do utilize surface science characterization methods to help investigate LEO environmental impacts on polymer samples.[45][46] Exposure to UV light is known to reduce tensile strength of PTFE, which is linked to chain scission.[47] Zhao et al. found that UV irradiation did not lead to mass loss, but did significantly alter the optical properties and the lead to defluorination, which was studied by XPS.[48] Synergistic degradation effects between UV and AO were observed by Zhao et al., as well as earlier research.[49] Similar experiments found an increase in the solar absorbance of PVF after UV exposure.[50] As no mass loss was reported for PVF in contrast to more fluorinated polymers, cross-linking of the CH bonds was proposed.[2] Similar to ultraviolet photons, X-ray photons also lead to degradation of fluoropolymers.[51] This effect is observable in the second publication of this work, where the PVF sample was significantly altered during the XPS measurements.[52]

By utilizing SEM and XPS, Morra et al. found changes in the surface morphology of PTFE after exposure to an oxygen plasma.[53] It should be noted here that this study was not motivated by the use of PTFE for space applications and is therefore harder to interpret, as no dose of AO was calculated. The researchers observed defluorination within the first minutes of plasma exposure, coinciding with an increase of oxygen content. After five minutes, this trend was reversed, leading to a surface composition similar to that of untreated PTFE, although the surface morphology had changed significantly. SIMS measurements were also conducted but peaks were not assigned to specific ions but rather C_X regions and not interpreted in more detail. This study stands out due to the short plasma exposure and the unusual finding of a chemically pristine PTFE surface after AO exposure. The aforementioned study by Zhao et al. observed an increase in the F/C ratio from 1.26 to 1.48 in XPS measurements, while oxygen content also slightly increased after exposure to AO in the 10^{20} atoms/cm² range.[48] In both studies, XPS was used to determine the elemental composition of the sample surface, without further unraveling any detail spectra.

Gonzales et al. did observe decreasing signal intensities for CXF (X=H,F) C1s signals after *in situ* exposure to AO.[54] However, as no reference samples (exposure to non AO conditions) were measured in that study, the possibility of that change being at least partially the result of X-ray damage cannot be completely excluded. At the same time, a slight shift in the binding energy of the F1s signal was visible for PTFE, but not PVF after oxygen exposure. The authors conclude that AO preferably reacts with the fluorinated carbon atom, a claim that is not undisputed and must be viewed with the possibility of X-ray damage in mind.

Defluorination for PVF and PTFE in XPS after exposure to AO, was observed by Hoflund et al.[55], who did not reach the same conclusion as Gonzales et at.[54] Instead, they propose a favored reaction between the oxygen and hydrogenated carbon in the polymer.[55] In this paper, very little chemisorption of oxygen was observed, indicating that carbon-carbon bonds are formed at the surface of the polymers. As the XP spectra of all polymers were calibrated on both C1s and F1s of PTFE, slight changes (±0.5 eV) in the binding energy of the F1s signal were observed throughout the measurements. Similarly, Vandencasteele et al. could detect a change in the fluorine content of PTFE from 66% to 36% after 1200 s of oxygen plasma exposure.[56] As the paper was written and the experiments were designed with a different motivation, it is not trivial to translate these results to LEO exposure experiments. Extreme changes as reported by Vandencasteele et al. in the chemical composition were not observed on samples exposed to real LEO conditions for 40 h, where PTFE showed no significant change at all and PVF experienced a loss of fluorine from 32.7% to 26%.[57] Theoretical computations by Gindulytè et al. yielded activation barriers for the chain breaking reaction of AO with a fluoropolymer and an alkane of 67 and 36 kcal/mol respectively, whereas the kinetic energy of LEO AO would be in the 100 kcal/mol range.[58][59] The scission of the polymer chain is therefore a possible and plausible mechanism to explain the chemical degradation of fluoropolymers in the LEO.

As spaceflights for research purposes are expensive and have limited payload capacity, all of the studies cited earlier in this section used ground-based facilities to simulate LEO conditions in a more cost-effective manner. These setups can range from relatively simple vacuum reactors to dedicated machines built to simulate multiple environmental impacts at the same time.[60][61][62] Due to AO being uniquely tied to the LEO, many simulation studies ignore these other factors. Radio frequency (RF) operated plasma reactors are the most common system to generate AO due to their affordability.[15] Major differences between such generated atomic oxygen and the one found in space include a lesser kinetic energy relative to the sample, as well as much higher densities. The latter point must not solely be understood as a detrimental inaccuracy, as it allows for ground-based setups to simulate months and years of LEO flights in mere hours to days. UV radiation may also be emitted during the generation of AO, which is typically not quantified, making an easy comparison between simulation experiments nontrivial.[15]

2.2. Methods

"Wissen und Erkennen sind die Freude und die Berechtigung der Menschheit […]."
„Knowledge and understanding are the joy and justification of humanity […]"
- Alexander von Humboldt[63]

This chapter contains introductions into the methods used in this work. Attention is given to capacitively generated low temperature oxygen plasmas, which were used in this work to partially simulate LEO conditions, as well as ToF–SIMS and XPS, two important characterization techniques used in surface science. While many other methods were used as well in the experimental research for this doctoral thesis, these two methods delivered the deepest insight into the degradation mechanisms, especially in combination with MVS methods (Chapter 2.3).

2.2.1. Plasma Discharges

When Crookes characterized gas discharges in 1879[64], only three states of matter, solid, liquid and gaseous, were known to science. This newly discovered fourth state of matter consisting of ionized gases remained unnamed until Langmuir proposed the name *plasma* in 1928.[65] Although the gas discharge phenomenon had been described before[66][67] and naturally occurring plasmas, such as flames, lightning or the northern lights (*aurora borealis*), have been observed by humanity since ages past, Crookes was the first to recognize plasma as the fourth state of matter.[64][68]

Many modern industrial and scientific processes utilize plasmas due to high energy densities that can be achieved at low cost.[68][69][70] At the same time, plasmas can contain high concentrations of chemically active species, making them ideally suited for surface modifications. Another important application for plasmas lies in ion thrusters used to propel spacecraft.[71][72]

Although plasmas consist of neutral as well as charged gas particles, overall they are quasi-neutral, i.e. the number of free electrons and negatively charged particles is roughly equal to the number of positively charged particles per volume.[70] In conventional laboratory plasmas, the degree of ionization is between 10^{-7} and 10^{-4}. Complete ionization is possible, but energy consuming and used less frequently.[68][73] If the thermal energy of electrons and ions is in equilibrium, e.g. in solar winds, the plasma is referred to as a thermal plasma.[70][74] Such a thermal equilibrium is, however, not necessarily the case in plasmas. In a non-thermal plasma, electrons exhibit a far higher temperature, often several eV or 10,000s K higher, than the remaining particles, which may even remain at room temperature.[75] Due to their high temperature, electrons will move faster and thus be lost faster from the plasma to the walls, charging the walls negatively. This generates a potential difference to the positively charged plasma volume, decelerating further electrons near the border of the plasma in the so-called *plasma sheath*.[70][76]

A common method to ignite a non-thermal plasma is by exposing a low-pressure gas to a radio frequency (RF) driven electromagnetic field. Once the gas is exposed to such a setup, free electrons in the gas, which are naturally generated by ionizing background radiation, are accelerated by the alternating potential. Neutral particles and ions, having higher masses than electrons, remain largely unaffected by the high frequency field due to inertia.[77] Collisions between the excited electrons and other gas particles then leads to secondary electron emission, which results in a cascade of collisions, gaseous ions and thus, plasma. In a capacitively coupled plasma (CCP) , such as the setup used in the work for this dissertation, two electrodes are placed in parallel, similar to a capacitor.[70][75] This setup was first used in 1893 and typically generates a less ionized plasma than inductively coupled plasma (ICP) setups, where a coil is used to excite electrons.[70][78] If the electrodes' geometries differ from one another, a self-induced DC-bias can form between the electrodes due to the different number of electrons lost to each electrode.[75] In this work, this bias was controlled to 150 V to prevent positively charged ions from impacting the sample on the grounded electrode.

The bias value was chosen with the goal of keeping the plasma power low, to maintain a small degree of ionization, and simultaneously stable. Naturally, this bias accelerated positively charged ions towards the driven electrode, potentially causing damage there. Although larger biases are often generated in similar setups to sputter a target on the driven electrode, significant sputter effects were not observed in this work.[79][80] At the same time, this bias accelerates electrons towards the sample, which is not ideal but was preferred over possible reactions with positively charged oxygen species.

The process of applying plasma to degrade a sample is usually called *plasma etching*.[75] The most important use for plasma etching currently lies in the fabrication of silicon circuits.[81][82] In which fluorine containing compounds are typically used for the plasma.[81] Other gases, such as argon can be used to remove contaminants from surfaces.[83] By reacting to form volatile species that are then ablated from the surface, oxygen plasmas provide great utility in cleaning surfaces from organic contaminants.[83] While this concept is similar to the application of oxygen plasma in this work, the goal here was not the efficient removal of organic material but understanding the process behind such unintended "surface cleaning" processes in the LEO. By approaching the reaction of plasma generated oxygen species with samples from yet another perspective, the topic of *plasma surface modification* comes up.[84] In this area of research, scientists employ plasmas to modify surface properties of materials, including polymers.

Oxygen plasmas consist of electrons, neutral, as well as positively and few negatively charged particles.[85] The degree of ionization depends on geometry, pressure and many further parameters.[86][87] In a different CCP setup, Kitajima et al. found the concentration of AO in the center of the plasma to differ with the radio frequency used to generate the plasma.[88] The concentration of AO then decays exponentially from the center towards the electrode due to diffusion.[88] At pressures used in sample preparation for this doctoral thesis (10 Pa), the main contributors to AO loss are not collisions within the plasma, but rather with walls.[87] In yet another setup, Tesrepi et al. found the concentration of AO to be in the low 10^{14} cm^{-3} range, corresponding to not more than 2.5%.[89] These values were in agreement with prior studies.[90][91]

Negatively charged oxygen species present a dilemma for this work. Due to the high electronegativity of oxygen, negative species are more likely to form than for other plasma gases. Because of the applied bias, these species are then driven towards the sample, creating unintended reaction pathways. Lichtenberg et al. found that lowering the pressure, as well as increasing the plasma power reduces the amount of negatively charged oxygen particles.[85] The plasma parameters used in this work (publication 1[92], 2[52]) were a compromise between a stable, and reproducible plasma and the detrimental impact of negatively charged oxygen ions.

2.2.2. Time-of-Flight Secondary Ion Mass Spectrometry

Identifying the chemical compounds at the surface of a given sample is crucial in many scientific applications.[93] Time-of-Flight Secondary Ion Mass Spectrometry (ToF–SIMS) is a common and powerful characterization technique in surface science.[94] During a measurement, primary ions (PI), often bismuth or argon clusters, are accelerated towards the sample surface.[95] During this bombardment, energy is transferred from the PIs to the surface, causing electrons, atoms, molecules and ions leave the surface. Ions generated this way are referred to as secondary ions (SI). It is important to note that SIs are not directly representative of the chemical structure of the sample surface, as they are the product of PI induced degradation of the sample, which includes chemical fragmentation. Additionally, the probability of ionization, which is necessary for the detection of the fragment, depends on the chemical surrounding of the particle from which the SI is generated. This is known as the *matrix effect*. Despite being only semi-quantitative, SIMS is of great use due to its low detection limit in the ppb range, down to 10^{12} atoms·cm^{-3}.[96] As only particles from the first nanometers of the surface get emitted, SIMS is extremely surface sensitive, marking another advantage over many other characterization techniques. By increasing the PI current, the surface sensitivity decreases as more material is destroyed during PI impact. This relation can be used to create depth profiles.[94][95]

The ToF detector works by accelerating the generated SIs in an electric field towards the detector. As the flight time depends on the mass to charge ratio m/z, the latter can be calculated by measuring the former. In contrast to other analyzers, such as orbitrap, ToF analyzers combine a high mass resolution with no lower limit on detectable masses. Mass resolution refers to the ability of an analyzer to separate two mass signals. In ToF–SIMS, mass resolution is typically in the 10^4 regime, i.e. it is possible to separate two signals that differ from one another by 0.01% of their m/z ratio. Even higher mass resolutions (10^5) are possible to achieve by utilizing multiple ion reflectors.[94][95][97]

Another common analyzer that has been used in SIMS and is still being employed in other MS applications is the quadrupole.[94][98] Four rods, hence the name, are oriented in parallel on the corners of a hypothetical square. By applying both a DC, and an RF electric field to these rods, only ions of a specific m/z ratio are kept on a stable path between the rods. By varying the frequency, the stable m/z ratio can be controlled. This analyzer works with relatively simple detectors, as only one m/z signal needs to be detected at a time, reducing the monetary cost. Due to the low mass accuracy obtainable with such an analyzer, it was phased out of use in SIMS in favor of more expensive, but more accurate detectors.[95] For this doctoral thesis, a quadrupole-MS was used to monitor the composition of the atmosphere inside the plasma chamber during exposure experiments.

2.2.3. X-ray Photoelectron Spectroscopy

Whereas SIMS is a destructive characterization method that derives information from ionic fragments, X-ray Photoelectron Spectroscopy (XPS) is a nondestructive technique that observes electrons. By irradiating a sample with X-rays, energy is transferred from the photons to electrons inside the material, causing some to leave the sample. The discovery of this *photoelectric effect* was the reason Einstein was awarded the Nobel Prize in 1921.[94][99][51][100] During an XPS measurement, monochromatic X-rays, i.e. photons with a defined wavelength and thus energy, are used to excite electrons, whose kinetic energy is then measured by detecting them on a multi-channel detector plate after passing through an analyzer, typically a hemispherical energy analyzer. The kinetic energy can then be translated back to the binding energy of the electron by the Einstein equation:[94]

$$E_{\mathrm{Binding}} = h\nu - E_{\mathrm{Kinetic}} - \Phi_{\mathrm{Spectrometer}} \qquad \textbf{(Eq. 1)}$$

Where E refers to the respective energy, h to the Planck constant, ν to the frequency of the X-ray and Φ to the work function of the spectrometer, i.e. the energy required to promote an electron to vacuum level. The binding energy (BE) contains information about the element and orbital, the electron was excited from, as well as the chemical state of that atom. The C1s electron of adventitious carbon, which is found on many samples and is usually used for calibration, has a BE of 284.8 eV. While in polymer science, the C1s value is commonly set to 285.0 eV, this work uses the 284.8 eV value.[101] If the carbon atom is bonded to a more electronegative atom, such as fluorine, a higher binding energy is observed.

The empty orbital resulting from X-ray irradiation can be filled by an electron of a higher orbital in the same atom. During this process, a photon is emitted that has an energy level equal to the energy difference between the two orbitals. If this energy level is high enough, it can be transferred to another electron that is then emitted. Such an electron is called an auger electron and its kinetic energy depends solely on the orbitals involved. As a typical XP spectrum uses the BE for the abscissa, Auger electrons are assigned a hypothetical BE value as well according to Eq. 1 that is dependent on the X-ray source used in the instrument.[94] By using relative sensitivity factors, XPS can be used as a quantitative analytical method. The detection limit, typically in the 0.1–1% range, and the surface sensitivity are slightly worse than in SIMS, as only electrons from the first ~10 nm can be detected.[94] Higher surface sensitivity can be achieved by lowering the angle between X-ray and sample.[102] The combination of XPS and (ToF–)SIMS is often employed in surface science, as these methods work complementary to another.[94]

2.3. Multivariate Statistical Analysis

"*Many other artes also there are which beautifie the minde of man: but of all other none do more garnishe & beautifie it, then those artes which are called Mathematicall.*"

- John Dee[103]

This section is intended to give the reader a basic understanding of the multivariate statistical (MVS) methods that were employed in the framework of this dissertation. While these methods are well established in many scientific communities, they are not used to their full potential in the field of surface science.

2.3.1. Principal Component Analysis

A fundamental challenge in science is the handling of large amounts of data. While most datapoints in a measurement will be useful to answer one or more scientific questions, they do not necessarily contain information that is relevant to the specific question they were gathered to answer. Manually checking each datapoint and trying to figure out if relevant information can be obtained by evaluating it further might have been cumbersome but possible in previous centuries, with the advent of digital data and automatic data collection and storage, this process would be a Sisyphean task today. A simple approach to handle this hurdle lies in establishing signpost datapoints, such as specific mass signals in a mass spectrum, that have proven useful to answer similar questions in the past. By focusing on these few points, data can be quickly and easily interpreted. At the same time, there is a huge risk that blindly omitting data outside of these subsets can easily lead to a false or simplified answer to the scientific question.

Principal Component Analysis (PCA) is a method that reorders data by statistical relevance and can therefore be used to quickly gain a better understanding of the data at hand.[104] While explaining the algorithm behind PCA in detail would go far beyond the scope of this chapter, a simplified overview is given below: During a measurement, n features are recorded. These features can be any property, as long as it can be represented numerically, such as a height, a flow rate or the signal intensity for a given detector channel.[105] If the same n features are measured l times, e.g. for l different samples, a n-dimensional plot with l datapoints can be created, where each feature is used as an axis. During PCA, the data is first centered around the origin, followed by a rotation of this n-dimensional coordinate system.[106] The rotated first axis, now called Principal Component 1 (PC1), is the best linear fit through the datapoints and therefore oriented along the largest variance. The second axis is orthogonal to the first and oriented along the largest remaining variance. The following axes are constructed the same way, resulting in a new coordinate system where all axes remain uncorrelated and are, in addition, ranked by variance. Therefore, it becomes possible to display a large portion of the dataset's variance with just the first two or three PCs, which translates well to the two-dimensional reality of a sheet of paper. The axis rotation just described can also be understood as a linear combination of the initial features. The multiplicator for a feature in a PC is called the loading of that feature in that PC. Loadings can have positive or negative values. A larger absolute loading value indicates that the feature is more relevant to the composition of the PC. The sign carries no meaning if observed in a vacuum, as the orientation of the rotated axes is arbitrary. If two features share a sign, they are positively correlated.

If not, there is a negative correlation between them. The coordinates of the initial measurements in the PC coordinate system are called scores. Like loadings, scores can have negative or positive values, and a similar score between two measurements along a single PC indicates a similarity along this PC. Loadings and scores can't be understood on their own but only in combination with another.

For PCA to be reasonably applicable to a dataset, some constraints must be observed: While PCA is a great tool to extract linear trends from a dataset, it is not suited to handle other relations such as quadratic or inverse. If, for example, a group of approximately circular structures of varying size is studied, PCA will be unable to show a direct correlation between diameter and area. On the other hand, diameter and circumference will be correctly identified as correlated. It is therefore best to screen a dataset and exclude data if a nonlinear relation can be observed before the PCA is applied.

Another issue is a difference in the numerical size of features: If e.g. pressure (Pa) and the number or particles per volume (#/cm³) in different gas samples were studied using PCA without proper preparation, the resulting loadings would imply that pressure is completely insignificant, as the number of particles will always be larger by many orders of magnitude. To obtain a more valuable result, both features would have to be normalized. Such a normalization can however create new issues, as it may overcorrect noise and reduce the variance explained by the first PCs. Choosing the right features to include and deciding if normalization needs to be conducted is therefore crucial.

2.3.2. Multivariate Curve Resolution

While the method behind PCA was envisioned by Pearson in 1901 with "physical, statistical and biological investigations"[107] in mind, the interpretation of negative loadings or scores can often be nontrivial. Multivariate Curve Resolution (MCR) was designed specifically with constraints leading to results that resemble actual measurement data more closely and can thus be interpreted easier. In particular, MCR was created to tackle the so-called mixture analysis problem, where the individual contributions of components in a mixture are to be identified. The first algorithms by Lawton and Sylvestre in 1971 were only able to determine two components.[108] In 1985, Borgen et al. solved a three component model, followed by a general multicomponent model in 1986.[109][110]

Mathematically speaking, the datamatrix **D** (m x n) is decomposed into the concentration profiles **C** (m x k) and the spectra matrix $\mathbf{S}^{\mathbf{T}}$ (k x n), where k represents the number of factors. The remaining variance is expressed by the error matrix **E** (m x n).[111][112]

$$D = CS^T + E \qquad \textbf{(Eq. 2)}$$

This showcases a key difference between PCA and MCR: While PCA can be conducted without additional knowledge about a dataset, MCR needs the number of components as additional input. Two MCRs applied to the same dataset with different numbers of components (or factors, as they are sometimes referred to in the context of MCR) will yield different results. Therefore, MCR is often preceded by a PCA to estimate the number of factors necessary to obtain a meaningful result.[113][114]

As a tool to overcome the mixture analysis problem, MCR results contain a concentration profile of the factors across all measurements (scores) and the calculated raw signal for each of the components (loadings). To achieve this, another important distinction between MCR and PCA is the inclusion of non-negativity, as a negative concentration is not chemically sensible.[115] Similarly, in spectroscopic measurements, which MCR was first envisioned to assist with, negative signal intensities cannot be obtained.[108] Thus, by preventing negative values, the resulting loadings closely resemble actual data and can be treated as such. The non-negativity constraint is true for many techniques in surface science as well, such as ToF–SIMS and XPS.

2.3.3. Use of Multivariate Statistical Methods in Surface Science

As early as the 1970s, serious efforts were undertaken to use computers for statistical calculations in the field of analytical chemistry under the newly coined term *chemometrics*.[116][117][118] Potential benefits of applying chemometrics to spectroscopic and mass spectrometric characterization techniques were immediately clear.[119] In 1986, the Journal *Chemometrics and Intelligent Laboratory Systems* was established, followed by the *Journal of Chemometrics* in 1987, showcasing the importance of the topic to the scientific community at that time.[120][121] In the past 40 years, over 300 combined volumes have been published in these two journals alone.

In (ToF–)SIMS, highly resolved mass spectra generate large amounts of data that are difficult to interpret on their own. This is further enhanced by the number of mass spectra generated during imaging or depth profiling. Although the matrix effect, i.e. the changing ionization probability depending on the chemical surrounding, prevents strict adherence to the linearity that is inherent to PCA and MCR, these tools still provide a lot of utility and can assist in better understanding the measured data.[94][122][123]

One of the first publications applying PCA to SIMS data was published in 1987 by Gaarenstroom.[124] Here, PCA was used to smooth the depth profile of Ho^+ on a Ho-doped PbTe wafer. Although the author concluded that PCA was even more useful on Auger spectra, the ability of PCA to remove interference of other mass signals was emphasized.[124]

More recently, Manaprasertsak et al. were able to investigate the changes in cancer cells that survived cisplatin treatment using ToF–SIMS imaging in combination with MVS methods in 2025.[125] The authors used PCA to separate untreated and surviving cells but found that it was not suited to further distinguish the cytoplasm from the rest of the cell. By applying MCR to the same dataset, they were not only able to fully distinguish the cytoplasm, but also gain meaningful insight into the mass signals that made up the surviving cancer cells.[125] Also in 2025, Seydoux et al. proposed a new denoising method for mass spectrometry imaging by using the Noise2Void algorithm on the score images obtained from PCA instead of the raw images.[126] The data preparation by PCA virtually improved the lateral resolution without changes to the experimental setup.[126]

Other methods in surface science, such as XPS and AES are even better suited for MVS, as the underlying principles align more closely with the linearity of MVS methods. In the 1980s, PCA was already used to improve data quality in AES depth profiling measurements and reduce the time required for a thorough analysis.[127][128] The time saved by applying PCA to XPS data, especially with large data sets or complex spectra, was also mentioned by Koenig et al. in 1986.[129]

Since the early 2000s, MCR is being used as well on XPS data to resolve spectra with overlapping signals, such as C1s spectra of polymer mixtures.[130][131] Moeini et al. showcased the benefits of combining XPS with MCR over PCA.[132] The authors cite the ease of interpretation and lack of need for data preprocessing. Instead of relying on PCA to estimate the number of necessary factors, Moeini et al. compared the results of MCR with 1-6 factors respectively based on their knowledge about the sample system and the resemblance to actual XPS data.[132]

In 2023, Fairley et al. used PCA to resolve the Fe2p spectrum of native iron oxides. Manual dissection of these spectra would require deeper knowledge about the distribution of said oxides on the sample.[133] The authors conclude that PCA is a great tool to resolve XP spectra of samples with carbonaceous contamination layers on transition metals.[133] Another application for PCA was shown in 2024 by Fernandez et al. in the form of data processing for XPS imaging.[134] The authors present the advantage of using PCA with data scaling in low signal-to-noise spectra of heterogenous samples to localize features that would remain hidden otherwise.[134]

Despite the great potential MVS methods evidently hold for the field of surface science for a variety of materials and scientific questions, they are still severely underutilized. At the time of writing, less than 2% of publications in the last 10 years in the field of XPS employ PCA and/or MCR (Table 1). Less than 10% of publications that mention SIMS also include one or both statistical methods. These numbers are also likely to be inflated as they may include publications that mention MVS methods in sections unrelated to surface characterization techniques. Additionally, publications referencing MCR often included PCA as well. The significant difference between MVS use in SIMS and XPS is unexplained, but the ready availability of said methods in common SIMS software, such as SurfaceLab, may play a role. At the same time, it is evident that MCR is ~4 times less frequently used than PCA. Again, the reason for this discrepancy is unclear, but familiarity with PCA is likely contributing to its preferred treatment. In this case, the niche constraints of MCR that make it very well suited for tasks in surface science may actually be a hindrance to its use. PCA, on the other hand, is far more widely known due to its broad applicability, lowering the barrier to use.

Table 1: Number of publications that mention MVS methods between 2015 and 2025 according to Google Scholar. Search terms were "secondary ion mass spectrometry" or "x-ray photoelectron spectroscopy", respectively. For MVS, the additional search terms included "principal component analysis" or "multivariate curve resolution", respectively.

	SIMS	***XPS***
Publications 2015-2025	36 900	267 000
Publications 2015-2025 incl. PCA	3 160	5 410
	8.56%	2.03%
Publications 2015-2025 incl. MCR	391	662
	1.06%	0.25%

2.3.4. Use of Multivariate Statistical Methods in this Dissertation

Usually, the results of a PCA are displayed in a scores biplot, where two PCs serve as ordinate and abscissa, respectively.[135][136] This is particularly useful when the measured samples are not directly related to another, such as different but similar materials that were investigated by ToF–SIMS. In such a case, the measurements can be grouped visually to show similarities and differences between groups of samples (Figure 2).

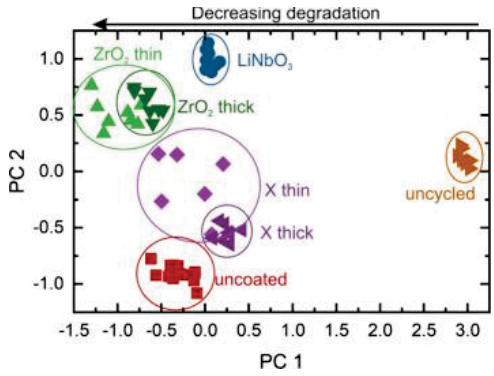

Figure 2: A typical PCA scores biplot by Hertle et al.[137] This type of plot is well chosen due to the variation in the investigated samples. Variance along PC1 corresponds to material degradation during cycling, whereas PC2 serves to distinguish different groups of samples from another.

Despite being the most common way to display PCA results, this dissertation did not utilize any biplots. This was done in a conscious matter, as the samples that were compared in each individual publication were all directly connected by a singular variable: The same material was exposed to the same plasma conditions for varying amounts of time. As a direct result, it is possible to display the different datapoints along the time axis (Figure 3).

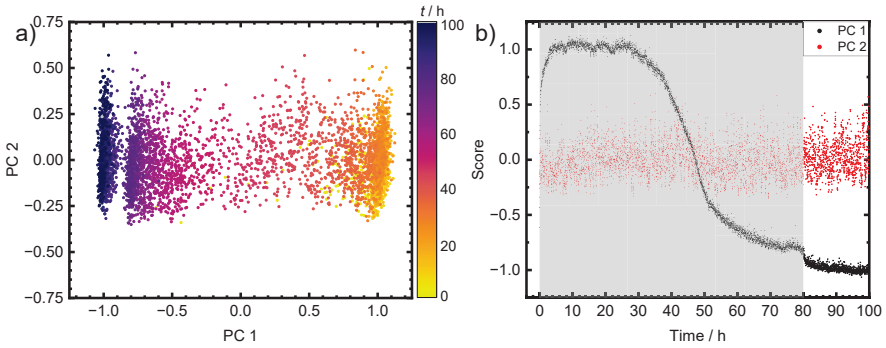

Figure 3: Two ways to display the same scores for two PCs. The dataset was taken from publication 2.[52] The classical biplot (a) would be a suboptimal choice here, as the plasma exposure time cannot directly be inferred for a given datapoint. The plot chosen for publication is more accessible due to the familiar abscissa.

The scores of PC1 and PC2 in (Figure 3b)[52] can be understood intuitively even by scientists unfamiliar with PCA to represent abstract signals that change throughout the experiment. It is immediately clear that PC1 is of interest, whereas PC2 is mostly noise. The loading plots (available in publication 2 and the corresponding SI)[52] then explain the makeup of the PCs by linear combination of mass signals, which, although nontrivial, is still relatively easy to understand for newcomers to PCA. The same cannot be reasonably said for the same data represented in a classical biplot (Figure 3a). Although the mass spectra can be clustered visually, it is far more difficult to correlate a data cluster to a more tangible concept. At the same time, the random nature of PC2 is not as directly obvious to the reader. Another important difference between the two plots is the ease of correlating a given measurement to the plasma exposure time. This is of key interest to the scientific question the investigation was launched to answer.

3. Results

At the beginning of the work for this doctoral thesis in 2019, the degradation of fluoropolymers under AO was already present in literature. Most of the work had been done in the past, especially during the early era of spaceflight. Studies were mostly concerned with the decay of material properties to the point of failure and the development of composites able to delay this. The chemical reactions involved were understood very broadly, but little effort had been made to obtain a more detailed understanding of it. Analytical methods that are commonly used in surface science, such as ToF–SIMS and XPS are completely absent or only rarely used, respectively. Measurements of the latter were mostly conducted to obtain the elemental composition of the sample, which does not exhaust the possible questions this method can be used to answer. Detail spectra were considered in some, but not all publications. The degradation of fluoropolymers under X-rays was well documented, but not well understood. Additionally, chemometric methods, although conceived during a period of increasing space flights, were not used to assist in obtaining a better understanding of the chemical degradation occurring in the LEO. The objectives of this work were therefore to obtain a better physical-chemical understanding of the processes between fluoropolymers and AO by finding and employing characterization methods from the surface science toolkit, as well as enhancing the quality of the obtained data by MVS methods.

In the first publication of this doctoral thesis, the reaction of the fluoropolymer PTFE with plasma generated AO was studied by SEM, ToF–SIMS and XPS. Additionally, the atmospheric composition inside the plasma chamber was monitored by operando QMS. Evaluation of the obtained mass spectra from SIMS and QMS was assisted by MVS methods and potential pitfalls for the application of these techniques were discussed. In the second publication of this doctoral thesis, the less fluorinated PVF and its reactivity towards AO were examined using the analytical techniques established in the first paper. The degradation of the polymer upon exposure to X-rays was also investigated with the help of PCA, in order to interpret the XPS data with more certainty.

3.1. Publication 1: “Long-term degradation study of Polytetrafluoroethylene in a low temperature oxygen plasma”

The first publication of this dissertation explores the degradation of polytetrafluoroethylene (PTFE) in a low temperature oxygen plasma. The samples were characterized by ToF–SIMS, XPS, SEM, and weighing. During the sample degradation in the plasma chamber a QMS monitored the composition of the plasma atmosphere.

By combining surface sensitive analysis techniques with QMS, the degradation mechanism could be studied in detail. Chain scission could be observed, as was defluorination. The application of PCA and MCR to the recorded mass and electron spectra was crucial to investigate the degradation in depth. ToF–SIMS depth profiles were also recorded but found not to be particularly useful to elucidate possible degradation beneath the surface due to the roughness of the sample.

The first author designed, planned and carried out and evaluated the experiments under the supervision of M. Rohnke and J. Janek. The manuscript was written by the first author and edited by the co-authors.

Reprinted with permission from T. Wagner, M. Rohnke, J. Janek, "Long-term degradation study of Polytetra-fluoroethylene in a low temperature oxygen plasma", *Polymer Degradation and Stability* **2024**, *229*, 110989; DOI 10.1016/j.polymdegradstab.2024.110989.

Polymer Degradation and Stability 229 (2024) 110989

Contents lists available at ScienceDirect

Polymer Degradation and Stability

journal homepage: www.journals.elsevier.com/polymer-degradation-and-stability

Long-term degradation study of Polytetrafluoroethylene in a low temperature oxygen plasma

Tobias Wagner, Marcus Rohnke *, Jürgen Janek *

Institute of Physical Chemistry and Center for Materials Research, Justus Liebig University Giessen, Heinrich-Buff-Ring 17, D 35392 Giessen, Germany

ARTICLE INFO

Keywords:
Low temperature oxygen plasma
Polymer degradation
Surface analysis
Degradation mechanism

ABSTRACT

Atomic oxygen (AO) is the most common gas species in the Low-Earth-Orbit (LEO) and responsible for material degradation of the outer shell of spacecrafts within this space region. Due to their similar properties, low temperature oxygen plasmas are suited for material degradation studies taking place on earth instead of quite expensive space studies. Here we focus on the long-term degradation of Polytetrafluoroethylene (PTFE), which is often employed on the outside of spacecrafts. Up to date, there is no complete understanding of the degradation process on molecular level, which is necessary for materials improvement and new materials development.

For the degradation studies, a self-constructed capacitively driven 13.56 MHz RF reactor was used to generate an oxygen plasma for the simulation of LEO conditions. PTFE was characterised in the pristine state and after AO treatment at different times by ToF-SIMS, XPS and SEM. During plasma treatment, the samples show a linear mass loss behaviour. ToF-SIMS surface analysis reveal mass fragments which show a clear chemical reaction of oxygen species with PTFE. The presence of these molecular indicators was verified by XPS, where additional carbon species were found after plasma treatment. SEM micrographs showed an inhomogeneous degradation on the surface in the first hours similar to actual LEO exposure. For a complete understanding of the degradation progress, operando mass spectrometric studies of the plasma composition were carried out to detect volatile degradation products.

In summary, a steady degradation has been observed that leads to constant mass loss, defluorination, chain shortening and insertion of oxygen into the polymer.

1. Introduction

The low-earth-orbit (LEO) plays a crucial role in modern space technology. Many satellites are operating within this region due to its proximity to the earth's surface. In contrast to other regions in space, the LEO has an atmosphere consisting mostly of atomic oxygen (AO), which is hazardous to most materials used in space applications. AO is mainly formed by solar UV photons below a wavelength of 243 nm breaking apart the molecular O_2 bond. Depending among other factors on the altitude and solar activity, a spacecraft traveling with a velocity of 8 $km \cdot s^{-1}$ is exposed to a flux of 10^{14}–10^{15} atoms of oxygen $cm^{-2} \cdot s^{-1}$ [1–3]. To simulate simplified LEO conditions, ground-based facilities are often used, utilizing oxygen plasmas to generate AO [4–7].

A material often used in space applications is polytetrafluoroethylene (PTFE), commonly known as Teflon [2,8]. Applications for PTFE in this context include space suits ("Beta cloth"), protective shields for satellites and rockets as well as wire insulation. Similar to many other polymers, it is a lightweight material, which is a crucial property [9]. Furthermore, PTFE has proven to be much more resistant to AO than most other materials, showing an erosion yield of $1.42 \cdot 10^{-25}$ $cm^3 \cdot atom^{-1}$, only [10]. The erosion yield is a material constant calculated from LEO flight experiments describing the volume loss per impacting oxygen atom. Due to the fluctuating conditions in the LEO, slightly different values have been reported from space flight experiments [11].

Many studies have investigated the changes PTFE undergoes after short AO treatment, often focusing on optical and mechanical properties [12–17]. Studies for long treatment times does not exist. Surface sensitive characterization methods, such as time-of-flight secondary ion mass spectrometry (ToF-SIMS) and x-ray photo emission spectroscopy (XPS), have also been employed in similar studies [18,19]. However, the potential of these methods has not yet been fully exploited. Valuable

Abbreviations: AO, atomic oxygen; PTFE, polytetrafluoroethylene; LEO, low-earth-orbit.

* Corresponding authors.
E-mail addresses: Marcus.Rohnke@pc.jlug.de (M. Rohnke), Juergen.Janek@pc.jlug.de (J. Janek).

https://doi.org/10.1016/j.polymdegradstab.2024.110989
Received 19 July 2024; Received in revised form 30 August 2024; Accepted 30 August 2024
Available online 31 August 2024

insights into ongoing degradation reactions can be obtained by the application of statistical tools for data evaluation. As shown in the literature, multivariate statistical methods such as principal component analysis (PCA) and multivariate curve resolution (MCR) can be used to evaluate SIMS data to gain a better understanding of the degradation mechanisms of different materials, including other polymers [20,21].

In the present work, we focus on the chemical surface analysis of PTFE samples before and after long-term oxygen plasma treatment. Scanning electron microscopy (SEM) was used to investigate the morphological changes during AO exposure. For a characterization of the chemical composition of the sample surface, ToF-SIMS analysis was carried out. To obtain more information from the mass spectra, multivariate statistical methods such as PCA and MCR were employed. While PCA is usually well known in the scientific community, MCR is often neglected. However, MCR can provide additional information, as it is designed specifically to solve the mixture analysis problem [22,23]. By this mean, spectra of mixtures are deconvoluted into a set of additive, and most importantly, chemically sensible spectra. Therefore, interpretation of MCR results can be more accessible than that of PCA results. Complementary to the SIMS measurements, XPS was used to validate these findings. Finally, operando quadrupole mass spectrometry (QMS) was used to obtain information on the changes occurring within the plasma composition during treatment. The obtained data was then subjected to multivariate statistical tools to gain further insight into the degradation process. This work aims to fully elucidate the degradation mechanism of PTFE in artificial space conditions.

2. Materials and methods

2.1. PTFE

A PTFE sheet (Merck – Sigma Aldrich) of 1 mm thickness was cut into samples of approximately 20 × 20 mm^2. For mass loss experiments, the samples were then weighted on a precision balance and placed on the grounded electrode of the plasma chamber. After plasma treatment, the samples were weighted again, and the mass loss calculated. Furthermore, the geometry and exposed surface area of the samples were measured.

2.2. Oxygen plasma

The capacitive oxygen plasma was generated in an apparatus consisting of a PFG 300 RF-Generator (TRUMPF Hüttinger GmbH, Germany) connected to a stainless-steel electrode (9 cm diameter, placed horizontally) via a PFM 1500 A matchbox (TRUMPF Hüttinger GmbH, Germany). A stainless-steel grounded electrode (9 cm diameter) is 9 cm below the driven electrode. After evacuation to 0.1 mbar, the chamber was flushed with 5.0 oxygen to 1 mbar and then evacuated to 0.1 mbar again. This procedure was then repeated for cleaning once before the plasma was ignited at 0.1 mbar. A negative bias of 150 V was applied to the driven electrode while the power was regulated and remained at 10 W. The RF-generator operated at a frequency of 13.56 MHz. During the plasma treatment, oxygen was supplied to the plasma chamber at a rate of 0.025 sccm while a rotatory pump connected via a valve kept the pressure constant at 0.1 mbar (± 0.03 mbar). An image of the apparatus can be seen in the Supplementary Information (**Figure S1**).

2.3. Operando-QMS

To perform operando measurements in the plasma reactor, a Prismapro QMG 250 quadrupole mass spectrometer from Pfeiffer Vacuum (Asslar, Germany) in combination with a turbomolecular pump were installed at a cross fitting via CF-40 flanges. The cross fitting was connected to the plasma chamber via a double-sided blind flange that was pierced by a capillary with a diameter of 5.5 mm and a length of 95 mm. This setup enabled the quadrupole mass spectrometer to operate in the 10^{-5} –10^{-6} mbar pressure range without disturbing the plasma pressure. Mass spectra were recorded with a dwell time of 16 ms, 20 points·amu^{-1}, a range of 0–200 *m/z*, and an activated electron multiplier.

2.4. SEM

SEM images were acquired with a Merlin high-resolution SEM (Carl Zeiss AG, Oberkochen, Germany) at a pressure in the low 10^{-6} mbar range, a probing current of 90 pA, and an electron acceleration voltage of 3 kV. An in-lens secondary electron detector was used for image acquisition. To prevent charging effects, the insulating samples were coated with 4 nm of Pt using an EM ACE 600 sputter coater (Leica, Wetzlar, Germany).

2.5. XPS

A PHI 5000 VersaProbe 4 Scanning ESCA Microprobe (Physical Electronics, Chanhassen, USA) with monochromatized Al K_α X-ray source (beam diameter of 100 μm, X-ray power of 100 W) was used to measure XP spectra. An analyzer pass energy of 27 eV, a step time of 50 ms, and a step size of 0.05 eV were used for measuring detail spectra. During the measurements, charge neutralization with slow electrons was applied. CasaXPS software was used for data evaluation and the charge correction was applied using the CF signal in the F1s (689.4 eV) spectrum as reference. For all fitted signals, a Shirley background was used.

2.6. ToF-SIMS

ToF-SIMS measurements were carried out with a M6 Hybrid-SIMS instrument (IONTOF GmbH, Münster, Germany), equipped with a 30 kV Bi cluster primary ion gun (Nanoprobe 50) for analysis and a 20 keV gas cluster ion beam (GCIB) for depth profiling. All measurements were carried out with electron neutralization of the low energetic flood gun. For additional neutralisation, the pressure inside the analysis chamber was increased to $5{\cdot}10^{-6}$ mbar Ar. A surface potential of +440 V was used for all measurements. Surface analysis and depth profiling were carried out in spectrometry mode with Bi_3^{+} as primary ions (FWHM $m/\Delta m$>5000 @ $m/z = 15.99$ (O^-)). The cycle time was set to 140 μs. An area of 100 × 100 $(\mu m)^2$ was analyzed with a 64 × 64 pixel field in random raster mode. For spectra, the stop condition was set to a primary ion dose of 10^{13} ions/cm^2. For depth profiling, Ar_{2000}^{+} clusters (250 × 250 $(\mu m)^2$, 10 kV, 10.76 nA) were used as sputter species. After 1 sputter frame with 2 s pause time, 1 analysis frame with 1 shot/frame and 64 × 64 pixels was recorded. The stop condition was set to 300 scans. For all measurements, negative polarity was used.

2.7. AFM-SIMS

Surface roughness measurements and sputter yield measurements were carried out with a M6 Plus instrument (IONTOF GmbH, Münster, Germany), equipped with a Gas Cluster Ion Beam for depth profiling and an integrated atomic force microscope (AFM). Depth profiles were carried out with the same conditions as in the M6 Hybrid SIMS machine. For calculation of the sputter yield line scans were measured in tapping mode® before and after depth profiling. The erosion yield was calculated to 44 nm^3/Ar-cluster and used for depth calibration of all depth profiles.

All SIMS data were evaluated with SurfaceLab 7.3 (IONTOF GmbH).

3. Results and discussion

3.1. Mass loss

To compare the plasma setup with LEO experiments, mass loss experiments were conducted. The change in mass was normalized to the

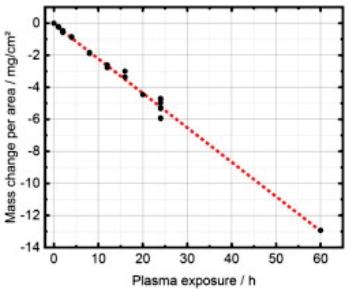

Fig. 1. Observed change in weight of PTFE samples after different plasma treatment times at 0.1 mbar, 150 V, 10 W, normalized to the exposed surface area. A linear change in mass can be observed.

exposed surface area of the samples. As can be seen in Fig. 1, the mass loss is linear even for long-term plasma exposure, indicating a steady degradation kinetics and no significant change in the degradation mechanism throughout the exposure.

From a linear fit with a R^2 of 0.989, a mass loss rate γ of $5.99 \cdot 10^{-8} \pm 0.15 \cdot 10^{-8}$ g·cm^{-2}·s^{-1} was calculated.

The volume degradation Γ can be calculated according to Eq. (1):

$$\Gamma = \gamma / \rho \tag{1}$$

Where Γ = volume degradation ρ = density (2.15 g·cm^{-3}) [2]

In a next step, the flux of atomic oxygen in the plasma chamber towards the sample surface f_{PC} can be approximated according to formula **(2)**. Here we use an erosion yield that was determined from experiments conducted in the LEO:

$$f_{PC} = \Gamma / E_S \tag{2}$$

Where f_{PC} = flux of atomic oxygen in the plasma chamber E_S = erosion yield ($1.42 \cdot 10^{-25}$ cm^3·atom^{-1}) [2].

For this setup, the flux of atomic oxygen f_{PC} was calculated to be approximately $2.0 \cdot 10^{17}$ atoms/cm^2/s, three orders of magnitude higher than the flux in the LEO [2]. This allows long-term LEO exposure to be simulated in a much shorter time frame. In general, the question arises what is the additional impact on degradation by typical plasma wall interactions. To rule out degradation effects induced by the plasma itself, reference experiments with an argon plasma were conducted. In contrast to oxygen plasma degradation for short exposure times (<24 h) the mass loss was less than the sensitivity of the scale used (0.1 mg) and a degradation rate could not be calculated. After 24 h a mass loss of 0.2 mg/cm^2 was calculated (**Figure S2**). From this, it can be estimated that the degradation rate is more than two orders of magnitude lower than in an oxygen plasma, indicating that the chemical reaction of oxygen with the sample was mainly responsible for the degradation.

Low temperature plasma discharges are non-equilibrium systems consisting of anions, cations, electrons and neutrals [24]. Whereas charged particles can take up energy from the electric field and cause in the case of heavy ions sputter damage during plasma-wall interactions, the energy of neutrals is close to room temperature and they should not contribute to physical degradation. In order to ensure that plasma generated high energetic positively charged species did not impact the sample surface, a DC-Bias was applied to accelerate them to the driven electrode instead. In general, the concentration of negatively charged species - with exception of electrons - is negligible in low temperature discharges. Electrons can reach energies of up to 10.000 K but have negligible momentum due to their small mass and cause little sputter effects. In contrast to oxygen discharges pure argon plasmas do not contain any reactive neutral species. For the reasons mentioned, the degradation observed for the oxygen plasma treatment can be mainly attributed to neutral species, such as, AO.

3.2. SEM

In Fig. 2, SEM images of PTFE surfaces after different periods of plasma treatment are shown. On the pristine PTFE sample (a), the presence of cracks in the surface on a nm scale is obvious. After 2 h (b), erosion is clearly visible around plateau-like structures. The cracks are still present on the plateaus of this sample and remain seemingly unaltered, indicating that they are not starting points for degradation. This suggests a degradation that is independent of the nanostructure at the initial polymer surface. After 4 h (c), most of the surface is covered with craters with few plateaus in between. With longer plasma treatment times (d), no more plateaus can be observed. Additionally, there is no further change in the topography of the surface between samples that were treated for >4 h. This indicates that the degradation at the surface is transitioning to a quasi-equilibrium, where, even though degraded material is steadily ablated from the sample, the bulk material serves as

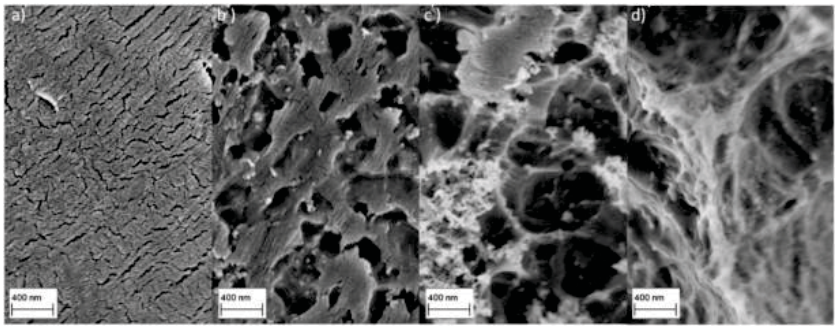

Fig. 2. Micrographs of samples treated for 0 h (a), 2 h (b), 4 h (c) and 12 h (d) in the oxygen plasma at 0.1 mbar, 150 V, 10 W. Increasing erosion of the surface with longer oxygen plasma treatment times can be observed.

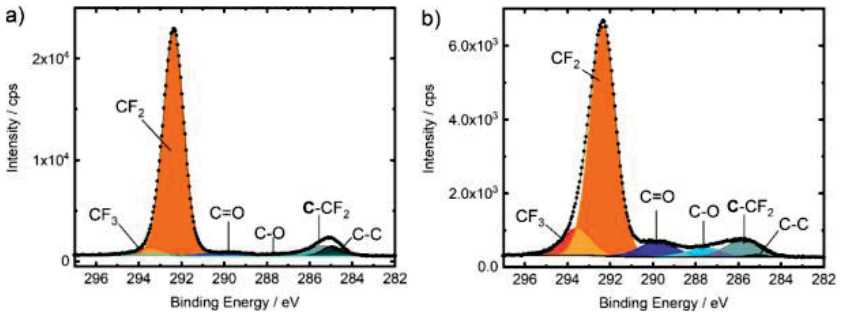

Fig. 3. C 1 s detail spectra from XPS measurements of an untreated (a) and a 2 h oxygen plasma treated (b) PTFE sample. Experimental conditions were 0.1 mbar, 150 V, 10 W. Recorded Datapoints are shown as dots, the outline as a black line. An increase in oxygenated and terminated carbon atoms can be observed.

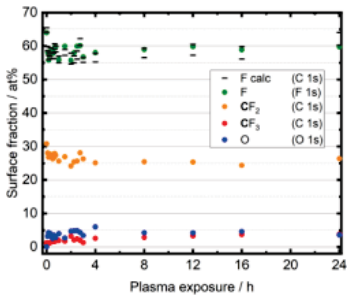

Fig. 4. Quantification results of XPS measurements on untreated ($t = 0$ h) and oxygen plasma treated PTFE samples. Starting with short plasma treatments (5 min), a decrease in fluorine content, as well as an increase in oxygen and terminated carbon content is visible.

an infinite reservoir of pristine PTFE. SEM micrographs of reference samples exposed to an argon plasma showed much less degradation at the sample surface (**Figure S3**).

3.3. XPS

In the C 1 s XPS detail spectra of an untreated (Fig. 3a) and a 2 h oxygen plasma treated sample (b), several signals can be observed. The most prominent peak in both spectra is the peak at 292.3 ± 0.1 eV, corresponding to CF_2. A smaller peak at 293.5 ± 0.1 eV can be assigned to terminated carbon chains. After plasma treatment, this signal increases in intensity relative to the main signal. Furthermore, two signals likely belonging to oxidized carbon species appear at 289.8 ± 0.1 eV and 287.5 ± 0.1 eV respectively. At lower binding energies, two further signals that were interpreted as unfluorinated and unoxidized carbon can be fitted. These peaks are located at 285.7 ± 0.1 eV and 285.1 ± 0.1 eV respectively.

In Fig. 4, the quantification results from C 1 s, F 1 s and O 1 s fits are shown. The quantification on the reference sample ($t = 0$ h) closely matches the theoretical values of 67 % fluorine and 33 % carbon in PTFE. Additionally, a theoretical fluorine content was calculated for all samples from the respective CF_2 and CF_3 C 1 s signals according to Formula (3):

$$F_{calc,\ lower\ limit} = 2 \cdot CF_2 + 2 \cdot CF_3 \quad F_{calc,\ upper\ limit} = 2 \cdot CF_2 + 3 \cdot CF_3 \quad (3)$$

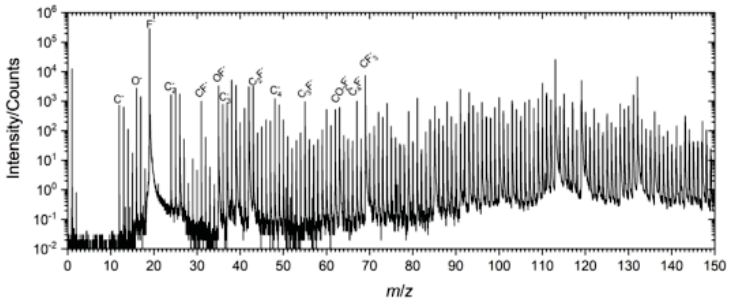

Fig. 5. Exemplary secondary ion mass spectrum in negative ion mode of a plasma treated ($t = 4$ h) PTFE sample surface.

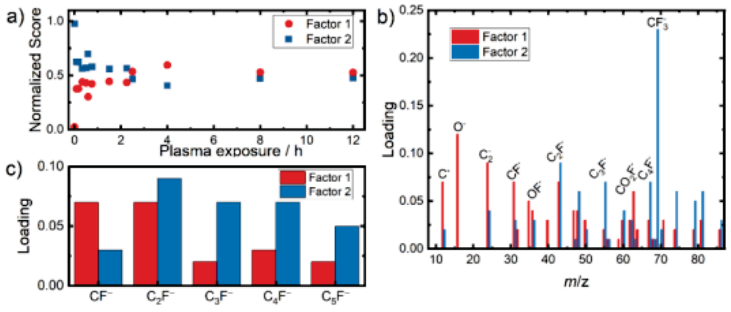

Fig. 6. Normalized Scores (a) and Loadings (b) obtained from a MCR with two factors applied to negative ion mode ToF-SIMS surface spectra of untreated ($t = 0$ h) and oxygen plasma treated PTFE samples. Factor 1 represents degradation products on the sample, whereas factor 2 corresponds to pure PTFE. Loadings of selected C_xF^- signals from the same MCR are shown in (c) to investigate a change in average chain length.

The lower limit was chosen to account for terminated and partially oxidized carbon (COF_2), which was assumed to appear during plasma treatment, whereas the upper limit accounts for only fully fluorinated carbon atoms (CF_3). As can be seen, the measured fluorine contents are indeed within these calculated limits. Generally, a trend can be observed where F 1 s content decreases during plasma treatment from 64 % to 56 %. As the observed values for fluorine content closely match the calculated values, carbon atoms inside the chain are likely either fully fluorinated or completely stripped of fluorine, as is evident from the presence of oxidized C 1 s species (C = O, C—O) after treatment. These signals increase from 1 % to 3.5 % and from <1 % to 2 % respectively. At the same time, an increase in oxygen content (O 1s: 0.5 to 4 %) is noted. Whereas CF_2 C 1 s decreases from 31 % to 25 %, the amount of CF_3 C 1 s increases from 1 % to 2 %, suggesting a higher presence of terminated carbon chains and therefore a shorter average chain length, resulting from degradation of the material. The composition of longer-treated samples does not change significantly. Elements other than carbon, oxygen and fluorine were not detected on any sample (**Figure S4**).

3.4. ToF-SIMS

Mass spectra generated from ToF-SIMS measurements, such as the one in Fig. 5, are usually quite complex and contain a lot of information. To obtain a better understanding of the differences between the mass spectra of plasma treated and untreated samples, both principal component analysis (PCA) and multivariate curve resolution (MCR) were applied.

A PCA on mass spectra of samples treated in the plasma up to 24 h revealed two principal components (PCs) to account for 98 % of variance. Therefore, a follow-up MCR was employed with two factors, the results of which can be seen in Fig. 6. The normalized scores of factors 1 and 2, plotted against the oxygen plasma treatment times, are shown in a). The score of factor 1 is neglectable on the reference sample without plasma treatment ($t = 0$ h), but shoes normalized scores of >0.3 on all plasma treated samples. After plasma treatment, the normalized score of factor 1 increases until 4 h treatment time, where a maximum value of 0.59 is reached. For longer plasma treatments, the score of factor 1 decreases slightly, but remains above 0.5. The loadings of factor 1 contain oxidized fragments, such as O^-, OF^-, and CO_2F^-, which clearly suggests that this factor can be assigned to the degradation products. Interestingly, C_2^- is also present in factor 1, further hinting at defluorination of some carbon atoms during treatment. The normalized score of factor 2 of 0.98 on the reference sample indicates that factor 2 represents the mass spectrum of pure PTFE. As can be seen from the loading plot in Fig. 6(b), factor 2 consists mainly of CF_3^-, with other $C_xF_y^-$ fragments also present, similar to an expected mass spectrum of pure PTFE. It should be

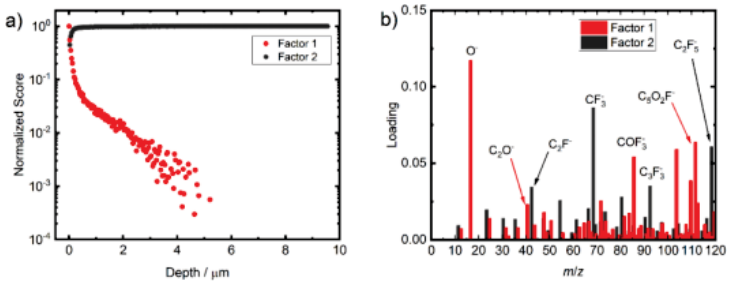

Fig. 7. Normalized scores (a) and loadings (b) obtained from a MCR with two factors applied to negative ion mode ToF-SIMS depth spectra of an oxygen plasma treated ($t = 4$ h) PTFE sample. Factor 1 is only present at the surface of the sample and represents degradation products, as well as surface contaminations. Factor 2 appears in the bulk material and corresponds to pristine PTFE.

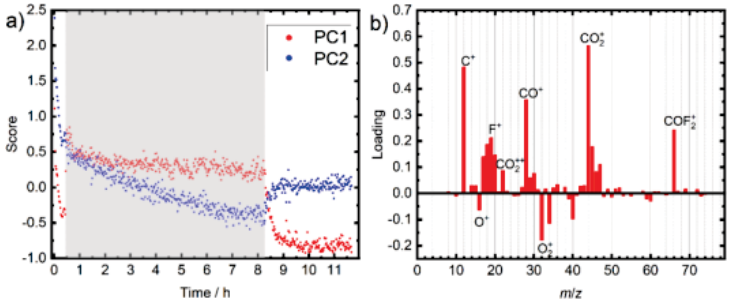

Fig. 8. Time dependent scores plot (a), as well as loading plot for PC1 (b) from the signal normalized PCA applied to operando mass spectra. Plasma treatment conditions were 0.1 mbar, 150 V, 10 W. The plasma treatment period is shown in grey. Positive loadings in b) correlate with plasma conditions, whereas negative loadings are associated with no plasma conditions.

noted here that surface contaminants, such as from handling the samples at air, are likely the same for all samples and thus have little impact on the loadings of factor 1.

The MCR loadings of selected C_nF^- mass signals with increasing carbon chain length (C_xF^-; $x = 1,\ldots,5$) can be seen in c). The highest loading in factor 2 belongs to C_2F^-, with longer carbon chains also contributing significantly. In factor 1, shorter CF fragments are more relevant, with larger fragments having the lowest loadings. This again indicates the fragmentation of longer carbon chains into shorter ones during plasma treatment.

3.5. AFM/ToF-SIMS

From AFM-SIMS measurements, the surface roughness, as well as the depth calibration for the depth profiles were obtained.

MCR was also applied to data of SIMS depth profiles. As can be seen from the normalized scores against sputtering depth in Fig. 7(a), factor 1 represents the composition of the surface in contrast to the bulk material, which is present in factor 2. The loadings plot (b) for both factors reveals that oxygenated fragments, most importantly O^-, define factor 1, whereas factor 2 consists of unoxidized fragments from carbon and fluorine. These loadings are notably different from those obtained from surface spectra of different samples (**Figure S5**), as here surface contaminants play a large role in the difference between surface and bulk material. The normalized score of factor 1 decreases to about 0.01 at a nominal depth of 2 μm. This value however needs to be considered in combination with the surface roughness R_a of the sample, which is 0.9 μm. An AFM line scan of the sample is depicted in **Figure S6**. Therefore, at this nominal depth, it is likely that the score of factor 1 does not represent explicitly oxidation within the bulk material. Instead, it appears that due to the roughness, surface that had been exposed to and oxidized by the plasma was detected within the first μm due to shading effects during 3D analysis. No significant correlation between plasma treatment and either score of factor 1 or signal intensity of O^- at any given depth could be found. Thus, we conclude that the chemical degradation is mainly occurring at the exposed surface of the material, leaving the bulk mostly unaffected.

3.6. Operando-QMS

By conducting QMS measurements during the plasma treatment, additional insights into the degradation process can be acquired. Again, statistical methods were effectively employed to reveal the differences in the gas phase composition of the plasma reactor during and after plasma treatment. A PCA of the received mass spectrometric data revealed that one principal component accounts for 99 % of variance. However, in this PCA only a few signals, such as O^+ and O_2^+, accounted for the variance as these were expectedly the most prominent signals in the oxygen atmosphere of the plasma chamber. Further information was revealed by normalizing each mass signal on itself, specifically to the highest intensity of this signal in all measurement cycles. The results of this follow-up PCA can be seen in Fig. 8. Here, PC1 accounts for 22.3 % of variance, whereas PC2 explains 9.1 %. While the positive score of PC1 aligns very well with the presence of plasma conditions (a), the score of PC2 shows a constant trend downwards until the end of the plasma. Further PCs showed no correlation between score and time, likely a by-product of the normalization approach. This indicates that PC1 represents the variance introduced by the plasma. As can be seen in the loading plot for PC1 (b), most signals with a positive loading are carbon and oxidized carbon fragments (C^+, CO^+, CO_2^+). Other signals with less loading are fluorine containing species (F^+, COF_2^+). Interestingly, no carbon species with only one fluorine atom attached could be observed. Pure oxygen species (O^+, O_2^+) exhibit a negative loading, likely due to the reactions that oxygen undergoes in the plasma. Above a m/z ratio of 75, no further signal exhibited significant loading. The presence of degradation related carbon fragments in PC1 further supports the hypothesis of fragmentation of the polymer into shorter chains, as longer carbon chains were not observed.

4. Discussion

Even though oxygen plasmas are commonly used to simulate degradation in the LEO, there are still differences between the two. The atmosphere in LEO consists mainly of atomic oxygen, followed by either N_2 or He, depending on the altitude. While atomic oxygen is also abundant in plasmas comparable to the one used in this study, such a plasma atmosphere also contains atomic and molecular oxygen ions, mostly cations [4]. These cations are prevented from reacting with the sample by the DC-Bias, which accelerates them towards the driven electrode, away from the sample. This may introduce a sputter-deposition like process, with the electrode serving as the target. XPS spectra revealed no observable amount of metal on any sample, indicating that this effect is, if present at all, neglectable. Other sources of degradation present in LEO, which may have synergistic effects on the oxygen-based degradation, such as UV-radiation, debris impact or cosmic radiation, were also not considered in this study.

The combined results of SEM, XPS, ToF-SIMS and Operando-QMS show the degrading effect an oxygen plasma has on PTFE. Even

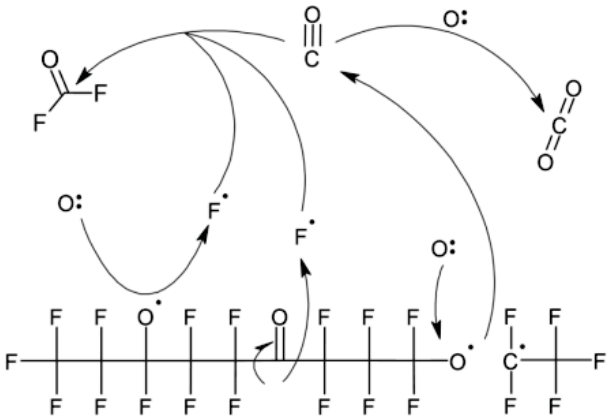

Fig. 9. Possible reaction scheme of the degradation occurring at the surface of PTFE with AO, as derived from surface analysis as well as operando mass spectrometry.

though the goal of the conducted experiments was to understand the long-term degradation of PTFE in an oxygen plasma, we were unable to replicate studies that showed harsh changes in surface composition after very short treatment times: Even though we also observed defluorination in XPS measurements, the change in fluorine content was not as strong as observed by Vandencasteele et al. [18], who reported a steadily declining fluorine content down to 36 % after 20 min of oxygen plasma treatment. Neither were we able to reproduce the observation by Morra et al. [16], who found that the fluorine content decreases within seconds after plasma ignition to 50 % and then rises back up to 61.4 % after 15 min. These differences might be attributable to a different plasma setup. Also, it is unclear whether the entire surface of the samples in literature had been degraded by the plasma. This point is especially relevant, as within the first hours of plasma treatment we found a heterogeneous distribution of degradation on the surface. Nonetheless, we were able to use QMS to observe the presence of CO, CO_2^+ and F in the plasma, as reported by Vandencasteele et al. [18], who used optical emission spectroscopy to detect these fragments.

While the exact degradation mechanism likely is highly complex and involves many different reactions, the following statements can be made:

- After 2–4 h of plasma treatment, the entire surface is degraded. This time corresponds to a fluence of approximately 2.5–5 mmol AO·cm^{-2}, or 174–348 days in the LEO at a constant flux of 10^{14} atoms·cm^{-2}. For longer plasma durations, a quasi-equilibrium is reached, where degradation is occurring at the same rate as before, however no changes in surface composition can be observed.
- The degradation process involves the stripping of fluorine from the carbon chain, as is evident from the reduced fluorine content measured in XPS, increased presence of defluorinated carbon species in ToF-SIMS, as well as the presence of F^+ during plasma conditions in QMS spectra.
- The slower degradation rate of PTFE in LEO compared to other, carbon chain based, polymers [10] indicates that the defluorination is the rate determining step in the degradation process.
- This defluorination likely results either in a bond between the defluorinated carbon atom and oxygen, or in a breaking of the carbon chain. This can be deduced from the decrease in fluorinated carbon atoms in XPS that matches the increase of oxygenated and terminated carbon.
- Once the first fluorine atom is removed from a carbon, the second fluorine is likely much more reactive, as no evidence of single fluorinated carbon was found in XPS.
- After the complete defluorination, the carbon atom breaks apart from the polymer chain and can be detected as either C^+ or oxygenated carbon, such as CO_2^+ in QMS measurements. Note that defluorination appears to not be necessary for the carbon atom to be ablated from the sample, as a mass signal could be attributed to carbonyl fluoride (COF_2), indicating that not every carbon atom removed from the sample is defluorinated beforehand. As no carbon fragment with a single fluorine atom was visible in QMS measurements, either complete or no defluorination appears to be the condition for carbon ablation from the sample.
- During the degradation process, the average polymer chain length at the surface of the sample decreases. This can be deduced from the increase in terminated carbon atoms visible in XPS, as well as from the increasing significance of shorter carbon chains in the loadings obtained from MCR on ToF-SIMS surface spectra.
- By combining these deductions, a simplified reaction scheme can be constructed, as seen in Fig. 9.

5. Conclusion

ToF-SIMS, XPS, SEM and operando-MS measurements were employed to investigate the degradation of PTFE in a low-temperature oxygen plasma. It was found that the surface undergoes significant changes within the first 4 h of plasma treatment, corresponding to a dose of 2.5–5 mmol atomic oxygen·cm^{-2}. Samples treated for longer durations exhibited no further changes in surface composition. A steady loss of mass was noted during the experiments, remaining linear even for extended treatment times. The degradation is likely taking place by stripping the fluorine from a carbon atom and subsequent ablation of the (oxygenated) carbon atom from the surface, breaking the polymer chain apart, resulting in an increase of both defluorinated and terminated carbon atoms, as well as overall shorter carbon chains. Significant

indicators of degradation are an increase in terminated carbon chains, verified by XPS, ToF-SIMS and mass spectrometric in operando measurements. At the same time, the bulk material remained unaffected by the plasma treatment.

CRediT authorship contribution statement

Tobias Wagner: Writing – original draft, Visualization, Validation, Investigation, Data curation. **Marcus Rohnke:** Writing – review & editing, Project administration, Methodology, Conceptualization. **Jürgen Janek:** Writing – review & editing, Supervision, Funding acquisition, Conceptualization.

Declaration of competing interest

The authors declare the following financial interests/personal relationships which may be considered as potential competing interests:

Juergen Janek reports financial support by European Commission and article publishing charges were provided by German Research Foundation. If there are other authors, they declare that they have no known competing financial interests or personal relationships that could have appeared to influence the work reported in this paper.

Data availability

Data will be made available on reasonable request.

Acknowledgements

Financial support by the European Union (IWB EFRE program) under project no FPG991 003/2019 is gratefully acknowledged. The authors thank also the German Federal Ministry for Education and Research (BMBF) for funding the PHI Versa Probe 4 and the M6 Plus SIMS (project PROGRAL, no 03XP0427) as well as the German Research Foundation (DFG) for funding the Hybrid-SIMS under grant number INST 162/544–1 FUGG.

Supplementary materials

Supplementary material associated with this article can be found, in the online version, at doi:10.1016/j.polymdegradstab.2024.110989.

References

[1] I. Gouzman, E. Grossman, R. Verker, N. Atar, A. Bolker, N. Eliaz, Advanced Materials (Deerfield Beach, Fla.), 31, 2019 e1807738.
[2] K.K. de Groh, B.A. Banks, S.K.R. Miller, J.A. Dever, Handbook of environmental degradation of materials (Third Edition) Chapter 28, Degradation of Spacecraft Materials (2018).
[3] J. Chen, N. Ding, Z. Li, W. Wang, Prog. Aerosp. Sci. 83 (2016) 37, https://doi.org/10.1016/j.paerosci.2016.02.002.
[4] X.-H. Zhao, Z.-G. Shen, Y.-S. Xing, S.-L. Ma, Polym. Degrad. Stab. 88 (2005) 275, https://doi.org/10.1016/j.polymdegradstab.2004.11.002.
[5] S. Abou Rich, P. Leroy, T. Dufour, N. Wehbe, L. Houssiau, F. Reniers, Surf. Interface Anal. 46 (2014) 164, https://doi.org/10.1002/sia.5403.
[6] Z. Shpilman, I. Gouzman, G. Lempert, E. Grossman, A. Hoffman, Rev. Sci. Instrum. 79 (2008) 25106, https://doi.org/10.1063/1.2885044.
[7] Y. Huang, X. Tian, S. Yang, P.K. Chu, Rev. Sci. Instrum. 78 (2007) 103301, https://doi.org/10.1063/1.2800766.
[8] Z. Hooshangi, S.A. Hossein Feghhi, R. Saeedzadeh, Acta Astronaut 119 (2016) 233, https://doi.org/10.1016/j.actaastro.2015.11.031.
[9] T. Ghidini, Nat. Mater. 17 (2018) 846, https://doi.org/10.1038/s41563-018-0184-4.
[10] K.K.de Groh, B.A. Banks, *Atomic Oxygen Erosion Data From the MISSE 2–8 Missions*, 2019.
[11] E.M. Silverman, Space Environ. Effects on Spacecraft: LEO Mater. Select. Guide (1995).
[12] S. Zanini, R. Barni, R.D. Pergola, C. Riccardi, J. Phys. D: Appl. Phys. 47 (2014) 325202, https://doi.org/10.1088/0022-3727/47/32/325202.
[13] C. Liu, R.D. Arnell, A.R. Gibbons, S.M. Green, L. Ren, J. Tong, Surf. Eng. 16 (2013) 215, https://doi.org/10.1179/026708400101517161.
[14] R. Zaplotnik, A. Vesel, M. Mozetič, Plasma Process Polym 15 (2018) 1800021, https://doi.org/10.1002/ppap.201800021.
[15] Y. Gudimenko, R. Ng, J.I. Kleiman, Z.A. Iskanderova, R.C. Tennyson, P.C. Hughes, Polymer Surface Modificat.: Relevance to Adhesion (2004) 325, https://doi.org/10.1201/b12183-18.
[16] M. Morra, E. Occhiello, F. Garbassi, Surf. Interface Anal. 16 (1990) 412, https://doi.org/10.1002/sia.740160186.
[17] A.A.-G.A. Atta, Indian J. Pure & Appl. Phys. (2016) 551.
[18] N. Vandencasteele, D. Merche, F. Reniers, Surf. Interface Anal. 38 (2006) 526, https://doi.org/10.1002/sia.2255.
[19] A. Vesel, M. Mozetic, A. Zalar, Surf. Interface Anal. 40 (2008) 661, https://doi.org/10.1002/sia.2691.
[20] D. Heller, B. Hagenhoff, C. Engelhard, Journal of Vacuum Science & Technology B, Nanotechnology and Microelectronics: Materials, Processing, Measurement, and Phenomena 34 (2016) 49, https://doi.org/10.1116/1.4948371.
[21] F. Awaja, J.B. Moon, M. Gilbert, S. Zhang, C.G. Kim, P.J. Pigram, Polym. Degrad. Stab. 96 (2011) 1301, https://doi.org/10.1016/j.polymdegradstab.2011.04.001.
[22] W.H. Lawton, E.A. Sylvestre, Technometrics 13 (1971) 617, https://doi.org/10.1080/00401706.1971.10488823.
[23] A. de Juan, J. Jaumot, R. Tauler, Anal. Methods 6 (2014) 4964, https://doi.org/10.1039/C4AY00571F.
[24] M.A. Lieberman, A.J. Lichtenberg, Principles of Plasma Discharges and Materials Processing, Wiley-Interscience, Hoboken, 2005.

3.2. Publication 2: "Investigation of the polyvinyl fluoride degradation mechanism under atomic oxygen exposure"

The second publication of this dissertation explores the degradation of polyvinyl fluoride (PVF) in a low temperature oxygen plasma. The samples were characterized by ToF–SIMS, XPS, SEM, and weighing. During the exposure of samples to the plasma, a QMS monitored the composition of the atmosphere inside the plasma chamber.

The combination of surface sensitive analysis techniques with QMS revealed new information on the degradation mechanism, such as carbonization of the polymer chain, as well as the presence of unoxygenated carbon species in the plasma atmosphere. Known phenomena, such as the defluorination of the polymer were also observed. The application of MVSA tools allowed for a better understanding of the sample system. Critically, PCA assisted in the observation and partial unraveling of X-ray induced degradation of the material during XPS measurements.

The first author designed, planned and carried out and evaluated the experiments under the supervision of M. Rohnke and J. Janek. J. Sann supported the analyses of the XPS data. The manuscript was written by the first author and edited by the co-authors.

Reprinted with permission from T. Wagner, M. Rohnke, J. Sann, J. Janek, "Investigation of the Polyvinylfluoride degradation mechanism under atomic oxygen exposure", *Polymer Degradation and Stability* **2025**, 111820; DOI 10.1016/j.polymdegradstab.2025.111820.

Polymer Degradation and Stability 244 (2026) 111820

Contents lists available at ScienceDirect

Polymer Degradation and Stability

journal homepage: www.journals.elsevier.com/polymer-degradation-and-stability

Investigation of the polyvinyl fluoride degradation mechanism under atomic oxygen exposure

Tobias Wagner, Marcus Rohnke *, Joachim Sann, Jürgen Janek *

Institute of Physical Chemistry and Center for Materials Research, Justus Liebig University Giessen, Heinrich-Buff-Ring 17, D 35392 Giessen, Germany

ARTICLE INFO

Keywords:
Low temperature oxygen plasma
Polymer degradation
Surface analysis

ABSTRACT

Materials degradation in the Low-Earth-Orbit (LEO) can be attributed to a combination of environmental factors, one of the most impactful of which is atomic oxygen (AO). Simulation of these conditions often employs ground-based facilities, such as low-temperature oxygen plasmas that contain AO. Here we focus on the degradation of polyvinyl fluoride (PVF), a material of interest in space applications. The degradation mechanism of PVF under AO is not completely understood, knowledge of which is essential for developing better materials for use in the LEO. A self-constructed capacitively driven 13.56 MHz RF low temperature reactor flooded with oxygen was used as the source of AO in this study. The chemical changes in the surface of PVF samples during the exposure to the oxygen plasma were investigated using surface sensitive techniques, such as scanning electron microscopy (SEM), X-ray photoelectron spectroscopy (XPS) and time-of-flight secondary ion mass spectrometry (ToF-SIMS). The composition inside the reactor was monitored using operando quadrupole mass spectrometry (QMS). Multivariate statistical methods were applied to the data to improve the analysis. The degradation occurs steadily, as evidenced by mass loss measurements, up to a point of a quasi-equilibrium after an exposure to $1.30 \bullet 10^{20}$ AO/cm^2. Water content in the sample and reactor increased during the exposure, as well as the presence of fragments indicating the chemical insertion of oxygen into the polymer. Fragments, such as CO_2^+, F^+ and H_2O^+ in the plasma atmosphere hint towards a near total oxidation of fragments that desorb form the PVF surface. SEM micrographs revealed changes in the morphology of the sample surface during the degradation process.

1. Introduction

In modern space flight, the Low-Earth-Orbit (LEO) plays a significant role. >2,500 objects have been launched into the LEO in 2024 [1]. While its proximity to earth is well suited for many applications, any object in the LEO is exposed to a combination of harsh conditions, such as extreme temperatures, X-Ray and UV radiation, and atomic oxygen (AO) [2–4]. In vast regions of the LEO, the most abundant gas species is AO, leading to a flux of 10^{14}–10^{15} atoms of oxygen cm^{-2} s^{-1} [5,6]. Each of these environmental factors on its own can have a destructive impact on materials, but their combination inside the LEO creates synergistic degradation effects, as evidenced by the tearing of the Hubble Space Telescope's thermal control blanket [7]. Ground based and cost-efficient facilities, such as plasma chambers, are often used to generate AO and simulate LEO conditions. The term *equivalent AO flux* is used to describe the flux of generated reactive oxygen species, which may also include ozone and charged oxygen species, inside such reactors [8–10].

Polymers, such as polyvinyl fluoride (PVF, $(CH_2CHF)_n$) are usually very lightweight, an important material property for usage in space. However, polymers also exhibit higher erosion yields, i.e., the volume lost per impacting oxygen atom, than other material classes [4]. When PVF is discussed in the context of space flight, the material in question usually is white Tedlar, a composite material consisting mainly of PVF with TiO_2 pigments. Such hybrid materials are known to reduce the erosion yield of the material, while not significantly affecting other properties [11,12]. In the case of PVF, the addition of TiO_2 reduces the erosion yield from $3.19 \bullet 10^{-24}$ cm^3 atom^{-1} to $1.01 \bullet 10^{-25}$ cm^3 atom^{-1}, roughly 30 times smaller [4]. This makes white Tedlar better suited for space applications than pure PVF, which is sold as clear Tedlar [3,13,14]. Nonetheless, pure PVF is used in degradation studies over white

Abbreviations: AO, atomic oxygen; PVF, polyvinyl fluoride; LEO, low-earth-orbit; XPS, X-Ray Photoelectron Spectroscopy; ToF-SIMS, Time-of-Flight Secondary Ion Mass Spectrometry; QMS, Quadrupole Mass Spectrometry.

* Corresponding authors.
E-mail addresses: Marcus.Rohnke@uni-giessen.de (M. Rohnke), Juergen.Janek@uni-giessen.de (J. Janek).

https://doi.org/10.1016/j.polymdegradstab.2025.111820
Received 12 September 2025; Received in revised form 11 November 2025; Accepted 27 November 2025
Available online 27 November 2025

Tedlar, as it gives a more direct and unequivocal understanding of the degradation of the organic material. Additionally, it allows for a better comparison to other polymers. Compared to other fluoropolymers, PVF has a low molecular weight, which is a desired attribute for usage in space.

Golub *et al.* have used XPS to investigate the changes polymers undergo during exposure to AO. However, their study focused more on the comparison of different polymers and did not seek to further unravel the chemical degradation of the PVF surface [15].Other studies use oxygen plasmas to etch the surface of PVF to obtain enhanced material properties in other contexts than space [16,17]. The difference between etching and polymer degradation is primarily in its intent, but not the mechanisms involved [18]. Grossman *et al.* approached the degradation of polymers in LEO by applying multiple conditions simultaneously and analyzing the transmission, as well as surface roughness changes by AFM scans of the materials [5].To this date, there is no study that involves the well-established [19,20] combination of XPS and ToF-SIMS to investigate the chemical changes at the surface of PVF after degradation in an oxygen plasma.

This study aims to unravel the chemical degradation PVF undergoes in a low-temperature oxygen plasma. Morphological changes during the plasma exposure were investigated using Scanning Electron Microscopy (SEM). The chemical composition of the samples was analyzed by X-Ray Photoelectron Spectroscopy (XPS), enhanced by Principal Component Analysis (PCA). These data were complemented by Time-of-Flight Secondary Ion Mass Spectrometry (ToF-SIMS) measurements, further supported by PCA as well as Multivariate Curve Resolution (MCR). This method was developed to tackle the mixture analysis problem and yields factors that are far more chemically sensible than principal components from PCA [21,22]. Although MCR is less established in the scientific community than PCA, its results are more straightforward to interpret and thus more accessible. To investigate changes in the makeup of the plasma during the exposure, operando quadrupole mass spectrometry (QMS) was employed and supported by the use of PCA.

2. Material and methods

2.1. PVF

A PVF film (Merck –Sigma Aldrich) of 50 μm thickness was cut into samples of approximately 20 × 20 mm^2. For the mass loss experiments, the samples were weighed on a precision balance and fixed between two 6 mm thick ceramic discs with a 10 mm diameter hole in the centre, providing a precise area of the sample exposed to the plasma. This was done to prevent bending of the sample that had been observed without the presence of the discs. This setup was placed on the grounded electrode of the plasma chamber. After plasma treatment, the samples were weighted again, and the mass loss calculated. For operando QMS measurements, a larger sample was used to generate more reaction fragments in the plasma and therefore more QMS signal intensity. Additionally, no ceramic disc was placed above the center of the sample. Instead, two discs were placed on opposite corners of the foil. This setup prevented the discs from suppressing mass signals, a phenomenon that was observed otherwise. Samples, as well as the PVF film were stored in a desiccator. For mass loss measurements, the samples were weighed immediately after removing them from the desiccator and again immediately after the plasma treatment.

2.2. Oxygen plasma

The capacitive oxygen discharge was generated in an apparatus consisting of a PFG 300 RF-Generator (TRUMPF Hüttinger GmbH, Germany) connected to a stainless-steel electrode (9 cm diameter, placed horizontally) via a PFM 1500 A matchbox (TRUMPF Hüttinger GmbH, Germany). A stainless-steel grounded electrode (9 cm diameter) was positioned 9 cm below the driven electrode. After reaching 0.04 mbar, the reactor chamber was flushed with oxygen (purity 5.0) to 0.4 mbar and then evacuated to 0.04 mbar again. Before igniting the plasma at 0.1 mbar, this process was repeated once for cleaning. A negative bias of 150 V was applied to the driven electrode while the power was regulated and remained at 10 W. The RF-generator operated at a frequency of 13.56 MHz. During the plasma treatment, oxygen was supplied to the plasma chamber at a rate of 0.025 sccm while a rotatory pump connected via a valve kept the pressure stable at 0.1 mbar (± 0.02 mbar). An image of the apparatus can be seen in the Supplementary Information (Figure S1) as well as in a previous publication [23].

2.3. Operando QMS

To perform operando measurements in the plasma reactor, a Prismapro QMG 250 quadrupole mass spectrometer from Pfeiffer Vacuum (Asslar, Germany) in combination with a turbomolecular pump were installed at a cross fitting via CF-40 flanges. The cross fitting was connected to the plasma chamber via a double-sided blind flange that was pierced by a capillary with an inner diameter of 0.55 mm and a length of 95 mm. This setup enabled the quadrupole mass spectrometer to operate in the 10^{-5}–10^{-6} mbar pressure range without disturbing the plasma pressure. Mass spectra were recorded with a dwell time of 16 ms, 20 points·amu^{-1}, a range of $0 \leq m/z \leq 200$, and an activated electron multiplier.

2.4. SEM

SEM images were taken using a GeminiSEM 560 (Carl Zeiss AG, Oberkochen, Germany) with a probing current of 90 pA, an electron acceleration voltage of 5 kV and a pressure in the low 10^{-6} mbar range. For image acquisition an in-lens detector was used. To prevent charging effects, the samples were coated with 4 nm of Pt before the measurement using an EM ACE 600 sputter coater (Leica, Wetzlar, Germany).

2.5. XPS

A PHI VersaProbe 4 Scanning XPS Microprobe (Physical Electronics, Chanhassen, USA) with monochromatized Al K_α X-ray source (High Power mode, beam spot of 100 μm scanned over 1.4 mm, X-ray power of 100 W) was used to measure XP spectra. An analyzer pass energy of 27 eV, a step time of 50 ms, and a step size of 0.05 eV were applied for measuring detail spectra. During the measurements, the samples were neutralized with the PHI dual beam neutralization consisting of a low current of 10 eV Ar^+ ions and 5 μA of 1 eV electrons, fixing the potential during the measurements at −1 V vs ground level. CasaXPS 2.3.26 software was used for data evaluation and the charge correction was applied using the CF signal at 686.94 eV in the F1s spectrum as reference [24]. For all fitted signals, a Shirley background was used. C1s signals were fitted by GL (30) shapes with a FWHM of 1–1.5 eV or 2 eV (oxygenated carbon).

2.6. ToF-SIMS

ToF-SIMS measurements were carried out with a M6 Hybrid-SIMS instrument (IONTOF GmbH, Münster, Germany), equipped with a 30 kV Bi cluster primary ion gun (Nanoprobe 50) for analysis. All measurements were carried out with electron neutralization of the low energetic flood gun. For additional suppression of charging effects, the pressure inside the analysis chamber was increased to $5{\cdot}10^{-6}$ mbar by gas flooding with Ar.

A surface potential of between +35 and +150 V was used depending on the sample. Surface analysis was done in spectrometry mode with Bi_3^{++} as primary ions (FWHM $m/\Delta m > 5000@m/z = 15.99$ (O^-)). The cycle time was set to 140 μs. An area of 100 × 100 $(\mu m)^2$ was analyzed with a 64 × 64 pixel grid in random raster mode. The stop condition was set to a primary ion dose of 10^{13} ions/cm^2. For all measurements,

negative polarity was used.

SurfaceLab 7.4 software was used for calibration and processing of the data, as well as for PCA and MCR.

3. Results and discussion

3.1. Mass loss

Due to the use of ceramic masks for sample fixation in this study, the setup differed from the one that was used in a previous study [23]. In order to recalculate the flux of AO per area and second, mass loss calibration measurements were performed with Kapton foil under the ceramic masks. Due to the well quantified erosion yield ($E_K = 3.0{\cdot}10^{-24}$ $cm^3{\cdot}atom^{-1}$) and density ($\rho_K = 1.42$ $g{\cdot}cm^{-3}$) of Kapton, this material is often used for calibration purposes [25]. The mass loss Δm_K and plasma treatment time t were obtained directly. The exposed area A was calculated from the diameter of the circular hole in the ceramic mask ($d = 1.0$ cm) to be $A = 0.785$ cm^2. From these calibration measurements, the flux of AO in the plasma chamber was calculated to be $f_{PC} = 4.5{\cdot}10^{15}$ $at{\cdot}cm^{-2}{\cdot}s^{-1}$ according to Eq. (1).

$$f_{PC} = \Delta m_K{\cdot}{\rho_K}^{-1}{\cdot}{E_K}^{-1}{\cdot}A^{-1}{\cdot}t^{-1} \quad (1)$$

The mass loss per area of PVF can be seen in Fig. 1, where a linear fit with an R^2 of 0.98796 reveals a degradation rate of $3.14{\cdot}10^{-8}$ $g{\cdot}cm^{-2}{\cdot}s^{-1}$. From this and the flux of AO in the plasma chamber, the erosion yield of PVF could be calculated to be $E_{PVF} = 3.35{\cdot}10^{-24}$ $cm^3{\cdot}atom^{-1}$ which is in good agreement with the value obtained from space flight experiments ($E_{PVF,\ Lit} = 3.19\text{-}3.53{\cdot}10^{-24}$ $cm^3{\cdot}atom^{-1}$ [3,26]). The decent linear fit indicates that the degradation is occurring without a significant change in reaction mechanism throughout the plasma treatment.

For plasma exposure extending 72 h, no further change in mass could be observed due to the total degradation of the 50 μm thick foil. Complete degradation of the exposed area was also visually confirmed and is consistent with the theoretical mass loss limit calculated from the known exposed area and density of the sample.

3.2. SEM

SEM micrographs of PVF after different durations of plasma exposure are shown in Fig. 2. Untreated PVF (a) shows little to no surface features. After oxygen plasma treatment (b), the surface exhibits inhomogeneities that increase in size during the plasma treatment (c-g). After 12 h (f), no further changes were observed on the surface. As the plasma parameters did not change during the exposure, we assume a steady rate of AO reaching the surface.

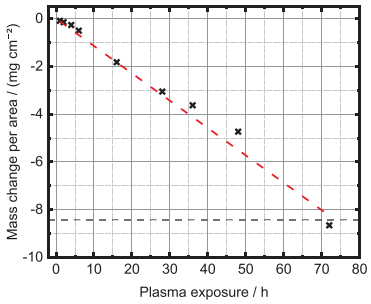

Fig. 1. Observed change in weight of PVF samples exposed to oxygen plasma at $p = 0.1$ mbar, U_{Bias}=150 V, P_{RF}=10 W. The dashed black horizontal line represents the theoretical limit, where the exposed sample is completely degraded.

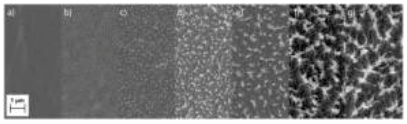

Fig. 2. SEM micrographs of PVF samples exposed to oxygen plasma at $p = 0.1$ mbar, $U_{Bias} = 150$ V, $P_{RF} = 10$ W for 0 h (a), 0.5 h (b), 2 h (c), 4 h (d), 8 h (e), 12 h (f) and 24 h (g). Ongoing erosion of the surface can be seen.

This indicates a degradation kinetics that reaches a quasi-equilibrium state between 8–12 h, where by further exposure to the oxygen plasma leads to the formation of volatile degradation fragments that desorb from the surface, leaving the underlying material exposed.

3.3. XPS

To investigate changes in the chemical composition of the PVF surface after exposure to the oxygen plasma, XPS measurements were conducted. In the survey spectra, the presence of carbon, fluorine, oxygen and marginal amounts (<1 %) of nitrogen were observed on all samples. The presence of oxygen on reference samples can be explained by residual water inside the polymer, as well as surface contaminations resulting from handling at atmosphere. This might also explain the presence of nitrogen. Chromium and manganese were also detected on all samples, with the amount increasing with plasma exposure up to <2 % (Fig. 3a, Figure S2). As these metals are present on the reference sample, albeit in almost undetectable amounts, they are likely remnants of the manufacturing process. During exposure to the oxygen plasma, the metals are likely not removed from the sample surface and accumulate as the polymer is being degraded, leading to a higher detection rate.

The 1s spectra of carbon, oxygen and fluorine were also used for quantification to observe changes in the chemical composition of the PVF samples (Fig. 3b). A general trend can be observed where the share of oxygen is increasing from ~10 % to ~25 % for longer plasma exposure. We attribute this to the likely formation of water during the reaction of the polymer with AO. At the same time, the carbon content is decreasing from ~80 % to ~60 %, while the fluorine content is decreasing at the same relative rate from ~20 % to ~15 %. The largest changes occur up to 12 h of plasma treatment.

Importantly, the ratio of fluorine/carbon is far smaller than the 1:2 ratio expected from the molecular structure of PVF, even for the untreated sample. To investigate this further, C1s detail spectra were recorded (Fig. 3c) that show two signals. The binding energies are in agreement with literature, with a signal representing the CHF carbon atom (written here as CHF) at 287.8 eV and another signal at 285.6 eV corresponding to the CH_2 carbon atom (CH_2) [24]. Even without fitting the two peaks, it is clearly evident that the areas of the two carbon peaks do not show the 1:1 ratio that would be expected for PVF. Instead, the CH_2 peak at lower binding energies is significantly larger than the CHF peak.

This phenomenon has been observed in literature before and can be explained by degradation of the polymer under X-rays, although the expected 1:1 ratio could be obtained for some XPS measurements of PVF [16,24,27,28]. The most in-depth study of this polymer behavior was conducted by Morgan *et al.*, who compared the degradation rates of different polymers under different X-ray sources [29]. However, the degradation process itself and the changes in the XP-spectrum during the exposure to X-rays remain unresolved. Although unraveling the degradation of polymers under X-rays is not the main focus of this work, we decided to investigate that change throughout the X-ray exposure in order to gain a better understanding of the measurements.

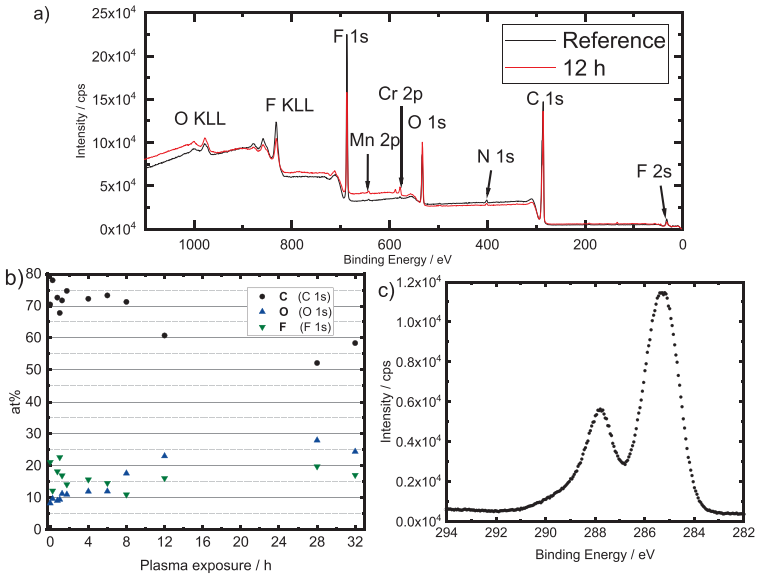

Fig. 3. XPS data on oxygen plasma treated PVF samples. The survey spectrum of pristine PVF, as well as of PVF treated for 12 h in the oxygen plasma (a) shows the presence of large amounts of oxygen on the sample as well as small amounts of contaminants. The quantification plot (b) reveals a steady increase in oxygen content during the exposure to the plasma, mostly at the cost of carbon. The C1s detail spectrum of untreated PVF (c) shows a deviation from the expected 1:1 ratio between the two carbon signals that are characteristic for PVF.

For this goal, the C1s spectrum was recorded continuously with less accuracy (0.2 eV steps, 20 ms/cycle) to achieve a shorter measurement time and thus better time resolution. During the degradation, the intensity of the CH_2 C1s signal increases, whereas the CHF C1s signal decreases in intensity. While the first scan showed the expected ratio between the two peaks of nearly 1:1, after 50 scans (~13 min of X-ray exposure), the ratio was 1.5:1 (Figure S3). This observed peak ratio corresponds to 20 % degradation, slightly higher than the 15 % Morgan *et al.* reported for a similar time [29]. Interestingly, Morgan *et al.* used a weaker (72 W) X-ray source on a ~1.7 times larger area (400 × 600 μm²), which leads to an X-ray dose per area that is only ~42 % of the value in this study [29].

To investigate how the sample changes during the X-ray exposure, a PCA was conducted on the set of continuous C1s spectra of untreated PVF. The first two principal components contained 98.96 % of variance (PC1: 98.10 %, PC2: 0.85 %), with subsequent PCs amounting for <0.1 % each. Loadings and scores plots of further PCs revealed no correlation to the X-ray exposure, making them not of interest in this study. The

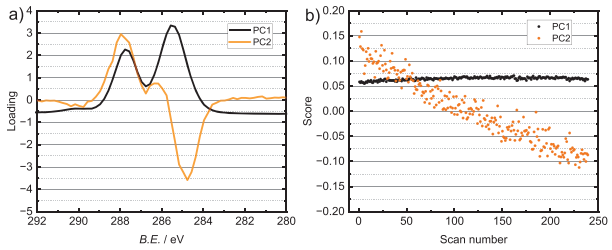

Fig. 4. Loadings plot (a) and scores plot (b) of the first two principal components obtained from a PCA conducted on a set of continuous X-ray photoelectron C1s spectra of untreated PVF.

the CHF and F quantification results. The slight overrepresentation of carbon over fluorine may be explained be the higher surface sensitivity of the F1s signal.

The C1s signal associated with oxygenated carbon is present in small amounts (~3 %) on the untreated PVF and reaches its long-term value of ~7 % after only 4 h of plasma treatment. The oxygen content also increases during the plasma treatment, however far more significantly: While the reference sample contained ~8 % oxygen, this value rises to ~25 % for longer exposure. Evidently, only a fraction of this oxygen can bind to carbon. Most oxygen atoms therefore likely exist as water, a product of the reaction of AO with the polymer sample that accumulates during the plasma exposure.

Identifying the beginning of the proposed quasi-equilibrium from these measurements is difficult, as the synergistic effects of degradation by oxygen plasma and degradation by X-Ray are unknown. Especially the reason for the intensity drop of the signals around 285 eV after 28 h remains unclear. Excluding this, the timeframe for the beginning of the quasi-equilibrium can be carefully proposed around 8–12 h.

3.4. ToF-SIMS

While XPS is useful to identify elements and their respective chemical states in a given sample, it can only provide limited information about the molecular structure of a sample. Therefore, XPS is often paired with complementary surface sensitive techniques, such as ToF-SIMS.

As a mass spectrum generated from a ToF-SIMS measurement usually contains hundreds of mass signals, it is difficult to evaluate the generated data by hand, especially if it is not yet known which peaks are of significant interest. Therefore, we employed PCA and MCR on a set of mass spectra of PVF samples that were exposed to the oxygen plasma for different durations. Notably, the F^-signal was excluded, as it oversaturated the detector during measurements.

PCA revealed 2 PCs accounted for 94.81 % of all variance between the measurements (PC1: 86.44 %, PC2: 8.37 %). The third PC still accounted for 3.91 % of variance, however its score indicates no correlation with plasma exposure. Therefore, the MCR was conducted with two factors, the results of which can be seen in Fig. 6.

The loadings plot (Fig. 6a) reveals vastly different compositions of the two factors: Factor 1 consists mostly of very small mass fragments, such as C^-, OH^- and C_2^-. At the same time, only a few mass signals are present in factor 1 at all. Factor 2 has loadings in nearly all detected mass signals with the highest contribution coming from $C_xH_y^-$ signals.

The scores plot (Fig. 6b) shows that factor 1 is not significantly present on samples exposed to the plasma for exposure times <2 h, however it rapidly becomes the dominant factor after 6 h of plasma treatment. For longer plasma exposure, the relative score reaches ~0.8 and fluctuates around that value. This again indicates that a quasi-equilibrium is achieved after ~8–12 h of plasma exposure.

When combining this information from both plots, it can be concluded that factor 1 must be associated with the degradation of PVF in the oxygen plasma, whereas factor 2 corresponds to the pristine state of PVF.

With the understanding that factor 1 represents the degradation products of the reaction of PVF with AO from the oxygen plasma, the mass signals contributing to factor 1 in the loadings plot can be interpreted even further: The absence of larger mass fragments, especially when compared to untreated PVF, indicate that the average carbon chain in the polymer becomes shorter during the exposure to oxygen plasma. However, it is important to keep in mind that the mass fragments detected during a SIMS measurement are the products of the interaction between the primary ion beam and the sample, rather than the composition of the surface itself. Nonetheless, it is noteworthy that only a single mass fragment (C_2O^-) contains both oxygen and carbon atoms. At the same time, this mass signal does not have any significant loading in both factors. The presence of oxygenated carbon species on the sample surface has been proven by XPS measurements, indicating that oxygenated carbon species are unstable secondary ions. Instead, those species likely fragment further into the single atom mass signals that are present in factor 1. The only other mass fragments containing oxygen atoms are O^- and OH^-, both of which can also be attributed to water that is formed during the oxidation of PVF.

When inspecting the carbon containing mass signals of factor 1 more closely, it becomes evident that they contain far less hydrogen than those of factor 2. Especially the C_x^- mass signals stand out here. For $x < 5$, these fragments are almost exclusive to factor 1, however starting with C_5^- they lose significance. It is unlikely that these ions are more stable secondary ions from a hydrogenated carbon chain than $C_xH_y^-$ fragments, as otherwise they would be expected to contribute significantly more to factor 2.

Therefore, their presence in factor 1 indicates the formation of oxygenated and less hydrogenated carbon chains that fragment during the primary ion bombardment into pure carbon and oxygen fragments.

3.5. Operando QMS

In order to gain further insight into the degradation process and to detect volatile degradation products, operando QMS was used during the plasma exposure of PVF. PCA was then applied to the consecutive mass scans to develop a better understanding of changes in the plasma composition. Each mass bin was normalized to the highest intensity of

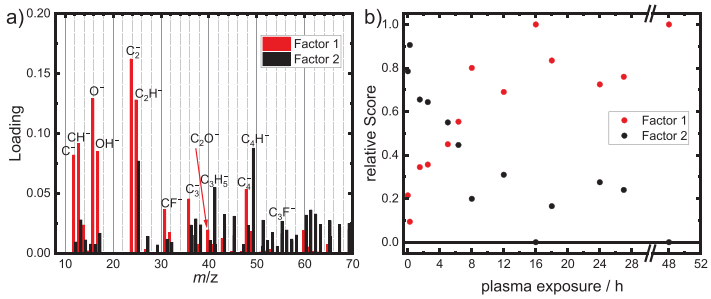

Fig. 6. Results of the MCR conducted on ToF-SIMS mass spectra of PVF samples exposed to the oxygen plasma for varying durations with two factors. The loadings (a) and scores (b) plots indicate that factor 1 is associated with damages from the oxygen plasma treatment, whereas factor 2 represents the pristine state of PVF.

loading plot of PC1 (Fig. 4) does not look close to the expected spectrum of pristine PVF. Instead, the peak representing the CHF signal at 287.8 eV is significantly smaller than the CH_2 peak at 285.6 eV. The scores plot reveals that PC1 serves as a "baseline" for all spectra as the score remains nearly constant throughout the measurement.

The second principal component appears to be of greater interest when trying to understand the degradation itself, as a correlation between the score and the scan number is clearly visible. At the start of the measurement, PC2 has a positive score, that decreases steadily during the X-ray exposure, eventually becoming negative. This is crucial to understand the loadings plot, as a positive loading corresponds to a signal observed at the beginning of the measurement, where the score is also positive. On the contrary, a negative loading multiplied by a positive score is subtracted from the early spectra. During later measurements, as the score also becomes negative, the product with the negative loading also becomes positive, which can be interpreted as the growth of a signal.

Three signals can be seen in the loadings plot for PC2: At 287.9 eV, a positive loading corresponds to the CHF signal that is present in the beginning of the measurement but degrades later on. At 286.1 eV, a far smaller, positive peak can be seen. We cautiously interpret this as a slight shift in the CH_2 signal towards higher binding energies due to the presence of a C-F bond on the neighboring carbon atom. During the degradation, as the amount of fluorinated carbon decreases, this shift is also reversed. While it might be possible that this is an over-interpretation of such a small signal, its peak-like shape and presence in the principal component that is without a doubt directly linked to the degradation, we are certain that reliable information is contained here.

The third peak is negative and has its minimum at 284.8 eV. We interpret this as adventitious carbon that is formed during the degradation of the CHF species. From the binding energy, a defluorination of the affected carbon atoms can be established.

The defluorination hypothesis is also supported by a simultaneous decrease in fluorine content. Importantly, the fluorine F1s signal only loses intensity, the binding energy does not change during the measurement. This was also confirmed by PCA conducted on a set of F1s spectra, where only PC1 showed a correlation with the scan number and its score steadily decreased during the experiment (Figure S4). Therefore, we do believe it is plausible to calibrate on the F1s signal at 686.9 eV, even though the signal is affected by degradation. At the same time, we cannot make statements regarding the chemical state of the fluorine atom after the degradation.

As the oxygen plasma induced degradation of PVF likely leads to a plethora of different carbon species on the sample, it was our goal to reduce noise in the C1s spectrum as much as possible. Therefore, before we noticed the degradation under X-rays, measurements took >1 h to get an optimal resolution. These measurement parameters had been employed on plasma treated PTFE, a material also reported to degrade under X-rays, in a previous study without observing any significant X-ray degradation [23]. Due to the structure of the measurement files, it is not possible to access the raw data for each spectrum, which would have enabled us to either investigate the first scans before the samples were significantly damaged by X-rays or apply a PCA to these measurements.

In Fig. 5(a), the C1s detail spectrum of PVF after 4 h of plasma exposure can be seen. To fit the recorded spectrum, 4 different Gauss-type curves were used: The peak at 289.1 eV is not present to this extend in PVF before the plasma treatment and has a very high FWHM of ~2 eV. Therefore, it can be attributed to an expected conglomeration of oxygenated carbon species that form during the oxygen plasma treatment. As we see no scientific benefit in attempting to fit a minute peak for each possible oxygenated species, a single, broad enveloping peak was used for quantification of the carbon atoms undergoing oxidation during the plasma exposure. In the following discussion, this will be referred to as "CO_x" in order to indicate oxygenated carbon.

The formation of many different species also serves as an explanation for the increased FWHM (~1.5 eV) of other peaks in the spectrum, as carbon-oxygen-bonds also affect the binding energy of the neighboring atom in the polymer chain. At 287.8 eV, the CHF C1s peak, one of the two characteristic signals of PVF, is visible. The other characteristic C1s peak of PVF, corresponding to CH_2, can be fitted at 285.7 eV. Due to the degradation of the sample under X-rays, as discussed in the previous section, this peak has a larger area than would be expected from PVF. To account for degradation of the material under X-rays, a second Gauss-type curve was used to simulate this behavior. Between all recorded spectra, the binding energies for all signals discussed varied ± 0.2 eV.

Quantification results from detail spectra of PVF samples exposed to the oxygen plasma for different durations can be seen in Fig. 5(b). Importantly, the data for the peak at ~285 eV is not shown individually, as the differentiation between the CH_2 and X-ray degraded CHF peak proved to be difficult to reproduce. Nonetheless, the PCA helped to clarify that the signal at 285 eV cannot be understood as a single peak and gave important insight into the makeup and evolution of this combined peak.

Due to the combination of two degradation processes (oxygen plasma and X-rays) on the sample, the observed trend of any given signal with increasing plasma exposure duration is more meaningful than the numerical value itself. The sum of content of CH_2 and X-ray degraded CHF decreases for samples treated for longer than 8 h from ~45 % to ~35 %. At the same time, the observed CHF signal decreased from ~22 % to ~17 %. As the fluorine content follows the same trend and has a similar value in all samples (±5 % absolute, geometric mean of CHF/F = 1.03), the vast majority of fluorine atoms are bound to CHF atoms. At the same time, this is an indicator that the oxygenated carbon is not bonded to fluorine, as in that case we would expect a larger divergence between

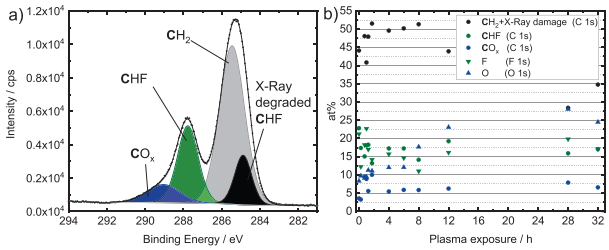

Fig. 5. Detail C1s spectrum of PVF exposed to the plasma for 4 h (a) as well as quantification results of XPS measurements on PVF exposed to the oxygen plasma for different durations (b). The C1s close-up reveals the presence of multiple, oxygenated carbon species, summarized in a broad ("CO_x") peak, as well as degradation induced by the X-rays. In the quantification plot, a steady increase of the oxygen content can be observed.

signal throughout all scans. This preparation of the data amplified changes in less detected mass fragments at the cost of mathematical accuracy. This cost is especially evident in the low variance contained in the first PCs. Due to the normalization, PC1 accounts for only 65.75 % of variance, followed by PC with 2.14 %. Nonetheless, the scores and loadings plots (Fig. 7, Figure S5) suggest that only PC1 is relevant to understand the changes occurring in the plasma atmosphere.

In the loadings plot of PC1 (Fig. 7a), only two signals exhibit significant negative loading: O^+ and O_2^+. Mass signals carrying a positive loading are far more numerous. These masses are associated with fragments containing hydrogen, carbon, oxygen and fluorine. It should be noted here that a higher positive value in the loadings plot does not necessarily indicate a high concentration of the mass fragment. Instead, due to the normalization used in the preparation of the data, it serves as an indicator that the corresponding mass signal is detected significantly more often in a scan where PC1 has a positive score compared to other scans. Similarly, a negative loading corresponds to a mass signal that is significantly more often detected in a scan with a negative score and less common in a scan with a positive score.

The scores plot (Fig. 7b) shows that only PC1 changes significantly during the experiment. Immediately after starting the plasma (marked gray), its score increases from negative values to positive ones and reaches a maximum after ~5 h. After ~29 h of active plasma, the score decreases until ~72 h, reaching negative values after ~ 46 h. Once the plasma is shut off after 80 h, the score drops even further.

When interpreting the scores plot, it becomes apparent that a positive score of PC1 must be associated with the reaction of the oxygen plasma with the PVF sample. Only while the plasma is active (gray background) and PVF is present in the chamber, the score is above 0. It becomes negative once the sample is degraded. It is important to note here that a slightly different setup was used here than in the experiments used in the preparation for mass loss and surface analysis. The presence of the ceramic mask that was necessary to define the exposed area and prevent bending of the sample proved to suppress mass signals in the operando QMS measurements. Therefore, the PVF sample was placed on two ceramic discs laying side by side and held in place by two masks lying on opposite ends of the sample. This led to higher exposure to AO and therefore higher degradation rates. As a result, the quasi-equilibrium discussed in the other sections of this study likely is reached already after ~5 h instead of 8 h. The full degradation of large parts of the sample after ~29 h (72 h with the other setup) was visually observed and is in agreement with the decreasing score after this exposure. Due to the inhomogeneity of the plasma in the plane of the PVF foil, the degradation of the sample was also inhomogeneous. While some parts of the sample were visually destroyed after 29 h of plasma exposure in this setup, other parts could still be observed, especially at the ends where the remains of the sample were held down by the ceramic mask. This serves as an explanation why the score does not reach its first minimum until much later (74 h of sample plasma exposure), as small amounts of PVF were still exposed to the oxygen plasma. This generated the mass signals coherent with degradation, albeit at much smaller scales than before. Another drop in the score of PC1 can be seen at 80 h, indicating the end of the active plasma.

When applying this knowledge to the loadings plot of PC1, it becomes evident that a positive loading in PC1 corresponds to mass signals being detected significantly more during the degradation of PVF in the oxygen plasma.

The mass signals with a significant positive loading consist of hydrogen, carbon, oxygen and fluorine and can therefore be interpreted as the products of the reaction between AO and the PVF sample. All these mass signals, such as CO_2^+, H_2O^+, HF^+ and C^+ are ions that would be expected as products from such a reaction. None of these fragments contain a CF-bond. Instead, the only fragments containing fluorine are F^+ and HF^+. From this, we can conclude that defluorination of the polymer carbon chain is an important step in the degradation process.

The oxygen species O^+ and O_2^+ both exhibit a negative loading, which means that these species are detected less commonly while PVF is being degraded. This is plausible, as oxygen species are reacting with the sample, and are thus no longer detected as pure oxygen and instead as ions such as H_2O^+ and CO_2^+.

Interestingly, no mass signal can be attributed to a mass fragment with more than one carbon atom, indicating that a complete scission of the carbon chain has taken place. We cannot immediately deduce whether that scission happened on the sample surface or afterwards, as the volatile fragments are exposed to the oxygen plasma before they can be detected by QMS. However, the significant loading of two fragments, C^+ and CO^+, in PC1 gives good evidence that a complete oxidation of the volatile fragments is not occurring. If a mean free path in the 10^{-3} m range is assumed, which is plausible for a gas discharge at 0.1 mbar, it is unlikely that a fragment reaches the capillary leading to the QMS at 15 cm distance from the sample without interacting with AO. Therefore, we assume that volatile fragments include small chains of more than one carbon atom that decay further, but are not completely oxidized on the way to the QMS detector. Due to the normalization that was employed in the data preparation for PCA, a high loading does not correlate to a large presence of a mass signal compared to other mass signals. Instead, the absolute detection currents of C^+, CO^+ and CO_2^+ need to be investigated to gain a deeper insight into the oxidation of carbon fragments.

All three detection currents of C^+, CO^+ and CO_2^+ (Fig. 8, Figure S6) reveal a similar trend after the plasma ignition, confirming the PCA results. All signals increase to a stable value and decrease simultaneously after ~29 h. Due to the logarithmic scaling, this is less visible than in the linear PCA scores plot. Importantly, between 0 and 29 h, the detection current of CO_2^+ is one order of magnitude larger than that of C^+

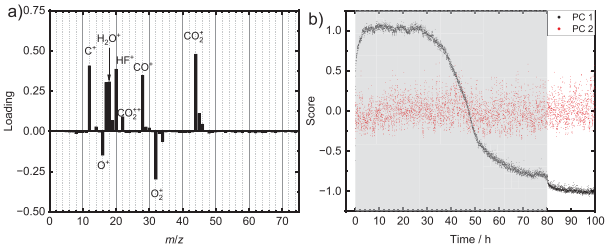

Fig. 7. Results of the PCA applied to consecutive mass spectra recorded by QMS during the PVF exposure to oxygen plasma. The loadings plot (a) shows the loadings of PC1, the only relevant principal component here. In the scores plot (b), the scores for both PC1 (black) and PC2 (red) can be seen. The period of active plasma is marked in gray.

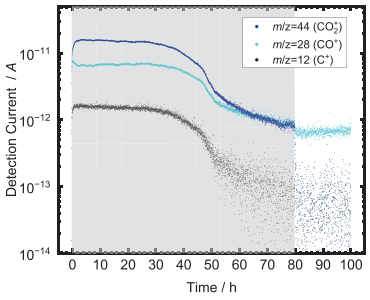

Fig. 8. Absolute detection currents of the mass signals corresponding to C^+, CO^+, and CO_2^+. The active plasma is shown in gray. All signals get detected more often after the start of the plasma and decline after the sample is completely eroded. CO_2^+, the most prominent signal is detected 10 times more often than C^+, the least abundant signal of the three.

and twice as large as that of CO^+. Although fragmentation of CO_2^+ might be possible inside the QMS, the large presence of C^+ and CO^+ can not plausibly explained solely by this fragmentation. Therefore, the presence of not fully oxidized carbon species serves as affirmation that a complete oxidation is not taking place inside the plasma.

Another interesting observation is the high base line for the mass signal associated with CO^+ after the end of the plasma. This can be explained by the shared nominal mass of 28 between CO and N_2. Although the mass resolution of the QMS cannot separate these two signals, an increase in N_2 content in the plasma chamber after the ignition is implausible whereas CO can easily be explained. After the end of the plasma, no further CO is being generated, however due to minor leaks, N_2 can enter the chamber from the atmosphere, explaining the relatively high detection current.

4. Discussion

Combining the results of mass loss experiments, SEM, XPS, ToF-SIMS and operando QMS measurements helps to gain a deeper understanding of the degradation mechanism of PVF in a low temperature oxygen plasma. The plasma consists mainly of free electrons, as well as positively charged oxygen species. Neutral species, such as AO make up a smaller, but still significant part, whereas negatively charged oxygen species only exist in even smaller amounts. To ensure that the degradation of PVF occurs by reaction with AO, a DC-Bias was used to prevent positively charged particles from colliding with the sample [30]. Instead, they were accelerated towards the driven electrode. The concentration of negatively charged oxygen species can be disregarded, leaving only neutral particles, as well as electrons to interact with the sample. Even though electrons can reach temperatures as high as 10,000 K under plasma conditions, their low mass prevents their kinetic impact from contributing to the degradation [30]. Nonetheless, the DC-Bias can lead to sputter effects at the driven electrode. While the amount of manganese and chromium on plasma treated samples might suggest sputter effects, their presence on reference samples not exposed to the plasma chamber provides a strong argument against sputter damage.

The mass loss experiments show linear degradation with time, indicating that the rate of the degradation process is not changing during the plasma exposure. Due to the minute mass losses in the first hours of mass loss experiments, the relative error margins are larger and it is difficult to exactly quantify the degradation rate for these points in time. Nonetheless, the observed mass losses were in very good agreement with the overall degradation rate, indicating no significant change in the degradation reaction throughout the experiments. Furthermore, the calculated erosion yield for PVF, obtained from the erosion yield of Kapton, was in good agreement with literature [3,26], indicating that the setup can be used to effectively simulate LEO conditions. The linear degradation is in very good agreement with the operando QMS data that showed no further change in the composition of the plasma atmosphere during the degradation. After ~8 h of plasma exposure, a quasi-equilibrium is reached where the degradation is steadily occurring, however the sample surface shows no change in morphology and composition. This could be concluded from SEM, XPS, ToF-SIMS and, to an extent, operando QMS measurements. A plasma exposure of 8 h corresponds to a fluence of $1.30 \bullet 10^{20}$ AO/cm² or 15 days in the LEO at a constant flux of 10^{14} atoms/cm². This fluence is one magnitude smaller than the value we obtained previously for the formation of a quasi-equilibrium at the surface of PTFE, a similar, but fully fluorinated polymer [23]. We interpret this as sign that the C-F bond stabilizes the polymer against reactions with AO. Increased fluorination of carbon atoms may therefore hinder the degradation of the polymer in LEO applications.

A key finding is the absence of CF fragments in both the loadings plot of factor 1 in the ToF-SIMS results, associated with degradation products on the surface of the sample, and in the operando quadrupole mass spectrum. This, again, can be understood as an indicator that the C-F bond is playing an important role in the degradation process. Since the XPS results also showed no presence of oxygenated and fluorinated carbon atoms, we see this as further support that of the two carbon atoms in the polymer, the unfluorinated one appears far more likely to react with AO.

Once oxidized, the carbon chain of the polymer becomes less chemically stable, as can be deduced from the absence of longer chain fragments in factor 1 of the ToF-SIMS results. This instability can lead to volatile fragments desorbing from the surface during the plasma exposure. These fragments are not limited to one carbon atom. Even though no fragment with a longer carbon chain was observed in operando QMS, we attribute this to further reactions of the volatile fragments with the oxygen plasma before detection.

Considering these insights, a simplified reaction scheme, which is presented in Fig. 9, can be devised. In a first step, AO breaks up the pristine polymer structure by inserting into the weak CH bond, followed by a second interaction with AO. This leads to the formation of water, which either diffuses into the polymer or desorbs into the plasma. The oxygenated carbon then likely reacts further, which may lead to small chain fragments desorbing from the surface. In the plasma, AO degrades

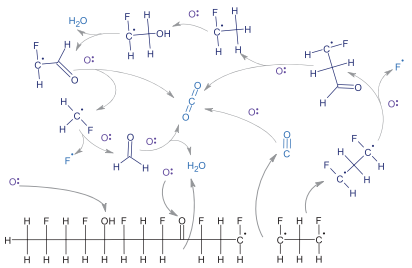

Fig. 9. Possible simplified reaction scheme for of the degradation of PVF (black) with atomic oxygen (purple). Changes in the sample that were detected during surface analysis, as well as further oxidation of possible volatile fragments (dark blue) are considered. Species detected during operando QMS measurements are shown in light blue.

these fragments further into F˙, H_2O, CO_2 and, in case of incomplete oxidation, CO.

To our knowledge, our result represents the most comprehensive study on the degradation of PVF in an oxygen plasma so far. While other studies have measured XPS on PVF treated with AO, the goal of these studies was not an in-depth understanding of the degradation reaction mechanism. Instead, XPS was used more qualitatively [15–17,29,31]. The combination of ToF-SIMS, XPS and QMS allowed us to gain insights into the degradation process that have not been observed before, such as the increased carbonization measured in ToF-SIMS or the presence of not fully oxidized carbon species in the plasma atmosphere detected by QMS. This allowed us to find further evidence for the protective properties of the CF bond against AO. We also observed the well-known phenomenon of defluorination of fluoropolymers [16,32]. While not directly relevant to the degradation of PVF under AO, the usage of PCA allowed us to gain a better understanding of the X-ray induced degradation of the polymer and the limitations of XPS measurements on fluoropolymers.

5. Conclusions

By using the combination of ToF-SIMS, XPS, SEM and operando QMS measurements together with multivariate statistical methods, we investigated the degradation of PVF in a low-temperature oxygen plasma to simulate low earth orbit conditions. The overall degradation rate does not change significantly during the plasma exposure. After 8 h, corresponding to a fluence of $1.30 \bullet 10^{20}$ oxygen atoms/cm^2, the sample has degraded to the extent that further exposure to AO will not significantly alter the composition or morphology of the surface. Instead, volatile fragments leave the surface and the underlying material becomes exposed. This quasi-equilibrium persists until the sample is completely degraded. The preferred reaction partner for AO is the unfluorinated carbon atom, making highly fluorinated polymers more durable in applications involving exposure to AO. During the degradation, the polymer chain becomes less stable and volatile, and not fully oxygenated fragments desorb from the surface. Furthermore, we were able to show that the F1s peak can be used for calibrating XP spectra of PVF despite the degradation the fluorinated carbon atom under X-Ray irradiation.

CRediT authorship contribution statement

Tobias Wagner: Writing – original draft, Visualization, Investigation, Formal analysis, Data curation. **Marcus Rohnke:** Writing – review & editing, Project administration, Conceptualization. **Joachim Sann:** Writing – review & editing, Formal analysis. **Jürgen Janek:** Writing – review & editing, Funding acquisition, Conceptualization.

Declaration of competing interest

The authors declare that they have no known competing financial interests or personal relationships that could have appeared to influence the work reported in this paper.

Acknowledgements

Financial support by the European Union (IWB EFRE program) under project no FPG 991003/2019 is gratefully acknowledged. The authors thank also the German Federal Ministry for Education and Research (BMBF) for funding the PHI Versa Probe 4 and the M6 Plus SIMS (project PROGRAL, no 03XP0427) as well as the German Research Foundation (DFG) for funding the Hybrid-SIMS under grant number INST 162/544-1 FUGG.

Supplementary materials

Supplementary material associated with this article can be found, in the online version, at doi:10.1016/j.polymdegradstab.2025.111820.

Data availability

Data will be made available on request.

References

[1] ESA Space Debris Office, *ESA´S ANNUAL SPACE ENVIRONMENT REPORT*, can be found under (2024). https://www.sdo.esoc.esa.int/environment_report/Space_Environment_Report_latest.pdf.
[2] B.J. Anderson, R.E. Smith, Natural orbital environment definition guidelines for use in aerospace vehicle development, NASA-TM-4527 (1994).
[3] J. Dever, B. Banks, K. de Groh, S. Miller, Degradation of Spacecraft Materials Handbook of Environmental Degradation of Materials, Elsevier, 2005.
[4] B.A. Banks, J.A. Backus, M.V. Manno, D.L. Waters, K.C. Cameron, K.K. de Groh, Prediction of atomic oxygen erosion yield for spacecraft polymers, J. Spacecr. Rockets 48 (14) (2011), https://doi.org/10.2514/1.48849.
[5] E. Grossman, I. Gouzman, Space environment effects on polymers in low earth orbit, Nucl. Instrum. Methods Phys. Res. B: Beam Interact. Mater. At. 208 (2003) 48, https://doi.org/10.1016/S0168-583X(03)00640-2.
[6] D. Angirasa, P.S. Ayyaswamy, Review of evaluation methodologies for satellite exterior materials in low earth orbit, J. Spacecr. Rockets 51 (2014) 750, https://doi.org/10.2514/1.A32742.
[7] K.K. de Groh, J.R. Gaier, R.L. Hall, M.P. Espe, D.R. Cato, J.K. Sutter, D. A. Scheimank, Insights into the Damage Mechanism of Teflon® FEP from the Hubble Space Telescope, High Perform. Polym. 12 (2000) 83, https://doi.org/10.1088/0954-0083/12/1/307.
[8] Z. Shpilman, I. Gouzman, G. Lempert, E. Grossman, A. Hoffman, rf plasma system as an atomic oxygen exposure facility, Rev. Sci. Instrum. 79 (2008) 48, https://doi.org/10.1063/1.2885044.
[9] J. Chen, N. Ding, Z. Li, W. Wang, Organic polymer materials in the space environment, Prog. Aerosp. Sci. 83 (2016) 37, https://doi.org/10.1016/j.paerosci.2016.02.002.
[10] Y. Huang, X. Tian, S. Yang, P.K. Chu, A ground-based radio frequency inductively coupled plasma apparatus for atomic oxygen simulation in low Earth orbit, Rev. Sci. Instrum. 78 (2007) 3220, https://doi.org/10.1063/1.2800766.
[11] K. Gotlib-Vainstein, I. Gouzman, O. Girshevitz, A. Bolker, N. Atar, E. Grossman, C. N. Sukenik, Liquid Phase Deposition of a Space-Durable, Antistatic SnO2 Coating on Kapton, ACS. Appl. Mater. Interfaces. 7 (2015) 3539, https://doi.org/10.1021/am5072817.
[12] I. Gouzman, O. Girshevitz, E. Grossman, N. Eliaz, C.N. Sukenik, Thin film oxide barrier layers. protection of kapton from space environment by liquid phase deposition of titanium oxide, ACS Appl. Mater. Interfaces 2010 2 (1835), https://doi.org/10.1021/am100113t.
[13] Bruce A. Banks, Grace C. Dill, R.J. Loftus, Kim K. de Groh, Sharon K. Miller, NASA/TM 2013 - 216613. Comparison of Hyperthal Ground Laboratory Erosion Yields with those in Low Earth Orbit, 2021.
[14] G. Broccia, *Cubesats in Low Earth Orbit. Perils and Countermeasures* (2021).
[15] M.A. Golub, T. Wydeven, R.D. Cormia, ESCA study of several fluorocarbon polymers exposed to atomic oxygen in low Earth orbit or within or downstream from a radio-frequency oxygen plasma, Polymer 30 (1989) 1571, https://doi.org/10.1016/0032-3861(89)90314-5.
[16] N. Vandencasteele, D. Merche, F. Reniers, XPS and contact angle study of N 2 and O 2 plasma-modified PTFE, PVDF and PVF surfaces, Surf. Interface Anal. 38 (2006) 526, https://doi.org/10.1002/sia.2255.
[17] T. Dufour, J. Hubert, N. Vandencasteele, P. Viville, R. Lazzaroni, F. Reniers, Competitive and synergistic effects between excimer VUV radiation and O radicals on the etching mechanisms of polyethylene and fluoropolymer surfaces treated by an atmospheric He–O 2 post-discharge", J. Phys. D: Appl. Phys. 46 (2013) 315203 https://doi.org/10.1088/0022-3727/46/31/315203.
[18] F.D. Egitto, Plasma etching and modification of organic polymers, Pure Appl. Chem. 62 (1990) 1699, https://doi.org/10.1351/pac199062091699.
[19] S.Abou Rich, P. Leroy, T. Dufour, N. Wehbe, L. Houssiau, F. Reniers, In-depth diffusion of oxygen into LDPE exposed to an Ar–O 2 atmospheric post-discharge. A complementary approach between AR-XPS and Tof-SIMS techniques, Surf. Interface Anal. 46 (2014) 164, https://doi.org/10.1002/sia.5403.
[20] P. Nancy, J. Joy, J. James, B. Joseph, S. Thomas, N. Kalarikkal, Spectroscopic and Mass Spectrometry Analyses of Plasma-Activated Polymeric Materials Non-Thermal Plasma Technology for Polymeric Materials, Elsevier, 2019.
[21] A. de Juan, J. Jaumot, R. Tauler, Multivariate Curve Resolution (MCR). Solving the mixture analysis problem, Anal. Methods 6 (2014) 4964, https://doi.org/10.1039/C4AY00571F.
[22] W.H. Lawton, E.A. Sylvestre, Self Modeling Curve Resolution, Technometrics 13 (1971) 617, https://doi.org/10.1080/00401706.1971.10488823.
[23] T. Wagner, M. Rohnke, J. Janek, Long-term degradation study of Polytetrafluoroethylene in a low temperature oxygen plasma, Polym. Degrad. Stab. 229 (2024) 110989, https://doi.org/10.1016/j.polymdegradstab.2024.110989.
[24] G. Beamson, D.J. Briggs, High resolution XPS of organic polymers. The Scienta ESCA300 Database, John Wiley, 1992. Chichester [etc.], op.

[25] Kim K.de Groh, Bruce A. Banks, Sharon K.R. Miller, Joyce A. Dever, "Chapter 28. Degradation of Spacecraft Materials".
[26] de Groh, K.K., Banks, B.A., Yi, G.T., Haloua, A., Imka, E.C., Mitchell, G.G., Asmar, O.C., Leneghan, H.A., Sechkar, E.A., "Overview of the MISSE 7 Polymers and Zenith Polymers Experiments After 1.5 Years of Space Exposure", *NASA-TM-2016-219167*2016.
[27] I. Mathieson, *Doctoral Thesis*, Loughborough University, 1995.
[28] D.T. Clark, W.J. Feast, D. Kilcast, W.K.R. Musgrave, Applications of ESCA to polymer chemistry. III. Structures and bonding in homopolymers of ethylene and the fluoroethylenes and determination of the compositions of fluoro copolymers, J. Polym. Sci. Polym. Chem. Ed. 11 (1973) 389, https://doi.org/10.1002/pol.1973.170110207.
[29] D.J. Morgan, S. Uthayasekaran, Revisiting degradation in the XPS analysis of polymers, Surf. Interface Anal. 55 (2023) 556, https://doi.org/10.1002/sia.7151.
[30] M.A. Lieberman, A.J. Lichtenberg, Principles of Plasma Discharges and Materials Processing, Wiley, 2005.
[31] S.D. Worley, C.H. Dai, J.L. Graham, A.T. Fromhold, K. Daneshvar, A.F. Whitaker, S. A. Little, Analyses of spacecraft polymeric materials, J. Spacecr. Rockets 23 (1986) 350, https://doi.org/10.2514/3.25810.
[32] M. Morra, E. Occhiello, F. Garbassi, Surface characterization of plasma-treated PTFE, Surf. Interface Anal. 16 (1990) 412, https://doi.org/10.1002/sia.740160186.

4. Conclusions

In this doctoral thesis, the degradation of two fluoropolymers, PTFE and PVF, during exposure to an oxygen plasma was studied. New insights into the degradation mechanism were gained by utilizing ToF–SIMS for characterization of the plasma treated samples, as well as operando QMS to monitor the plasma composition. Established techniques, such as XPS and SEM were also used to great effect. Importantly, the utilization of XPS has been refined from the approach in literature, where XPS is mostly used to obtain the fraction of each element at the sample surface. This is, to use a German idiom, *shooting sparrows with cannons*. It gets the job done, but the potential benefits of the methods are completely unused. Although not exhaustive, this work spotlights approaches to obtain deeper insight into the sample surfaces without needing to alter the instrumental setup.

As another result of this work, the established suite of characterization techniques employed in the study of space material degradation is shown to lack insight into the chemical makeup of the sample surface. ToF–SIMS is a method that works complementary to XPS and has been shown in the two papers of this dissertation to be ideally suited for the study of material decay in the LEO. Although the sample systems used in this work are not ideal SIMS samples due to their thickness and lack of electrical conductivity, ToF–SIMS measurements vastly expanded the information about the chemical composition of the polymer surface after AO exposure. Similarly, operando QMS provided additional insight into the degradation mechanism by analyzing the volatile products of the degradation reaction. This insight is extremely valuable, as it cannot easily be obtained in real space flight experiments.

Furthermore, MVS methods fit well into the aforementioned new (at least to space material degradation) characterization methods. As a ToF–SIMS data set contains a high information density and many hundreds of thousands of datapoints, chemometrics are shown in this work to provide important noise reduction and showcase trends, which lead to a more complete understanding of the obtained data. The application of PCA to XP spectra was shown here to lead to a better understanding of the degradation of PVF under X-rays, which in turn was critical to formulate a recommendation for the calibration of fluoropolymer XPS data. The results in this work show that MVS methods are underrepresented in spacecraft material studies, as well as in surface science as a whole.

The approach in this doctoral thesis to characterize the surface of AO treated fluoropolymers by a physical-chemical method suite provides new insight into the degradation mechanism by identifying both reaction products in the atmosphere and species on the sample surface. The application of PCA and MCR yielded deeper insights into the changes occurring in the system during plasma treatment. Fluorine was identified to delay chemical reactions of atomic oxygen with the polymer.

5. Outlook

This work presents chemical analysis techniques novel to the field of material degradation in the LEO that can complement current understanding. In order to fully evaluate whether these methods hold up for other material classes and different environmental conditions, more studies need to be conducted. Although QMS is one of the mentioned techniques, the potential of its use is limited to LEO environmental degradation that leads to material loss in the form of volatile fragments that can be detected. ToF–SIMS should prove more generally suited for the field of research. Especially if used in tandem with chemometrics, SIMS measurements promise high information densities that can supplement current characterization methods. A closer inspection of XPS results by the evaluation of C1s detail spectra, as well as the survey spectra, similarly revealed further insights that were not present in previous publications.

Fluorine was identified to make the material more resistant towards chemical reactions with AO. It stands therefore to reason that increasing the degree of fluorination in other, more complex polymers than polyethylene-derivates, such as Kapton, may also lead to increased resistance against AO. Currently, composite materials are used in the LEO to counteract erosion by oxygen, but a more stable polymer matrix could increase the lifespan of such materials under space conditions even further. Studies on the feasibility of such fluorination and the suitability of the resulting polymer for the intended use would of course need to be conducted as well.

More generally than the two points above, the advantage provided by the application of PCA and MCR was highlighted in this work on multiple occasions. These tools, and chemometrics in general, are severely underutilized in the field of surface science. The cost to feed a dataset into the algorithm, which is inherently possible in both the OriginLab and SurfaceLab software is negligible, whereas the potential benefits are tremendous. The recently created *Data Science* course of study at Justus–Liebig–University indicates a promising trend, if deeper connections between the chemical institutes and students of this degree can be established.

6. References

[1] Albertus, *De mineralibus et rebus metallicis libri quinque*, Apud I. Birckmannum & T. Baumium, Coloniæ, **1569**.

[2] J. Dever, B. Banks, K. de Groh, S. Miller in *Handbook of Environmental Degradation of Materials* (Ed.: M. Kutz), William Andrew Publishing, Norwich, NY, **2005**, pp. 465–501.

[3] "Online Index of Objects Launched into Outer Space", can be found under https://www.unoosa.org/oosa/osoindex/search-ng.jspx?lf_id=&utm. 2026-02-08.

[4] NASA, "Hubble", can be found under https://science.nasa.gov/mission/hubble/. 2026-02-25.

[5] NASA, "FIRMS", can be found under https://www.Earthdata.nasa.gov/data/projects/lance#ed-lance-disclaimer. 2026-02-25.

[6] NASA, "ISS", can be found under https://www.nasa.gov/international-space-station/. 2026-02-25.

[7] B. E. Holmes, V. T. Oiko, P. C. Roberts, "A review of satellite-based atomic oxygen sensing methods", *Progress in Aerospace Sciences* **2023**, *137*, 100886; DOI 10.1016/j.paerosci.2023.100886.

[8] M. R. Reddy, "Effect of low Earth orbit atomic oxygen on spacecraft materials", *JOURNAL OF MATERIALS SCIENCE* **1995**, *30*, 281; DOI 10.1007/BF00354389.

[9] de Groh, K.K., Banks, B.A., Yi, G.T., Haloua, A., Imka, E.C., Mitchell, G.G., Asmar, O.C., Leneghan, H.A., Sechkar, E.A, "Overview of the MISSE 7 Polymers and Zenith Polymers Experiments After 1.5 Years of Space Exposure", *NASA-TM-2016-219167* **2016**.

[10] T. Ghidini, "Materials for space exploration and settlement", *Nature Mater* **2018**, *17*, 846; DOI 10.1038/s41563-018-0184-4.

[11] E. Grossman, I. Gouzman, "Space environment effects on polymers in low Earth orbit", *Nuclear Instruments and Methods in Physics Research Section B: Beam Interactions with Materials and Atoms* **2003**, *208*, 48; DOI 10.1016/S0168-583X(03)00640-2.

[12] K. M. Chang, D. Das, L. Salvati III., L. M. Dean, R. Keshari, M. Garg, D. D. Dlott, I. Chasiotis, N. R. Sottos, "Durable and impact-resistant thermoset polymers for the extreme environment of low Earth orbit", *Extreme Mechanics Letters* **2023**, *64*, 102089; DOI 10.1016/j.eml.2023.102089.

[13] B. A. Banks, J. A. Backus, M. V. Manno, D. L. Waters, K. C. Cameron, K. K. de Groh, "Prediction of Atomic Oxygen Erosion Yield for Spacecraft Polymers", *Journal of Spacecraft and Rockets* **2011**, *48*, 14; DOI 10.2514/1.48849.

[14] J. D. Williams, C. C. Farnell, P. B. Shoemaker, J. A. Vaughn, T. A. Schneider, "Ground-Based Simulation of Low-Earth Orbit Plasma Conditions: Plasma Generation and Characterization", can be found under https://ntrs.nasa.gov/citations/20040111049. 2026-03-09.

[15] Z. Shpilman, I. Gouzman, G. Lempert, E. Grossman, A. Hoffman, "rf plasma system as an atomic oxygen exposure facility", *Review of Scientific Instruments* **2008**, *79*, 48; DOI 10.1063/1.2885044.

[16] J. Chen, N. Ding, Z. Li, W. Wang, "Organic polymer materials in the space environment", *Progress in Aerospace Sciences* **2016**, *83*, 37; DOI 10.1016/j.paerosci.2016.02.002.

[17] H. Nobis, B. Sticker, *BAND II De revolutionibus libri sex: Neue synoptisch-kritische Ausgabe des lateinischen Textes der Editio prima und des Autographs*, AKADEMIE VERLAG, Berlin, **1949;** DOI 10.1524/9783050082677.

[18] N. H. Crisp, P. Roberts, S. Livadiotti, V. Oiko, S. Edmondson, S. J. Haigh, C. Huyton, L. A. Sinpetru, K. L. Smith, S. D. Worrall et al., "The benefits of very low Earth orbit for Earth observation missions", *Progress in Aerospace Sciences* **2020**, *117*, 100619; DOI 10.1016/j.paerosci.2020.100619.

[19] L. A. Teichman, B. A. Stein, "NASA/SDIO Space Environmental Effects on Materials Workshop, part 1", can be found under https://ntrs.nasa.gov/citations/19890014157. 2026-03-24.

[20] N. H. Crisp, P. Roberts, S. Livadiotti, V. Oiko, S. Edmondson, S. J. Haigh, C. Huyton, L. A. Sinpetru, K. L. Smith, S. D. Worrall et al., "The benefits of very low Earth orbit for Earth observation missions", *Progress in Aerospace Sciences* **2020**, *117*, 100619; DOI 10.1016/j.paerosci.2020.100619.

[21] E. Murad, "The shuttle glow phenomenon", *Annual review of physical chemistry* **1998**, *49*, 73; DOI 10.1146/annurev.physchem.49.1.73.

[22] P. M. Banks, P. R. Williamson, W. J. Raitt, "Space shuttle glow observations", *Geophysical Research Letters* **1983**, *10*, 118; DOI 10.1029/GL010i002p00118.

[23] C. Xu, B. Sun, T. Gustafsson, K. Edström, D. Brandell, M. Hahlin, "Interface layer formation in solid polymer electrolyte lithium batteries: an XPS study. An XPS study", *J. Mater. Chem. A* **2014**, *2*, 7256; DOI 10.1039/C4TA00214H.

[24] A. C. Tribble, "The Space Environment: Implications for Spacecraft Design" **2020;** DOI 10.2307/j.ctvzxx9nh.

[25] A. Tan, *Theory Of Satellite Fragmentation In Orbit (Second Edition)*, World Scientific, **2025**.

[26] ESA Space Debris Office, *ESA'S ANNUAL SPACE ENVIRONMENT REPORT*, **2024,** can be found under https://www.sdo.esoc.esa.int/environment_report/Space_Environment_Report_latest.pdf.

[27] "Germany eyes lasers, spy satellites in military space spending splurge", can be found under https://www.reuters.com/science/germany-eyes-lasers-spy-satellites-military-space-spending-splurge-2026-02-03/. 2026-02-27.

[28] E. M. Silverman, "Space environmental effects on spacecraft: LEO materials selection guide, part 1", can be found under https://ntrs.nasa.gov/citations/19960000860. 2026-03-24.

[29] E. M. Silverman, "Space environmental effects on spacecraft: LEO materials selection guide, part 2", can be found under https://ntrs.nasa.gov/citations/19960000861. 2026-03-24.

[30] Thomas G. Roberts, "Space Launch to Low Earth Orbit: How Much Does It Cost?", can be found under https://aerospace.csis.org/data/space-launch-to-low-Earth-orbit-how-much-does-it-cost/. 2026-03-10.

[31] Z. Iskanderova, M. Tagawa, J. Kleiman, S. Nishioka, S. Horimoto, "Space polymers erosion in simulated LEO and VLEO environments", *IOP Conf. Ser.: Mater. Sci. Eng.* **2023**, *1287*, 12039; DOI 10.1088/1757-899X/1287/1/012039.

[32] S. Packirisamy, D. Schwam, M. H. Litt, "Atomic oxygen resistant coatings for low Earth orbit space structures", *JOURNAL OF MATERIALS SCIENCE* **1995**, *30*, 308; DOI 10.1007/BF00354390.

[33] J. Kleiman, Z. Iskanderova, R. Ng, A. Tang, "New Materials for LEO, GEO and Planetary Environments: Preliminary Results from MISSE-17 Experiment", *IOP Conf. Ser.: Mater. Sci. Eng.* **2025**, *1328*, 12017; DOI 10.1088/1757-899X/1328/1/012017.

[34] X. Zhao, Z. Li, P. Yang, Y. Liang, "A ground-based experimental study of atomic oxygen effects on polymer-matrix composite", *Journal of Thermoplastic Composite Materials* **2025;** DOI 10.1177/08927057251344162.

[35] K. M. Chang, D. Das, L. Salvati III., L. M. Dean, R. Keshari, M. Garg, D. D. Dlott, I. Chasiotis, N. R. Sottos, "Durable and impact-resistant thermoset polymers for the extreme environment of low Earth orbit", *Extreme Mechanics Letters* **2023**, *64*, 102089; DOI 10.1016/j.eml.2023.102089.

[36] S. R. White, N. R. Sottos, P. H. Geubelle, J. S. Moore, M. R. Kessler, S. R. Sriram, E. N. Brown, S. Viswanathan, "Autonomic healing of polymer composites", *Nature* **2001**, *409*, 794; DOI 10.1038/35057232.

[37] K. M. Chang, "Autonomous materials for active erosion resistance in low-Earth orbit", can be found under https://www.ideals.illinois.edu/items/129398. 2026-03-24.

[38] L. Pernigoni, U. Lafont, A. M. Grande, "Self-healing materials for space applications: overview of present development and major limitations", *CEAS Space J* **2021**, *13*, 341; DOI 10.1007/s12567-021-00365-5.

[39] J. Chen, N. Ding, Z. Li, W. Wang, "Organic polymer materials in the space environment", *Progress in Aerospace Sciences* **2016**, *83*, 37; DOI 10.1016/j.paerosci.2016.02.002.

[40] E. Grossman, I. Gouzman, G. Lempert, Y. Noter, Y. Lifshitz in *Protection of Materials and Structures from Space Environment*, Springer, Dordrecht, **2004**, pp. 379–390.

[41] T. J. Patrick, "Space environment and vacuum properties of spacecraft materials", *Vacuum* **1981**, *31*, 351; DOI 10.1016/S0042-207X(81)80042-5.

[42] K. K. de Groh, B. A. Banks, "Atomic Oxygen Erosion Data from the MISSE 2-8 Missions", can be found under https://ntrs.nasa.gov/citations/20190025445. 2026-03-24.

[43] Z. Hooshangi, S. A. Hossein Feghhi, R. Saeedzadeh, "The effects of low Earth orbit atomic oxygen on the properties of Polytetrafluoroethylene", *Acta Astronautica* **2016**, *119*, 233; DOI 10.1016/j.actaastro.2015.11.031.

[44] A. Goto, K. Yukumatsu, Y. Tsuchiya, E. Miyazaki, Y. Kimoto, "Changes in optical properties of polymeric materials due to atomic oxygen in very low Earth orbit", *Acta Astronautica* **2023**, *212*, 70; DOI 10.1016/j.actaastro.2023.07.036.

[45] M. Schulze, K. Bolwin, E. Glzow, W. Schnurnberger, "XPS analysis of PTFE decomposition due to ionizing radiation", *Fresenius J Anal Chem* **1995**, *353*, 778; DOI 10.1007/BF00321370.

[46] F. Awaja, J. B. Moon, S. Zhang, M. Gilbert, C. G. Kim, P. J. Pigram, "Surface molecular degradation of 3D glass polymer composite under low Earth orbit simulated space environment", *Polymer Degradation and Stability* **2010**, *95*, 987; DOI 10.1016/j.polymdegradstab.2010.03.013.

[47] H. S. Judeikis, "Space Radiation Effects on Teflon Films", can be found under https://apps.dtic.mil/sti/html/tr/ADA076613/. 2026-03-24.

[48] X.-H. Zhao, Z.-G. Shen, Y.-S. Xing, S.-L. Ma, "An experimental study of low Earth orbit atomic oxygen and ultraviolet radiation effects on a spacecraft material – polytetrafluoroethylene", *Polymer Degradation and Stability* **2005**, *88*, 275; DOI 10.1016/j.polymdegradstab.2004.11.002.

[49] E. Hoyer, "McKellar, J. F.(†), Allen, N. S.: Photochemistry of man-made polymers. Hrsg. Applied Scienc Publishers Ltd., London 1979. 306 S., 138 Abb., 37 Tab., London: Applied Science Publishers Ltd. 1979. £24,00", *J. Prakt. Chem.* **1982**, *324*, 1071; DOI 10.1002/prac.19823240634.

[50] W. K. Stuckey, M. J. Meshishnek, "Space Environmental Stability of Tedlar with Multi-Layer Coatings: Space Simulation Testing Results", can be found under https://apps.dtic.mil/sti/html/tr/ADA387139/. 2026-03-24.

[51] G. Beamson, D. J. Briggs, *High resolution XPS of organic polymers. The Scienta ESCA300 database*, John Wiley, Chichester [etc.], **1992**.

[52] T. Wagner, M. Rohnke, J. Sann, J. Janek, "Investigation of the Polyvinylfluoride degradation mechanism under atomic oxygen exposure", *Polymer Degradation and Stability* **2025**, 111820; DOI 10.1016/j.polymdegradstab.2025.111820.

[53] M. Morra, E. Occhiello, F. Garbassi, "Surface characterization of plasma-treated PTFE", *Surface and Interface Analysis* **1990**, *16*, 412; DOI 10.1002/sia.740160186.

[54] R. I. Gonzalez, S. H. Phillips, G. B. Hoflund, "In situ atomic oxygen erosion study of fluoropolymer films using X-ray photoelectron spectroscopy", *J of Applied Polymer Sci* **2004**, *92*, 1977; DOI 10.1002/app.20009.

[55] G. B. Hoflund, M. L. Everett, "Chemical Alteration of Poly(tetrafluoroethylene) (TFE) Teflon Induced by Exposure to Hyperthermal Atomic Oxygen", *J. Phys. Chem. B* **2004**, *108*, 15721; DOI 10.1021/jp048975j.

[56] N. Vandencasteele, F. Reniers, "Surface characterization of plasma-treated PTFE surfaces. An OES, XPS and contact angle study", *Surface & Interface Analysis* **2004**, *36*, 1027; DOI 10.1002/sia.1829.

[57] M. A. Golub, T. Wydeven, R. D. Cormia, "ESCA study of several fluorocarbon polymers exposed to atomic oxygen in low Earth orbit or within or downstream from a radio-frequency oxygen plasma", *Polymer* **1989**, *30*, 1571; DOI 10.1016/0032-3861(89)90314-5.

[58] A. Gindulytė, L. Massa, B. A. Banks, S. K. R. Miller, "Direct C−C Bond Breaking in the Reaction of O(3 P) with Flouropolymers in Low Earth Orbit", *J. Phys. Chem. A* **2002**, *106*, 5463; DOI 10.1021/jp0132578.

[59] A. Gindulytė, L. Massa, B. A. Banks, S. K. Rutledge, "Can Hydrocarbon Chains Be Disrupted by Fast O(3P) Atoms?", *J. Phys. Chem. A* **2000**, *104*, 9976; DOI 10.1021/jp001817h.

[60] H. N. Yeritsyan, A. A. Sahakyan, N. E. Grigoryan, V. V. Harutyunyan, V. V. Arzumanyan, V. M. Tsakanov, B. A. Grigoryan, H. D. Davtyan, V. S. Dekhtiarov, C. J. Rhodes et al., "Space low Earth orbit environment simulator for ground testing materials and devices", *Acta Astronautica* **2021**, *181*, 594; DOI 10.1016/j.actaastro.2021.01.030.

[61] Chae-Hwan Lim, Jae-Won Shim, Seong-Haeng Heo, Won-Ho Choi 2 and Young-Woo Nam, *Space Oxide/Oxide Ceramic Composites with Atomic Oxygen Resistance for VLEO Stealthy Satellites.* 1st International Conference on Drones and Unmanned Systems (DAUS' 2025), **2025;** DOI 10.13140/RG.2.2.18747.94240.

[62] R. Yang, K. Tang, X. Lang, C. He, Y. Liu, Y. Liu, "Design of Low-Cost Simulation Space Micro Debris Launch Device", *Aerospace* **2024**, *11*, 577; DOI 10.3390/aerospace11070577.

[63] Alexander von Humboldt, *Kosmos*, Cotta, Stuttgart, Tübingen, **1845**.

[64] "XVI. Contributions to molecular physics in high vacua. Magnetic deflection of molecular trajectory. - Laws of magnetic rotation in high and low vacua. - Phosphorogenic properties of molecular discharge", *Phil. Trans. R. Soc.* **1879**, *170*, 641; DOI 10.1098/rstl.1879.0076.

[65] I. Langmuir, "Oscillations in Ionized Gases", *Proc. Natl. Acad. Sci. U.S.A.* **1928**, *14*, 627; DOI 10.1073/pnas.14.8.627.

[66] William Robert Grove, "VII. On the electro-chemical polarity of gases", *Phil. Trans. R. Soc.* **1852**, *142*, 87; DOI 10.1098/rstl.1852.0008.

[67] E. Becquerel, "RECHERCHES SUR LA TRANSMISSION DE L'ÉLECTRICITE AU TRAVERS DES G AZ A DES TEMPÉRATURES ÉLEVÉES", *Annales de Chimie* **1853**, 355.

[68] A. Fridman, *Plasma Chemistry*, Cambridge University Press, **2009;** DOI 10.1017/CBO9780511546075.

[69] T. Mieno, *Plasma Science and Technology - Progress in Physical States and Chemical Reactions*, InTech, **2016;** DOI 10.5772/60692.

[70] M. A. Lieberman, A. J. Lichtenberg, *Principles of plasma discharges and materials processing*, Wiley-Interscience, Hoboken, N.J., **2005**.

[71] P. Dietz, W. Gärtner, Q. Koch, P. E. Köhler, Y. Teng, P. R. Schreiner, K. Holste, P. J. Klar, "Molecular propellants for ion thrusters", *Plasma Sources Sci. Technol.* **2019**, *28*, 84001; DOI 10.1088/1361-6595/ab2c6c.

[72] G. E. Berg, *FINAL SNAPSHOT PERFORMANCE REPORT*, Office of Scientific and Technical Information (OSTI), **1966;** DOI 10.2172/4474823.

[73] F. F. Chen, *Introduction to Plasma Physics and Controlled Fusion*, Springer International Publishing, Cham, **2016;** DOI 10.1007/978-3-319-22309-4.

[74] M. I. Boulos, P. Fauchais, E. Pfender, *Thermal Plasmas. Fundamentals and Applications*, Springer US; Imprint: Springer, New York, NY, **1994;** DOI 10.1007/978-1-4899-1337-1.

[75] G. Janzen, *Plasmatechnik. Grundlagen, Anwendungen, Diagnostik*, Hüthig, Heidelberg, **1992**.

[76] Y. P. Raizer, M. N. Shneider, N. A. Yatsenko, *Radio-Frequency Capacitive Discharges*, CRC Press, **2017;** DOI 10.1201/9780203741337.

[77] B. M. Smirnov, *Theory of Gas Discharge Plasma*, Springer International Publishing, Cham, **2015;** DOI 10.1007/978-3-319-11065-3.

[78] H. Ebert, E. Wiedemann, "Ueber electrische Entladungen. Erzeugung electrischer Oscillationen und die Beziehung von Entladungsröhren zu denselben", *Annalen der Physik* **1893**, *285*, 1; DOI 10.1002/andp.18932850502.

[79] M. Göttlicher, M. Rohnke, Y. Moryson, J. Thomas, J. Sann, A. Lode, M. Schumacher, R. Schmidt, S. Pilz, A. Gebert et al., "Functionalization of Ti-40Nb implant material with strontium by reactive sputtering", *Biomater Res* **2017**, *21*, 1; DOI 10.1186/s40824-017-0104-8.

[80] M. Sackers, C. Busch, T. V. Tsankov, U. Czarnetzki, P. Mertens, O. Marchuk, "Plasma parameters and tungsten sputter rates in a high-frequency CCP", *Phys. Plasmas* **2022**, *29;* DOI 10.1063/5.0083613.

[81] V. M. Donnelly, A. Kornblit, "Plasma etching: Yesterday, today, and tomorrow. Yesterday, today, and tomorrow", *Journal of Vacuum Science & Technology A* **2013**, *31*, 10; DOI 10.1116/1.4819316.

[82] G. S. Oehrlein, S. M. Brandstadter, R. L. Bruce, J. P. Chang, J. C. DeMott, V. M. Donnelly, R. Dussart, A. Fischer, R. A. Gottscho, S. Hamaguchi et al., "Future of plasma etching for microelectronics: Challenges and opportunities", *J. Vac. Sci. Technol. B* **2024**, *42;* DOI 10.1116/6.0003579.

[83] S. Sammut, "A Comprehensive Review of Plasma Cleaning Processes Used in Semiconductor Packaging", *Applied Sciences* **2025**, *15*, 7361; DOI 10.3390/app15137361.

[84] R. Morent, N. de Geyter, T. Desmet, P. Dubruel, C. Leys, "Plasma Surface Modification of Biodegradable Polymers: A Review. A Review", *Plasma Processes & Polymers* **2011**, *8*, 171; DOI 10.1002/ppap.201000153.

[85] A. J. Lichtenberg, V. Vahedi, M. A. Lieberman, T. Rognlien, "Modeling electronegative plasma discharges", *J. Appl. Phys.* **1994**, *75*, 2339; DOI 10.1063/1.356252.

[86] C. Lee, D. B. Graves, M. A. Lieberman, D. W. Hess, "Global Model of Plasma Chemistry in a High Density Oxygen Discharge", *J. Electrochem. Soc.* **1994**, *141*, 1546; DOI 10.1149/1.2054960.

[87] M. Rohnke, *Kinetische Untersuchungen an der Phasengrenze zwischen Sauerstoffionenleitern und Niedertemperatur-Sauerstoffplasmen*, **2003;** DOI 10.22029/jlupub-9971.

[88] T. Kitajima, K. Noro, T. Nakano, T. Makabe, "Influence of driving frequency on oxygen atom density in O 2 radio frequency capacitively coupled plasma", *J. Phys. D: Appl. Phys.* **2004**, *37*, 2670; DOI 10.1088/0022-3727/37/19/010.

[89] A. D. Tserepi, T. A. Miller, "Spatially and temporally resolved absolute O-atom concentrations in etching plasmas", *Journal of Applied Physics* **1995**, *77*, 505; DOI 10.1063/1.359032.

[90] G. Hancock, M. J. Toogood, "Laser-induced fluorescence of oxygen atoms in a plasma reactor", *Applied Physics Letters* **1992**, *60*, 35; DOI 10.1063/1.107486.

[91] E. J. H. Collart, J. A. G. Baggerman, R. J. Visser, "Excitation mechanisms of oxygen atoms in a low pressure O2 radio-frequency plasma", *J. Appl. Phys.* **1991**, *70*, 5278; DOI 10.1063/1.350237.

[92] T. Wagner, M. Rohnke, J. Janek, "Long-term degradation study of Polytetrafluoroethylene in a low temperature oxygen plasma", *Polymer Degradation and Stability* **2024**, *229*, 110989; DOI 10.1016/j.polymdegradstab.2024.110989.

[93] A. Benninghoven, "Die Analyse monomolekularer FestkörperoberflÄchenschichten mit Hilfe der SekundÄrionenemission", *Z. Physik* **1970**, *230*, 403; DOI 10.1007/BF01394486.

[94] J. C. Vickerman, I. S. Gilmore, *Surface Analysis – The Principal Techniques*, Wiley, **2009;** DOI 10.1002/9780470721582.

[95] P. van der Heide, *Secondary ion mass spectrometry*. *An introduction to principles and practices*, Wiley, Hoboken, NJ, **2014;** DOI 10.1002/9781118916780.

[96] H. Gnaser, "SIMS Detection in the 1012 Atoms cm-3 Range", *Surface & Interface Analysis* **1997**, *25*, 737; DOI 10.1002/(SICI)1096-9918(199709)25:10<737::AID-SIA294>3.0.CO;2-M.

[97] S. Maharrey, R. Bastasz, R. Behrens, A. Highley, S. Hoffer, G. Kruppa, J. Whaley, "High mass resolution SIMS", *Applied Surface Science* **2004**, *231-232*, 972; DOI 10.1016/j.apsusc.2004.03.197.

[98] A. Benninghoven, "Surface analysis by Secondary Ion Mass Spectrometry (SIMS)", *Surface Science* **1994**, *299-300*, 246; DOI 10.1016/0039-6028(94)90658-0.

[99] A. Einstein, "Über einen die Erzeugung und Verwandlung des Lichtes betreffenden heuristischen Gesichtspunkt", *Annalen der Physik* **1905**, *322*, 132; DOI 10.1002/andp.19053220607.

[100] J. F. Watts, J. Wolstenholme, *An introduction to surface analysis by XPS and AES*, Wiley, Hoboken, NJ, **2020;** DOI 10.1002/9781119417651.

[101] C. M. Chan, L.-T. Weng, "Surface Characterization of Polymer Blends by XPS and ToF-SIMS", *Materials* **2016**, *9*, 655; DOI 10.3390/ma9080655.

[102] C. S. Fadley, "Angle-resolved x-ray photoelectron spectroscopy", *Progress in Surface Science* **1984**, *16*, 275; DOI 10.1016/0079-6816(84)90001-7.

[103] John Dee, "The Mathematicall Praeface to Elements of Geometrie of Euclid of Megara", can be found under https://www.gutenberg.org/ebooks/22062. 2026-03-24.

[104] F. L. Gewers, G. R. Ferreira, H. F. D. Arruda, F. N. Silva, C. H. Comin, D. R. Amancio, L. D. F. Costa, "Principal Component Analysis", *ACM Comput. Surv.* **2022**, *54*, 1; DOI 10.1145/3447755.

[105] M. Greenacre, P. J. F. Groenen, T. Hastie, A. I. D'Enza, A. Markos, E. Tuzhilina, "Principal component analysis", *Nat Rev Methods Primers* **2022**, *2*, 559; DOI 10.1038/s43586-022-00184-w.

[106] I. T. Jolliffe, J. Cadima, "Principal component analysis. A review and recent developments", *Philosophical transactions. Series A, Mathematical, physical, and engineering sciences* **2016**, *374*, 20150202; DOI 10.1098/rsta.2015.0202.

[107] K. Pearson, "LIII. On lines and planes of closest fit to systems of points in space", *The London, Edinburgh, and Dublin Philosophical Magazine and Journal of Science* **1901**, *2;* DOI 10.1080/14786440109462720.

[108] W. H. Lawton, E. A. Sylvestre, "Self Modeling Curve Resolution", *Technometrics* **1971**, *13*, 617; DOI 10.1080/00401706.1971.10488823.

[109] O. S. Borgen, B. R. Kowalski, "An extension of the multivariate component-resolution method to three components", *Analytica Chimica Acta* **1985**, *174*, 1; DOI 10.1016/S0003-2670(00)84361-5.

[110] O. S. Borgen, N. Davidsen, Z. Mingyang, Ø. Øyen, "The multivariate N-Component resolution problem with minimum assumptions", *Mikrochim Acta* **1986**, *89*, 63; DOI 10.1007/BF01207309.

[111] A. de Juan, R. Tauler, "Multivariate Curve Resolution. 50 years addressing the mixture analysis problem – A review", *Analytica Chimica Acta* **2021**, *1145*, 59; DOI 10.1016/j.aca.2020.10.051.

[112] L. W. Hantao, H. G. Aleme, M. P. Pedroso, G. P. Sabin, R. J. Poppi, F. Augusto, "Multivariate curve resolution combined with gas chromatography to enhance analytical separation in complex samples. A review", *Analytica Chimica Acta* **2012**, *731*, 11; DOI 10.1016/j.aca.2012.04.003.

[113] A. de Juan, J. Jaumot, R. Tauler, "Multivariate Curve Resolution (MCR). Solving the mixture analysis problem", *Anal. Methods* **2014**, *6*, 4964; DOI 10.1039/C4AY00571F.

[114] C. Ruckebusch, L. Blanchet, "Multivariate curve resolution. A review of advanced and tailored applications and challenges", *Analytica Chimica Acta* **2013**, *765*, 28; DOI 10.1016/j.aca.2012.12.028.

[115] S. D. Brown, S. T. Sum, F. Despagne, B. K. Lavine, "Chemometrics", *Anal. Chem.* **1996**, *68*, 21; DOI 10.1021/a1960005x.

[116] B. R. Kowalski, "Chemometrics. Views and Propositions", *J. Chem. Inf. Comput. Sci.* **1975**, *15*, 201; DOI 10.1021/ci60004a002.

[117] M. Otto, *Chemometrics. statistics and computer application in analytical chemistry*, Wiley-VCH; John Wiley & Sons, Inc, Hoboken, NJ, **2024**.

[118] A. Smilde, R. Bro, P. Geladi, *Multi-Way Analysis with Applications in the Chemical Sciences*, Wiley, **2004;** DOI 10.1002/0470012110.

[119] B. R. Kowalski, "Chemometrics", *Anal. Chem.* **1980**, *52*, 112; DOI 10.1021/ac50055a016.

[120] D. L. Massart, "Editorial", *Chemometrics and Intelligent Laboratory Systems* **1986**, *1*, 1; DOI 10.1016/0169-7439(86)80001-6.

[121] B. Kowalski, S. Brown, B. Vandeginste, "Editorial", *Journal of Chemometrics* **1987**, *1*, 1; DOI 10.1002/cem.1180010102.

[122] T. Lombardo, F. Walther, C. Kern, Y. Moryson, T. Weintraut, A. Henss, M. Rohnke, "ToF-SIMS in battery research. Advantages, limitations, and best practices", *Journal of Vacuum Science & Technology A* **2023**, *41*, 2101181; DOI 10.1116/6.0002850.

[123] N. P. Lockyer, S. Aoyagi, J. S. Fletcher, I. S. Gilmore, van der Heide, Paul A. W., K. L. Moore, B. J. Tyler, L.-T. Weng, "Secondary ion mass spectrometry", *Nat Rev Methods Primers* **2024**, *4*, 32; DOI 10.1038/s43586-024-00311-9.

[124] S. W. Gaarenstroom, "Application of factor analysis to elemental detection limits in sputter depth profiling", *Applied Surface Science* **1986**, *26*, 561; DOI 10.1016/0169-4332(86)90127-3.

[125] A. Manaprasertsak, R. Rydbergh, Q. Wu, M. Slyusarenko, C. Carroll, S. R. Amend, S. Mohlin, K. J. Pienta, P. Malmberg, E. U. Hammarlund, "Chemical profiling of surviving cancer cells using ToF-SIMS and MCR analysis discriminates cell components", *Anal. Methods* **2025**, *17*, 2263; DOI 10.1039/D4AY02238F.

[126] C. Seydoux, M. Bryan, J.-P. Barnes, P.-H. Jouneau, "Efficient Denoising of Shot-Noise in Mass Spectrometry Images by PCA-Assisted Self-Supervised Deep Learning", *Anal. Chem.* **2025**, *97*, 12925; DOI 10.1021/acs.analchem.5c00825.

[127] J. S. Solomon, "Applications of factor analysis to electron and ion beam surface techniques", *Surface & Interface Analysis* **1987**, *10*, 75; DOI 10.1002/sia.740100204.

[128] S. W. Gaarenstroom, "Principal component analysis of Auger line shapes at solid—solid interfaces", *Applications of Surface Science* **1981**, *7*, 7; DOI 10.1016/0378-5963(81)90056-8.

[129] M. F. Koenig, J. T. Grant, "Comparison of factor analysis and curve-fitting for data analysis in XPS", *Journal of Electron Spectroscopy and Related Phenomena* **1986**, *41*, 145; DOI 10.1016/0368-2048(86)80036-6.

[130] M. R. Keenan, P. G. Kotula, "Recent Developments in Automated Spectral Image Analysis", *MAM* **2005**, *11;* DOI 10.1017/s1431927605502708.

[131] K. Artyushkova, J. E. Fulghum, "Identification of chemical components in XPS spectra and images using multivariate statistical analysis methods", *Journal of Electron Spectroscopy and Related Phenomena* **2001**, *121*, 33.

[132] B. Moeini, N. Gallagher, M. R. Linford, "Surface analysis insight note. Multivariate curve resolution of an X-ray photoelectron spectroscopy image", *Surface & Interface Analysis* **2023**, *55*, 853; DOI 10.1002/sia.7260.

[133] N. Fairley, P. Bargiela, W.-M. Huang, J. Baltrusaitis, "Principal Component Analysis (PCA) unravels spectral components present in XPS spectra of complex oxide films on iron foil", *Applied Surface Science Advances* **2023**, *17*, 100447; DOI 10.1016/j.apsadv.2023.100447.

[134] V. Fernandez, N. Fairley, D. Morgan, P. Bargiela, J. Baltrusaitis, "Surface science insight note. Imaging X-ray photoelectron spectroscopy", *Surface & Interface Analysis* **2024**, *56*, 669; DOI 10.1002/sia.7337.

[135] S. Chatterjee, B. Singh, A. Diwan, Z. R. Lee, M. H. Engelhard, J. Terry, H. D. Tolley, N. B. Gallagher, M. R. Linford, "A perspective on two chemometrics tools. PCA and MCR, and introduction of a new one: Pattern recognition entropy (PRE), as applied to XPS and ToF-

SIMS depth profiles of organic and inorganic materials", *Applied Surface Science* **2018**, *433*, 994; DOI 10.1016/j.apsusc.2017.09.210.

[136] K. M. Mc Evoy, M. J. Genet, C. C. Dupont-Gillain, "Principal component analysis. A versatile method for processing and investigation of XPS spectra", *Anal. Chem.* **2008**, *80*, 7226; DOI 10.1021/ac8005878.

[137] J. Hertle, F. Walther, T. Lombardo, C. Kern, B. Pavlovic, B. Mogwitz, X. Wu, H. Schneider, M. Rohnke, J. Janek, "Benchmarking of Coatings for Cathode Active Materials in Solid-State Batteries Using Surface Analysis and Reference Electrodes", *ACS Applied Materials & Interfaces* **2024**, *16*, 9400; DOI 10.1021/acsami.3c15723.

7. Appendix

7.1. Supporting Information

7.1.1. SI Publication 1

Title: Long-term Degradation of Polytetrafluoroethylene in a Low Temperature Oxygen Plasma

Tobias Wagner[a], Marcus Rohnke[a*] and Jürgen Janek[a*]

[a] Institute of Physical Chemistry and Center for Materials Research, Justus Liebig University Giessen, Heinrich-Buff-Ring 17, D 35392 Giessen, Germany

*Juergen.Janek@pc.jlug.de

*Marcus.Rohnke@pc.jlug.de

Supporting Information:

Plasma chamber

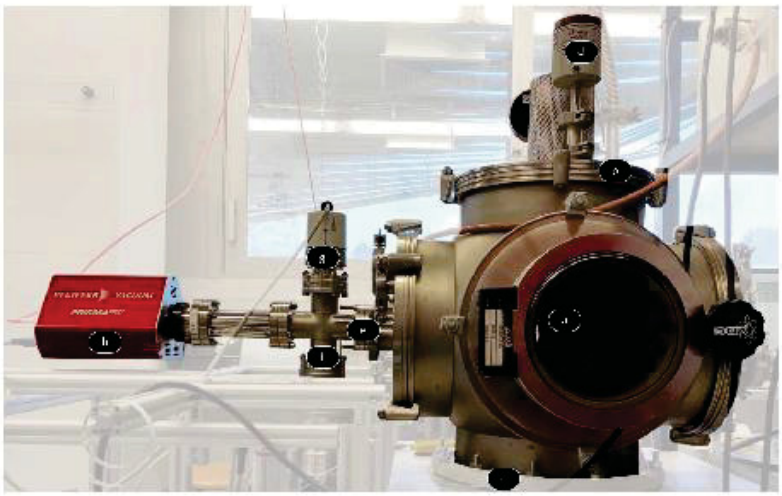

Figure S1: The plasma apparatus consisting of the main chamber (a), gas inlet (b), rotatory pump (below c), pressure sensor (d), double blind flange with capillary (e), turbomolecular pump (f), second pressure sensor (g) and quadrupole mass spectrometer (h).

Mass loss

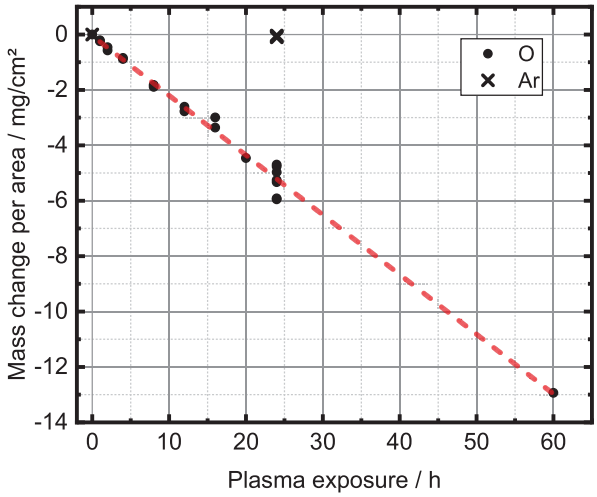

Figure S2: Observed change in weight of PTFE samples after different plasma treatment times at 0.1 mbar, 150 V, 10 W, normalized to the exposed surface area. A linear change in mass can be observed for samples treated in the oxygen plasma. Samples exposed to an Ar plasma under the same conditions experienced minimal mass loss, starting with 24 h of treatment. Shorter Ar treatments resulted in no detectable mass loss.

SEM

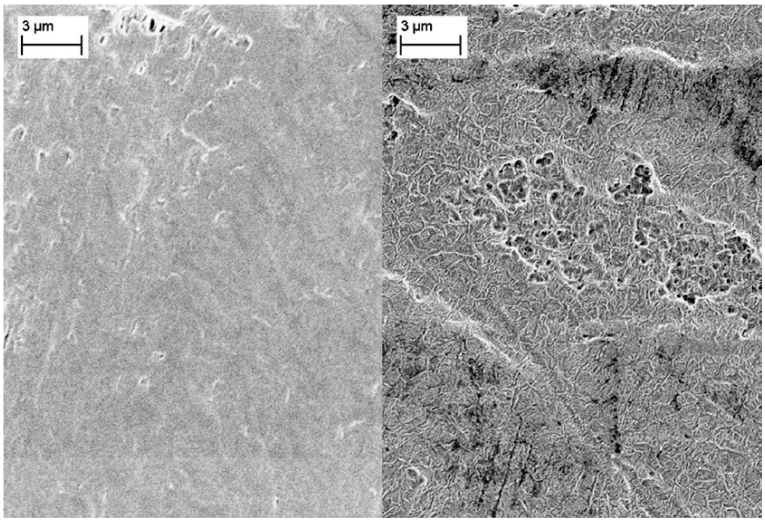

Figure S 3: Micrographs of an untreated (l) and an Ar plasma treated (t=4 h, r) PTFE sample. The plasma treatment conditions were 0.1 mbar, 150 V, 10 W. Contrary to the extreme surface changes observed for oxygen plasma treated samples, the Ar plasma treated sample exhibits only minimal erosion at the surface after the same treatment duration. This indicates that the degradation within the oxygen plasma is the result of a chemical reaction of the material with oxygen, rather than a physical process strated by plasma conditions.

XPS

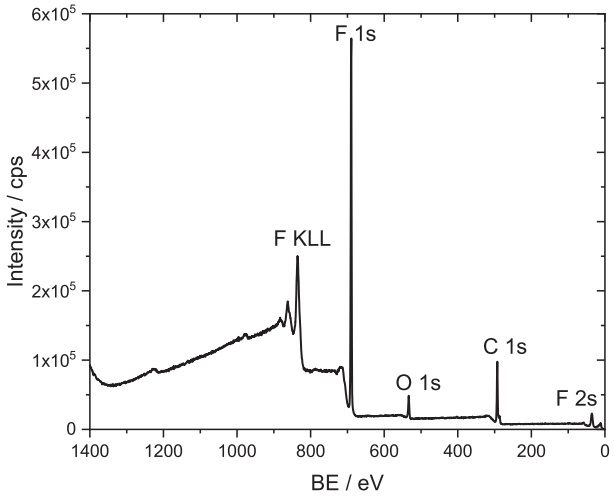

Figure S4: XP Survey spectrum of a 2 h oxygen plasma treated PTFE sample. Survey spectra were recorded with an analyzer pass energy of 224 eV, a step time of 50 ms, and a step size of 0.8 eV. Plasma treatment conditions were 0.1 mbar, 150 V, 10 W. No elements other than Carbon, Oxygen and Fluorine were detected on any of the samples.

AFM/ToF-SIMS

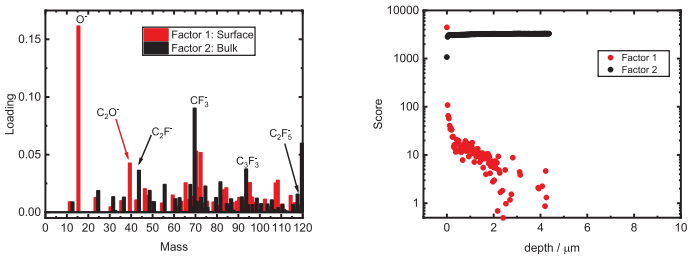

Figure S5: Loadings (l) and Scores (r) obtained from an MCR with two factors applied to negative ion mode ToF-SIMS depth spectra of an untreated (t = 0 h) PTFE sample. Factor 1 is only present at the surface of the sample and represents surface contaminations, such as oxygen and oxidized carbon fragments. Factor 2 appears in the bulk material and corresponds to pristine PTFE without any oxygen containing fragments.

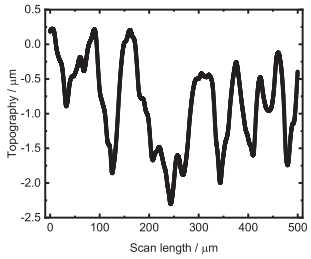

Figure S6: SPM scan of a PTFE sample treated at 0.1 mbar, 150 V, 10 W for 4 h. The surface roughness Ra of the sample was calculated to be 0.9 µm, rendering an accurate depth profiling of the near-surface region of plasma treated samples impossible.

7.1.2. SI Publication 2

Article Title: Investigation of the Polyvinylfluoride degradation mechanism under atomic oxygen exposure

Author Names: Tobias Wagner[a], Marcus Rohnke[a*], Joachim Sann[a] and Jürgen Janek[a*]

Affiliations: [a] Institute of Physical Chemistry and Center for Materials Research, Justus Liebig University Giessen, Heinrich-Buff-Ring 17, D 35392 Giessen, Germany

*Juergen.Janek@uni-giessen.de
**Marcus.Rohnke@uni-giessen.de

Supporting Information:

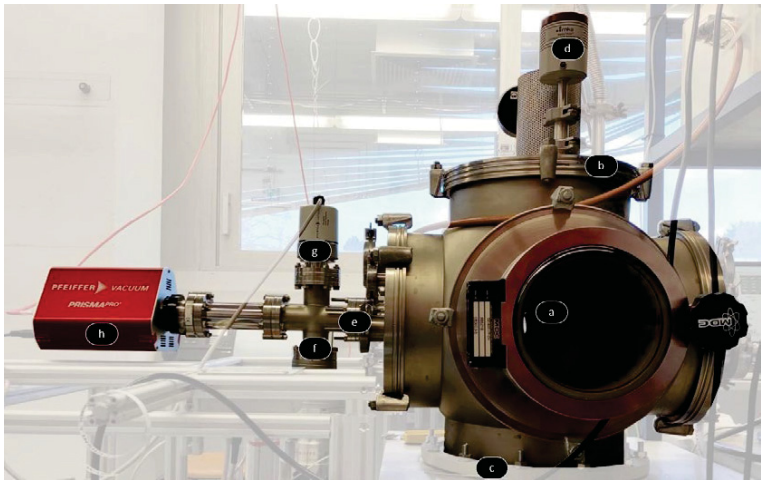

Figure S1: The plasma apparatus consisting of the main chamber (a), gas inlet (b), rotatory pump (below c), pressure sensor (d), double blind flange with capillary (e), turbomolecular pump (f), second pressure sensor (g) and quadrupole mass spectrometer (h).

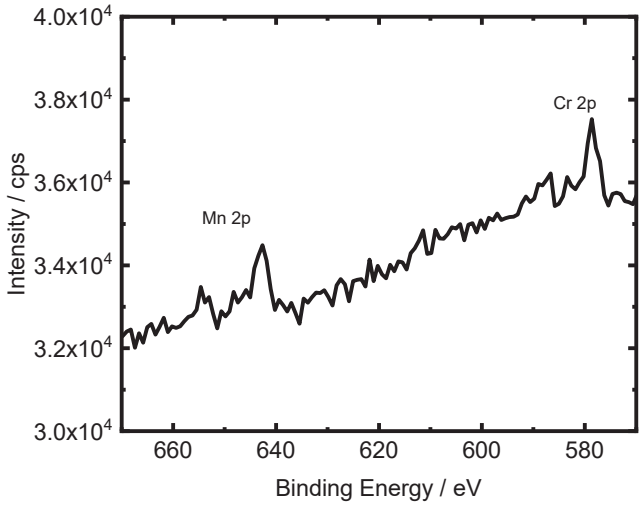

Figure S2: A close-up on the XPS survey spectrum of pristine PVF. Small peaks associated with chromium and manganese can be observed. Although these signals are too minute to be interpreted in detail, their existence indicated tha t these metals are present on the reference sample without any exposure to the plasma chamber.

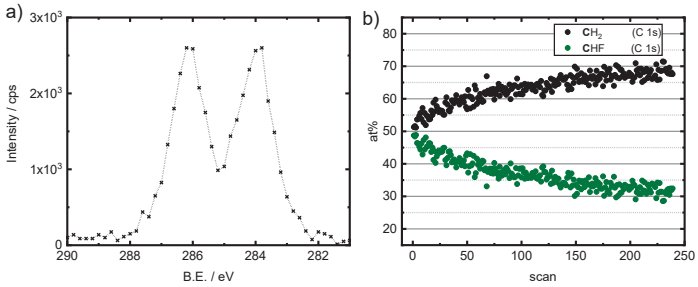

Figure S3: The first XPS C 1s detail spectrum of pristine PVF before X-Ray induced degradation of the material is observed (a). *The two characteristic peaks of PVF (CH_2 at lower BE, CHF at higher BE) can be seen. Both peaks have the same area, in agreement with the expected 1:1 ratio. Importantly, as the F 1s spectrum was not recorded, therefore the binding energy could not be cali brated. The changing composition of the C 1s spectrum can be seen in* (b). *After 50 scans (~13 min of X-ray exposure), the CHF signal has degraded significantly to a ratio of 1.5:1 (CH_2:CHF). After 175 scans, the ratio is at 2:1 with a continuing trend.*

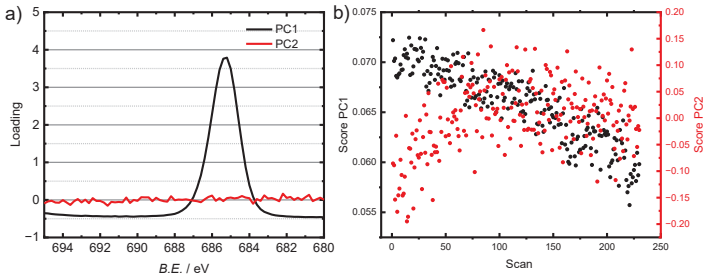

Figure S4: Results of a PCA applied to the uncalibrated F 1s XP Spectra of pristine PVF resolved over the scan number. The loadings plot (a) *reveals that PC1 (99,43% of variance) contains a peak-shaped signal at 685.4 eV. No other signal is visible in either principal component. In the scores plot* (b)*, a continuous decrease of the score of PC1 can be observed, while the score of PC2 (0.05% of variance) increases with the scan number. Nonet heless, the absence of significant loadings in PC2 indicates that this principal component is not relevant for interpretation of the data.*

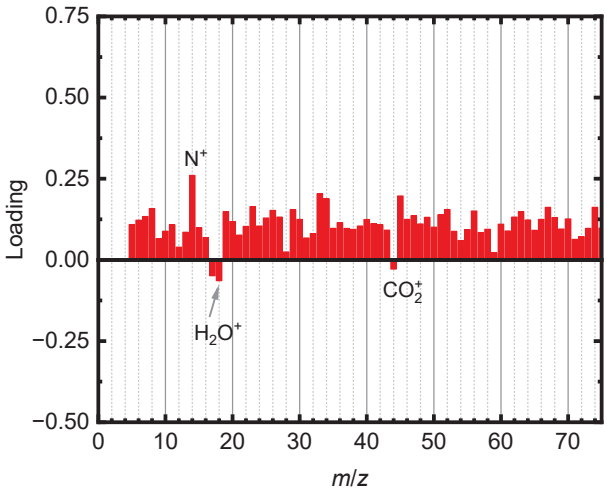

Figure S5: The loading plot of PC2, obtained from the PCA applied to consecutive mass spectra recorded by QMS during the PVF exposure to oxygen plasma. Very few mass signals exhibit significant loading. The most intense positive signal is at m/z = 28, attributed to N^+. As the score does not show any statistical relevance, PC2 does not conta in significant information regarding the degradation of PVF during the exposure to an oxygen pla sma.

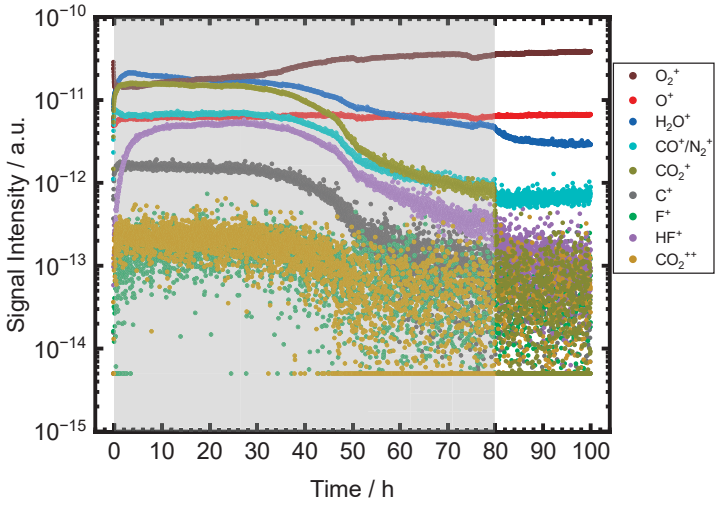

Figure S6: The raw signal intensities from QMS measurements. The plasma was active for 80 h, as can be seen by the grey overlay. The most abundant signals in absolute terms are O_2^+,O^+, H_2O^+, CO_2^+ and CO^+/N_2^+(m/z=28). After ~29 h, the signals linked to the degradation of PVF begin to decrease, with a sharp drop at ~46 h, where we assume that the sample is completely degraded. After the end of the plasma, O_2^+,$O^+$and H_2O^+ remain the most abundant species, followed by N_2^+.

7.2. List of Scientific Contributions

2025 T. Wagner, M. Rohnke, J. Sann, J. Janek, "Investigation of the Polyvinylfluoride degradation mechanism under atomic oxygen exposure", *Polymer Degradation and Stability* **2025**, 111820; DOI 10.1016/j.polymdegradstab.2025.111820.

2024 Poster Presentation: *ION-TOF User BeneFrance Meeting*, Leuven, Belgium: “Investigating the degradation of PTFE in a Low Temperature Oxygen Plasma.”

2024 T. Wagner, M. Rohnke, J. Janek, "Long-term degradation study of Polytetra-fluoroethylene in a low temperature oxygen plasma", *Polymer Degradation and Stability* **2024**, *229*, 110989; DOI 10.1016/j.polymdegradstab.2024.110989.

2022 Oral Presentation: *AVS 68*, Pittsburgh, USA (11/2022): “Long-Term Degradation of PTFE in a Low Temperature Oxygen Plasma.”

2020 T. Wagner, D. Valbusa, L. Bigiani, D. Barreca, A. Gasparotto, C. Maccato, "XPS characterization of Mn2O3 nanomaterials functionalized with Ag and SnO2", Surface Science Spectra 2020, 27, 1367; DOI 10.1116/6.0000331.